–Ph.D. Thesis–

Process Development for Recovery of Valuable Metals from Metallurgical Wastes using Hydrometallurgical Processes

湿式製錬法による鉱業廃棄物からの有用金属回収プロセスの開発

LABONE LORRAINE GODIRILWE

September 2022

Graduate School of International Resource Sciences

AKITA UNIVERSITY

PREFACE

Pyrometallurgical operations generate large amounts of slag as a waste product during the extraction of copper and/or nickel. These slags are oftentimes stockpiled and abandoned, which gradually present environmental problems to the immediate surroundings. Due to metal entrapment during the smelting process, the discarded slag still contains some valuable metals, which substantially accumulate over the years of continuous smelter operations. Recently, metallurgical waste is globally being explored as a potential secondary resource of valuable metals due to the depletion of primary ore resources. Hydrometallurgical processing is lately being preferred as an alternative route from conventional pyrometallurgical processing for metal extraction because of its great potential to process complex and low-grade ores with reduced environmental impact. This research aims to develop an efficient hydrometallurgical process to recover Ni, Cu, and Co from discarded copper/nickel granulated smelter slag. The high-pressure oxidative acid leaching (HPOAL) method was used to effectively leach Ni, Cu, and Co from slag, with low Fe tenors to the pregnant leach solution (PLS). The high-pressure leaching technology can operate at elevated temperatures and oxygen overpressure, these operating conditions provide the advantages of increased reaction kinetics, enhanced metal selectivity, and the generation of stable residues. This technology was further applied to low-grade secondary material (flotation tailings) and a difficult-to-treat complex ore of high impurity content (carbonaceous sulfide ore), for the extraction of copper. The solvent extraction technique was also used to selectively extract and enrich copper from the dilute PLS. Furthermore, selective precipitation techniques were used to separate value metals from impurities and also achieve individual value metals. This Ph.D. thesis is composed of five (5) chapters, addressing the different aspects of the hydrometallurgical processes developed to recover valuable metals from the low–grade waste material and difficult-to-treat ore resources.

Thesis Summary

Chapter 1: Introduction

This chapter introduces the pyrometallurgical production of nickel, and copper from sulfide nickel ore, including the description of the smelting process that results in the generation of slag as a waste product. A worldwide current situation regarding the production statistics and predicted data is outlined. Slag is explained and how metal losses are incurred in slag. Environmental consequences due to discarded slag are demonstrated. The importance of re-processing slag is outlined, as well as the objective of this research. The technologies and analytical methods used in this research are introduced. Previous research studies related to the re-processing of slag are cited.

Chapter 2: Direct atmospheric leaching (AL) and high-pressure oxidative acid leaching (HPOAL) of slag

This chapter mainly discusses the results of atmospheric leaching and high-pressure leaching of slag. Initially, the characterization of the electric furnace slag sample is illustrated. The characterization analysis tests include size analysis, XRF, XRD, and SEM observations which showed that the slag sample has an amorphous structure and the dominant mineral composition is fayalite with the matte phase locked in the fayalite phase. The valuable metals content of Ni, Cu, and Co were 0.36%, 0.36%, and 0.17%. Various leaching parameters such as sulfuric acid concentration, temperature, oxidant concentration/total pressure, and leaching time were investigated during the leaching of slag. The atmospheric leaching results showed poor extractions of Ni below 40%, with high Fe dissolution of about 80% when utilizing 1.0 M sulfuric acid and 0.6 M hydrogen peroxide reagent suite. The formation of a passive layer of amorphous silica was suspected to hinder oxidant access for sulfides dissolution and/or Fe precipitation. On the other hand, under optimized leaching conditions, high-pressure oxidative

acid leaching yielded excellent extractions of Ni, Cu, and Co from slag with the highest metal recoveries of Ni, Cu, and Co of 99%, 84%, and 99%, respectively with low Fe extraction of less than 2%. Acidity and temperature are important parameters for optimum dissolution of valuable metals from slag and control the stability of silicic acid to prevent polymerization to silica gel which clogs dissolution pores and hinders slag leaching. Leach residue elution tests were performed for evaluation of their environmental stability.

Chapter 3: Selective separation of metals from leach liquor by solvent extraction, precipitation, and xanthate complexation.

This chapter presents various separation techniques to selectively separate metal ions from the pregnant leach solution (PLS) and possibly upgrade or enrich the metal content from the dilute PLS. The solvent extraction technique was used to effectively extract and enrich copper from a simulated leach solution obtained from the high-pressure leaching of the smelter slag. The multicomponent leach solution contained 0.3 g/L Cu, 0.34 g/L Ni, 0.13 g/L Co, and 2.96 g/L Fe. Batch solvent extraction tests were carried out using a countercurrent two-stage mixer settler extraction column. Copper was selectively extracted using LIX 984N (10%v/v) with Isoper M as a diluent and stripped with sulfuric acid (H_2SO_4) solution. Fundamental parameters influencing the extraction process such as pH, mixing speed, H_2SO_4 concentration, and organic/aqueous (O/A) phase ratio were investigated. For copper enrichment in solution, a combination of two extraction stages and two stripping stages were employed. About 97% of copper was extracted from the simulated solution with coextraction of Fe, Ni, and Co of about 5.90%, 1.47%, and 2.53%, respectively. A final Cu-rich solution of about 23 g/L Cu was obtained with a very low Fe concentration of 0.05 g/L and no Ni and Co coextraction in the second stage. Additionally, for iron removal from the Ni/Co raffinate solution, more than 99% of iron was precipitated at pH 4 by the addition of a calcium carbonate ($CaCO_3$) suspension, with low coprecipitation of nickel and cobalt of around 3.68% and 2.27%, respectively. Subsequently, 99.3 % nickel and 99.9% cobalt were co-precipitated from the solution by

potassium amyl xanthate (PAX) solution (55 g/L) at pH 6 forming Ni and cobalt xanthates. Selective dissolution of nickel xanthate using ammonia solution was achieved while more than 99% Co remained as cobalt xanthate precipitate, which was roasted and recovered as CoO powder of about 25 wt.% Co.

Chapter 4: Application of hydrometallurgical processes to mine tailings and complex carbonaceous sulfide ore.

This chapter presents the application of high-pressure leaching technology to extract valuable metals from other metallurgical waste material (flotation tailings) and a complex ore of high impurity content (complex carbonaceous sulfide ore). High-pressure leaching was used to treat the flotation tailings to convert the AMD supporting minerals to more stable forms, for reduction of environmental loading while simultaneously valorizing the mine tailings. A combination of hydrometallurgical processes of high-pressure oxidative leaching (HPOL), solvent extraction (SX), and electrowinning (EW) were utilized to recover copper from mine tailings. An overall copper recovery of 86% was obtained, while pyrite, which is primarily in the mine tailings, was converted into hematite after HPOL. A stability evaluation of the solid residue confirmed almost no elution of metal ions. Complex carbonaceous sulfide ores are extremely difficult to treat due to their mineralogical complexity and impurities of organic carbon and carbonates. This study focuses on the development of a hydrometallurgical process for efficient copper extraction from complex carbonaceous sulfide ore which contains chalcopyrite, carbonates (dolomite and calcite), and carbonaceous gangue minerals. High-pressure leaching of complex carbonaceous sulfide ore in oxygenated sulfuric acid solution was performed. Selective dissolution of copper from iron can be achieved by controlling free acidity in the pregnant leach solution (PLS). The highest copper extractions achieved was 97.55% respectively. More than 99.9% of copper was precipitation of copper from the PLS by NaSH sulfidization.

Chapter 5: Conclusion

This chapter provides a summary of the data discussed in the previous chapters, highlighting the major findings and conclusions of each chapter. An overall process flow chart of the developed hydrometallurgical processes for valuable metal recovery slag is presented. Future work recommendations are also outlined.

Contents

List of figures

Chapter 1: Introduction

Chapter 2: Direct atmospheric leaching (AL) and high-pressure oxidative acid leaching (HPOAL) of slag

Chapter 4: Application of hydrometallurgical processes to mine tailings and complex carbonaceous sulfide ore

Chapter 5: Conclusion

List of tables

Chapter 1. Introduction

Large amounts of low-grade metallurgical wastes are produced every year in copper-nickel smelters, containing significant amounts of valuable metals such as cobalt (Co), nickel (Ni), and copper (Cu). Due to the increasing demand for metals, which is primarily driven by the rapid growth in the human population, the global industrial revolution, and advancing modern technological developments, the continuity of mining and supply of these metals is important. Unfortunately, this results in an in-evitable huge generation of metallurgical wastes, and due to the absence of efficient technologies for extraction of these metals from slag, they remain accumulated in enormous masses worldwide. It has been estimated that for every ton of nickel produced, 6–16 tons of nickel slag are produced [11]. Gorai et al. [12] estimated an annual slag generation at about 24.6 million tons from copper-smelting slags from world copper production. However, with the recent challenges in the mining industry such as the decline in ore grades, these waste masses are expected to increase due to large amounts of gangue material that has to be removed during the processing of low-grade ores.

Copper, nickel, and cobalt are important metals that are of great vitality to the development of societies today. Of the roughly 2 million tons of nickel produced every year, more than 2 thirds are used in alloys, such as stainless steel and superalloys [1]. Nickel increases an alloy's resistance to corrosion and can withstand extreme temperatures. Equipment and parts often used in harsh environments such as those in chemical plants, petroleum refineries, jet engines, and power generation facilities are often made of nickel-bearing alloys [2]. Copper is one of the most important industrial metals due to its excellent properties of electrical and thermal conductivity, corrosion-resistant and malleability. Demand for copper is primarily in construction, electronics, machinery, and consumer goods [14]. On the other hand, cobalt has unique properties such as a high melting point of about 1493°C and is ferromagnetic, with the ability to retain its magnetic properties up to 1100°C [13]. These properties make cobalt to be

highly sought for high-tech purposes. Cobalt's primary use is in making lithium-ion batteries needed to power electric vehicles and portable electronic devices. It is thus considered a critical metal due to the essential role it plays in ensuring a low carbon future and enabling technological development.

1.1 Sulfide nickel ore occurrence

There are two major types of nickel ore deposits today: magmatic sulfide deposits found in Canada, Russia, Australia, China, and South Africa, etc., and laterite deposits found in Cuba, New Caledonia, Indonesia, Philippines, Burma, Vietnam, and Brazil [3]. Magmatic sulfide deposits contain about 40% of global nickel resources while laterite deposits host approximately 60% of the world's nickel resources.

Sulfide nickel ores consist principally of nickeliferous pyrrhotite (Fe_7S_8), pentlandite $(Ni,Fe)_9S_8$, and chalcopyrite ($CuFeS_2$). Other minerals which occur in small but significant amounts include magnetite (Fe_3O_4), ilmenite ($FeTiO_3$), pyrite (FeS_2), etc. The typical grade for sulfide ores is 0.4–2.0 % nickel, 0.2–2.0% copper, 10–30 % iron, and 5–20 % sulfur. The most common of the sulfide minerals is pentlandite, while nickeliferous pyrrhotite is usually the most abundant phase in nickel ore. It contains nickel in solid solution (0.2–0.5 % Ni) in addition to very finely divided pentlandite inclusions [4]. Chalcopyrite is the most important copper mineral in the sulfide nickel ores. Although the major minerals are the same in all large sulfide ore bodies, the relative amounts of pyrrhotite, pentlandite, and chalcopyrite vary widely. In addition to nickel production, a large number of valuable by-products can be recovered from sulfide ores, including copper, cobalt, or platinum-group metals. Cobalt occurs principally in solid solution in pentlandite, at concentrations ranging from 1–5 % of the nickel content. The treatment processes are normally designed to yield optimum overall recovery of metal values.

Currently, sulfide nickel ores are the main source of more than one-half of the world's nickel supply. However, production from laterite ores is likely to increase as the nickel resources in existing sulfide mines are getting depleted [2, 26]. The Sudbury Igneous Complex in Canada is the second-largest nickel sulfide deposit in the world. The major nickel-producing countries include Indonesia, Russia, China, Canada, Cuba, Australia, the Philippines, and New Caledonia [2,3], while the top three consumers of nickel include China, the USA, and Japan [5].

Figure 1.1: A sample of nickel ore from the Sudbury Igneous Complex shows a specimen of pentlandite in pyrrhotite [2].

1.2 Pyrometallurgical Production of Nickel, Copper, and Cobalt

Most sulfide nickel ores are processed by concentration through a froth flotation or a magnetic separation process. Over 90% of the world's nickel sulfide concentrates produced follow the pyrometallurgical extraction processes to form nickel-containing mattes [4]. Most nickel producers produce a bulk concentrate that contains pentlandite, pyrrhotite, and chalcopyrite as smelter feed. Nickel copper concentrates typically range in grade from 5 to 15 % Ni + Cu. At a nickel-copper mine in Botswana the pyrrhotite/pentlandite ratio in the ore averages about 13:

1 and the pyrrhotite contains over 30 % of the nickel either in solid solution or as small pentlandite inclusions. Therefore, high nickel recoveries from pyrrhotite are achieved by producing a bulk pentlandite-pyrrhotite-chalcopyrite concentrate, with a typical composition of 2.8 % Ni and 3.2% Cu [4]. Some major nickel smelters with their production capacities and composition of the feed concentrate and product matte are listed in Table 1.1.

The pyrometallurgical treatment of nickel concentrates such as at the copper-nickel mine in Botswana, includes smelting, and converting. Smelting is carried out in a flash furnace, where pre-dried copper/nickel concentrate (chalcopyrite, pentlandite, and pyrrhotite) and silica flux with oxygen are injected into the furnace using a concentrate burner mounted at the top of the reaction shaft. At operating temperatures of about 1100^{o}C, the injection of these materials into the hot furnace causes the sulfide minerals (e.g., FeS_2) in the concentrate to react rapidly with the oxygen blast. The subsequent reactions are exothermic and result in large thermal energy which provides all the heat required for smelting.

Table 1.1: Major nickel sulfide smelters' data [4]

Smelter	*Feed concentrate, %*		*Matte product, %*		*Nominal capacity, t/a Ni*
	Ni	*Cu*	*Ni*	*Cu*	
Inco, Copper Cliff	13	2.7	63	15	110 000
Inco, Thompson	10.5	0.4	73	3	50 000
Western Mining	11.4	0.85	72	5	60 000
Falconbridge	6.7	5.6	40	34	45 400
Outokumpu	8-9	2-4	64	26	18 000
BCL, Botswana	2.8	3.2	38	40	20 000
Rustenburg	3.2	2.0	47	27	19 000
Bindura	10.6	3.4	70	20	14 400

The oxygen selectively reacts with iron to form iron oxide, FeO, which combines with silica flux to form a fayalite slag, leaving copper and nickel in the form of the sulfide, Cu_2S, and Ni_3S_2 (matte). The matte and slag form separate layers and are tapped at opposite ends of the furnace. The separation of the liquidus slag and matte is influenced by the addition of silica.

Figure 1.4 demonstrates that when silica is added to the mixture of FeO, and FeS at 1200°C, a liquid-state miscibility gap appears, which widens with more silica addition. The heavy arrow shows that adding SiO_2 to an oxy-sulfide liquid causes it to split into FeS-rich matte and FeS-lean slag.

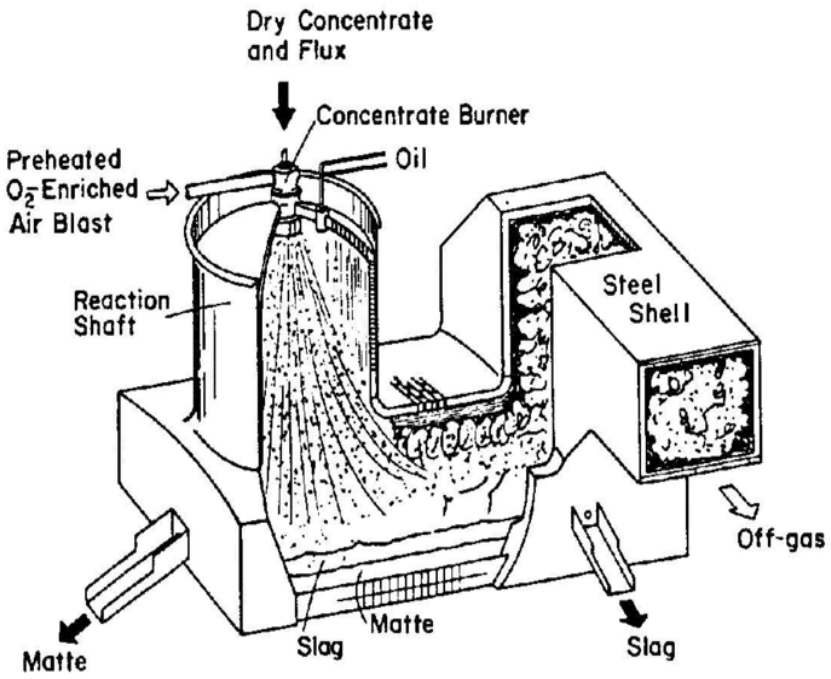

Figure 1.2: The schematic view of an Outokumpu flash furnace [15].

Nickel flash furnace mattes typically grade 50-55 % Ni and Cu, and the grade is controlled by adjusting the ratio of oxygen to concentrate in the furnace. The furnace matte has a grade of around 30% (Ni + Cu), which is further treated in Peirce-Smith converters with oxygen-enriched air to upgrade the matte product by forming iron oxides and removing sulfur as sulfur dioxide. Silica flux is added to the converters to combine with iron oxides and form an iron silicate slag having the approximate composition of fayalite ($2FeO.SiO_2$) by reaction 7. The final product from the converters is a high-grade matte typically of 74% or 92% nickel plus copper which is transferred from the converters to a ladle granulation point. The slag from the converters is further treated in the converter slag cleaning vessel (CSCV) for further recovery of cobalt.

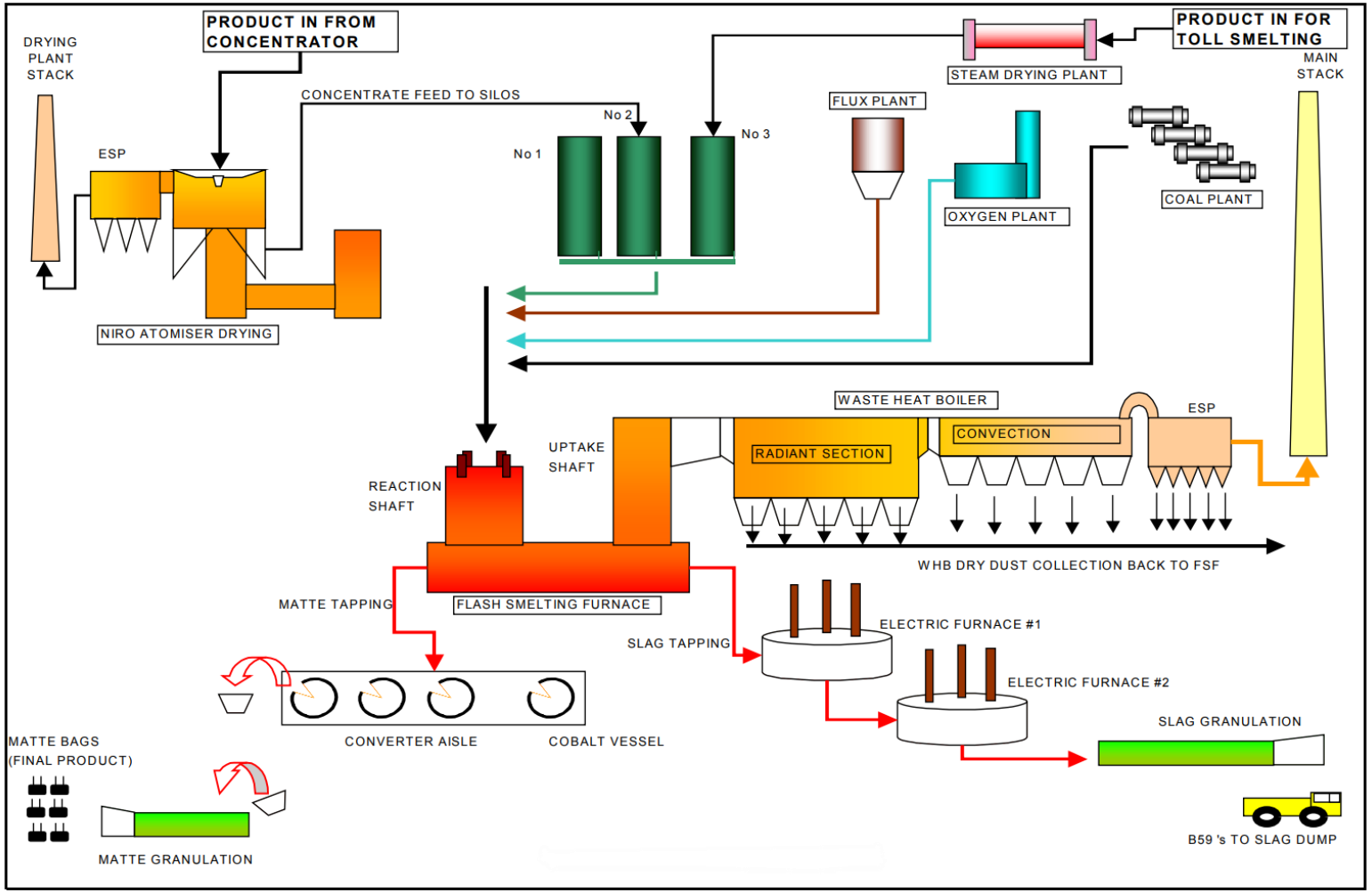

Figure 1.3: Process flow diagram of a Cu-Ni smelter in Botswana [44]

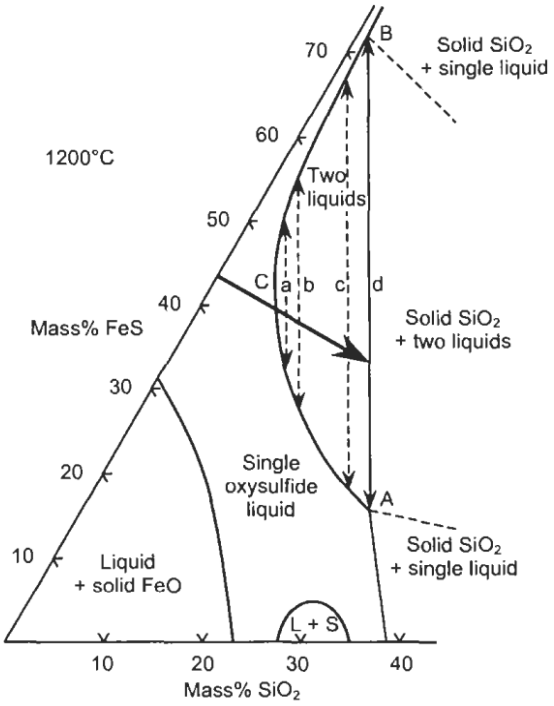

Figure 1.4: A simplified partial phase diagram for the Fe-O-S-SiO_2 system showing slag-matte separation behavior as influenced by SiO_2 addition [8, 10]

The main reactions, which take place during smelting and converting are as follows:

$CuFeS_2$	→	$CuS + FeS$	(1)
$2CuS + O_2$	→	$Cu_2S + SO_2$	(2)
$3NiS + O_2$	→	$Ni_3S_2 + SO_2$	(3)
$2FeS_2 + 5O_2$	→	$2FeO + 4SO_2$	(4)
$2FeS + 3O_2$	→	$2FeO + 2SO_2$	(5)
$6FeO + O_2$	→	$2Fe_3O_4$	(6)
$2FeO + SiO_2$	→	$2FeO \cdot SiO_2$	(7)

The overall reactions can be represented by the equations:

$2CuFeS_2 + {}^5/_2O2 + SiO_2 \rightarrow Cu_2S.FeS + FeO.SiO_2 + 2SO_2 + heat$ (8)

(Chalcopyrite) (Flux) (Matte) (Slag)

$2FeS + 3O_2 + SiO_2 \rightarrow 2FeO.SiO_2 + 2SO_2$ (9)

(Air) (Flux) (Slag) (Gas)

The following are the essential reactions forming base metals in the converter:

$[CoS] + O_2 \rightarrow [Co] + SO_2$ (10)

$[Ni_3S_2] + 2O_2 \rightarrow 3[Ni] + 2SO_2$ (11)

$[Cu_2S] + O_2 \rightarrow 2[Cu] + SO_2$ (12)

The flash furnace slag contains residual metals present both in an entrained metallic or sulfide form, and in a dissolved oxidized form, typically 2.0% nickel plus copper. The slag is tapped continuously from beneath the flash furnace uptake shaft, into the slag cleaning electric furnaces to recover the contained valuable metals (such as Co, Ni, and Cu) with the lowest possible iron content. The final slag to be discarded is laundered to be quenched by water and granulated at a rate of approximately 120 t/h. The slag losses are normally 0.20% nickel and 0.32% copper, and the slag is transported to the dump.

Sulfur dioxide (SO_2) and carbon dioxide are off-gases and pollutants also produced during smelting. The flash furnace off-gas contains about 10 to 30 % volume of sulfur dioxide (SO_2). These dust-laden gases from the uptake shaft of the flash furnace enter the waste heat boiler at around 1400^{o}C boiler where the heat content of the gas is recovered as high-pressure steam. The off-gas is cleaned in electrostatic precipitators to recover entrained dust before being dispersed to

the atmosphere through the stack. The technology is available to produce sulfuric acid economically from sulfur dioxide in the high-strength off-gas streams produced by the modern smelting techniques. However, there is not always a market for large amounts of acid within an economic shipping distance of the nickel smelter, so some smelters such as the BCL smelter vent SO_2-containing off-gases to the atmosphere.

Table 1.2: Metallurgical data for smelters [4]

Smelter		Outokumpu	Botswana	Western Mining
Capacity, t/a concentrate		190 000	800 000	600 000
Concentrate, %	Ni	8–9	2.8	11.4
	Cu	2–4	3.2	0.9
	Fe	24–27	43.52	38
	S	19–22	31.0	32
Furnace matte, %	Ni	33	15	44
	Cu	19	17	3
	Fe	18		27
	S	25		22
Converter matte, %	Ni	58	36	72
	Cu	32	40	5
	Fe	0.5	<1	<1
	S	6	20	21
Discard slag, %	Ni	0.15	0.15	0.28
	Cu	0.32	0.34	0.08
Smelter recovery, %		95	91.5	96

1.3 Slag

Slag is produced as a by-product during the extraction of nickel and/or copper from sulfide ores in pyrometallurgical operations. Slag is a solution of molten oxides [10], and the main slag composites are FeO, Fe_2O_3, and SiO_2, considering reactions 4–7 and thus are referred to as fayalite

slags. Small amounts of sulfides can also be dissolved in FeO-SiO_2 slags [10]. The solidification of slag is formed from molten material through air-cooling or instant granulation by quenching with water. Upon cooling the molten slag, fayalite (Fe_2SiO_4) precipitates, which is a dense and glassy material. The rate and method of cooling affect the properties of the slag, air-cooled Ni slags usually contain a majority of crystalline phases, while water-quenched Ni slag is mainly amorphous and appears glossy [7]. The amount of slag produced is usually of comparable tonnage to the tonnage of the feed concentrate [6]. Other research estimated that producing 1 ton of Ni in a flash smelting furnace or electric arc furnace will generate around 6–16 tons of slag [7], while others noted that for every ton of copper produced, an average of 2.2 tons of slag is formed [9, 12]. Figures 5 and 6 show that the world Ni and Cu production has been growing significantly over the years, showing an exponential growth trend since 1960 [26], this consequently translates to an exponential generation of slag waste worldwide.

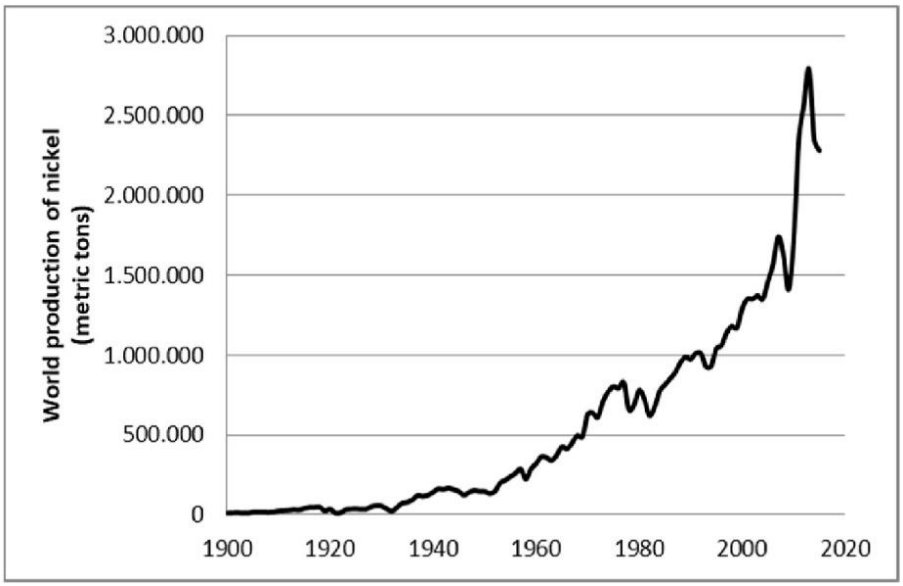

Figure 1.5: World nickel production between 1900 and 2017 [27].

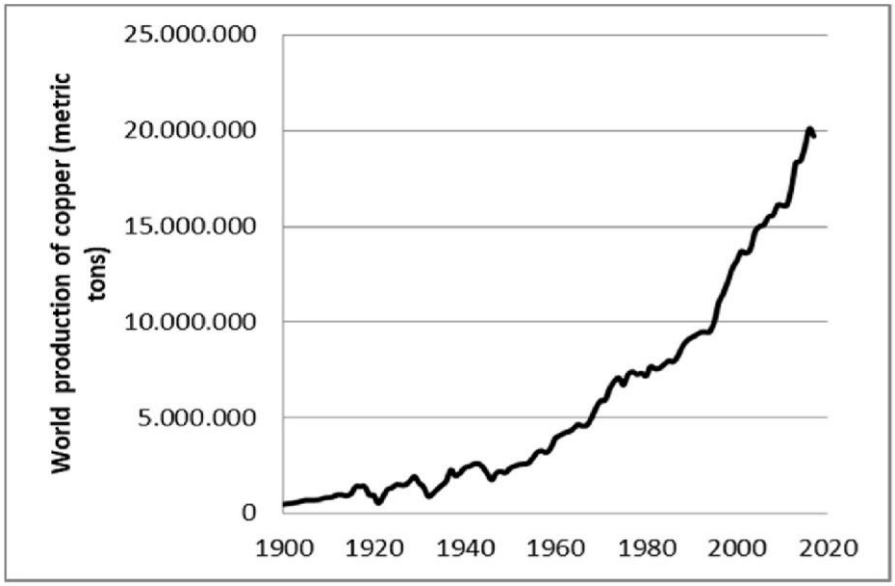

Figure 1.6: World copper production between 1900 and 2017 [27]

1.3.1 Metal losses in slag

Entrained matte in slag is the main way in which the smelter incurs metal losses. Entrained matte represents 50–90% of the copper contained in smelter slag [8]. There are several causes of entrained matte in slags, some of which are mentioned below.

a. Losses of nickel and copper to the slag tend to increase with the oxidation potential of the system, so metal losses to slag in the electric furnace where melting is carried out under reducing conditions are less than in the flash smelting furnace where the smelting conditions are strongly oxidizing [4]. A more reducing environment also decreases the content of magnetite (Fe_3O_4) in the slag and thus encourages settling [10].

b. Droplets of matte that have failed to settle completely through the slag layer are one of the common ways that can result in entrained matte in slag, especially the smallest droplets. The rate at which matte droplets settle through the molten slag has been predicted as follows [8]:

$$V = (\rho_M - \rho_S)\, gr^2/3\eta_S$$

Where V is the settling rate of the matte droplets (m/s), g is the gravitational constant (9.8 m/s^2), ρ_M is the matte density (3900 – 5200 kg/m^3), ρ_S is the slag density (3300 – 3700 kg/m^3), η_S is the slag kinematic viscosity, and r is the radius (m) of the settling matte droplet.

c. Temperature and slag silica content have a major influence on the settling rate [10]. Higher temperatures and lower silica levels decrease slag viscosities resulting in an increased matte settling rate. Magnetite content has also been noted to have a significant effect on the viscosity of fayalite slags [16]. Additionally, the matte grade has been noted to influence settling rates in that low-grade mattes have lower densities and therefore settle at slower rates than high-grade mattes [8].

d. Matte droplets can become suspended in smelter slags by mechanical means such as being floated into the slag by SO_2 bubbles that originate in the molten matte layer according to reaction 13. While some matte droplets may be lost in the slag by precipitation in colder areas of the smelting furnace [16].

$$3Fe_3O_{4(s)} + FeS_{matte} \rightarrow 10FeO_{slag} + SO_2\,(g) \qquad (13)$$

At the copper-nickel smelter in Botswana, slag losses are controlled in the flash furnace settler by the addition of lump coal, which floats on the surface of the slag and reduces the metal oxides. The slag is further cleaned with a carbonaceous reducing agent in two electric furnaces (DC-arc furnaces) connected in series before being discarded. The slag cleaning furnaces rely largely on a gravity settling mechanism, whereby the entrained sulfide and metallic droplets are

simultaneously collected. A quantity of matte may be added to the slag to enhance the coalescence of entrained matte droplets. However, conditions are not usually sufficiently reducing to recover much of the cobalt, and because of the similarities in the reduction behavior of cobalt and iron, some loss of cobalt is inevitable while separating the iron from the nickel and copper. Cobalt recoveries may be as low as 20%. The most effective means for the recovery of metals involves the addition of a reductant (such as carbon) to capture some of the metals present in an oxidized form. Typical metallurgical data of the copper-nickel smelter is presented in Table 1.2.

1.3.2 Environmental Impacts of Discarded Slag

There is an increasing concern worldwide over the potential environmental impacts of slag. The vast amount of discarded slag does not only result in the wasting of valuable metals but also poses a major environmental hazard depending on their physical, chemical, and mineralogical composition and behavior under certain environmental conditions. Numerous slag dumps exist worldwide, holding a massive amount of slag that has accumulated over the past decades of years, this only has resulted in less availability of land suitable for landfills [17].

The slag dump sites generally undergo natural weathering; that is a wide range of chemical, biological processes, and environmental factors such as pH variations, the presence of inorganic and organic acids, and microbial conditions [17]. Long-term exposure of slag to weathering may encourage oxidation of entrained sulfur to sulfuric acid promoting slow leaching of heavy metals into the nearby environment [18]. The high concentrations of potentially toxic metals in the vicinities of slag dumps is a concerning environmental issue for numerous slag disposal sites. However, other authors noted that the potential environmental risk of the slag is limited due to the immobility and the entrapment of small inclusions of more reactive sulfide and metallic alloys

containing Cr, Cu, Ni, Zn, and Sn in relatively stable silicate glass and oxides [24]. Soils in the areas around historic smelters, which were active between the 14th and 16th centuries, were reported to be still highly polluted with metal(loids)s due especially to the centuries-long dissolution of smelter wastes into the soils [19]. Similarly, Motswaiso et al. [20] conducted a geochemical investigation around the BCL mine area and found a high degree of enrichment of Cu and Ni in the soil and sediment of areas closer to the BCL waste dumps when compared with other parts of the mine area. High concentrations of Cu, Ni, and Cr in the Mathathane river, which flows very close to the tailings dump and slag pile when compared to other rivers around the mine area. Since the amount of the generated slag is estimated to be comparable to the tonnage of concentrate processed [21], the BCL slag dump can be estimated at 35 million tons since its operation in 1974, demonstrating that the slag dump is a large feature of the BCL mine site, which can cause significant environmental deterioration.

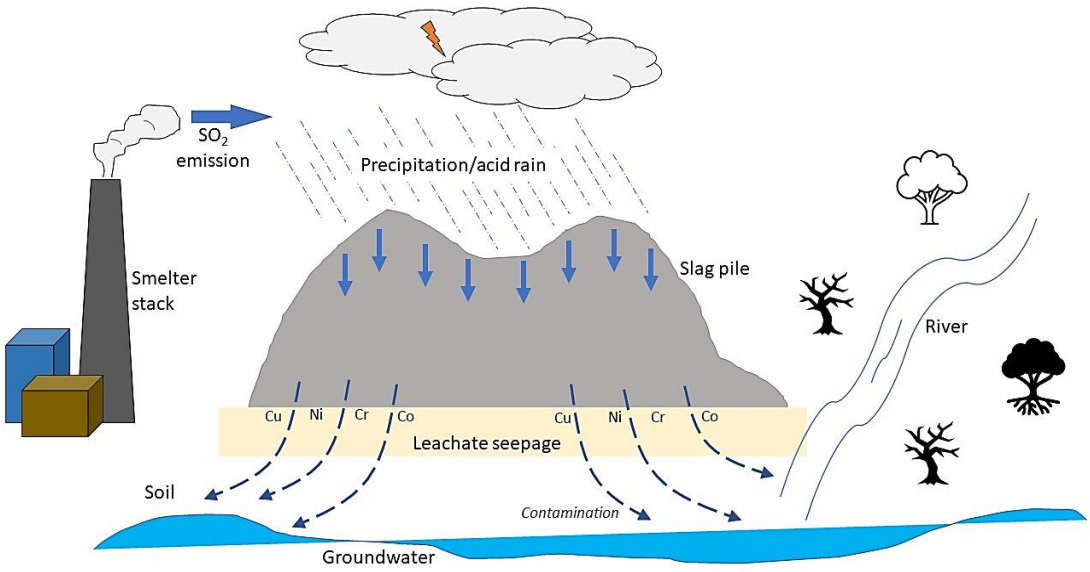

Figure 1.7: Illustration of the environmental impact of discarded slag

Concentrate feed to the copper-nickel smelter is a nominal 2600 tons per day, containing 30% sulfur, of which only 8% is captured and the difference is emitted to the atmosphere [22]. The high amounts of sulfur dioxide gas emitted into the atmosphere are the major cause of acid rain, as it chemically reacts to form a sulfuric acid mist [25]. As this acid rain falls onto the slag pile, it further promotes the dissolution of toxic metals from the slag as illustrated in figure 1.7. When these toxic metals accumulate in the environment, they become a major source of contamination to water sources and potentially endanger ecosystems and human health [23]. Therefore, the management of these slag piles is extremely important, as well as developing effective long-term strategies to reduce the environmental footprint of the mining industry.

1.3.3 Why process the smelter slag?

The three main reasons that motivate the re-use of slag include the mounting evidence of the adverse environmental impacts caused by slag piles [17-20]; the decreasing availability of land to be used for landfills due to the rapid growth of global industrialization [17]; and the significant quantities of valuable metals in slag that have accumulated over many years of operation of nickel and copper smelters. Alternative re-uses of slag are widely being explored mainly in the areas of construction, metal recovery from slag, and slag use in environmental remediation applications [11, 24, 28].

Current challenges in the mining industry, such as a decline in ore grade (figure 1.8) and depletion of Ni sulfide ore resources, have led to low-grade secondary sources of metals being exploited. To meet future demand for Ni, there is an increasing amount of Ni being mined from laterite ores and projected to remain high (figure 1.9), leading to increased energy and greenhouse gas emission costs for Ni production [26]. With the increased global production of Ni and Cu (Figures 5 and 6)

especially with the processing of low-grade ore, slag generation is expected to increase. China's copper output in 2019 reached 9.8 million tons, producing more than 20 million tons of copper slag, while the accumulative stockpile of copper slag exceeds 120 million tons [28]. Zhang et. al [11] estimated that the annual discharge of nickel slag in China is 81.05 million tons. A further decline in ore grade makes it difficult to increase recovery efficiency substantially, which is a balance between mainly energy costs and commodity returns [27]. This makes slag a potential raw material that not only needs to be processed to decrease the slag's footprint on the environment but also for its economical benefits.

The copper-nickel smelter in Botswana has generated millions of tons of granulated slag which has accumulated over 41 years of continuous smelter operation. In order to disrupt the slag weathering process and prevent further metal elution into the environment [20], environmental remediation actions need to be initiated. Over the years of the mine's operations, values of metal recoveries in the matte were reported to be low as there was a high degree of metal losses reported in the slag phase. The slag was oxidized with a high amount of magnetite thereby affecting the settling of entrained metal particles and resulting in high metal losses to the slag. There is a need, therefore, to recover the entrained metals (Ni, Cu, and Co) in the slag.

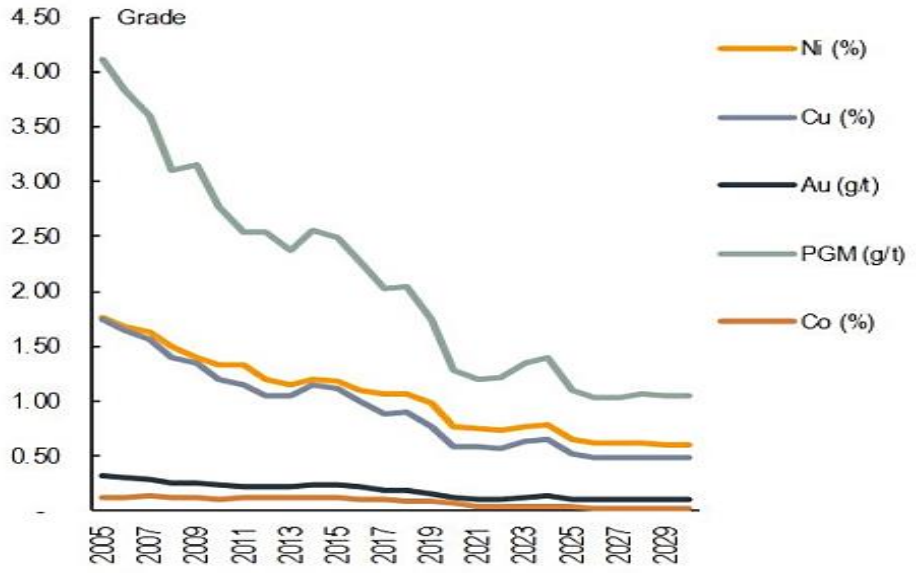

Figure 1.8: Average ore grades for various metals, past and future predictions [https://www.amegroup.com/Website/FeatureArticleDetail.aspx?faId=159]

In the past, the lack of a framework of environmental sustainability and limited scientific evidence of the slag's environmental behavior had resulted in the main focus only being the exploitation of resources with little concern regarding the slag waste and its long-term effects or re-use potential. However, with the recent technological advancements and holistic international legislations and goals, such as the sustainable development goals (SDGs) there is a possible way to have a balance between resource use and environmental management.

With the advanced and more efficient metallurgical processing techniques becoming available, it provides a possibility to develop viable methods to process the numerous heaps of slag and extract valuable metals such as Ni, Cu, and Co. In the current years, a growing interest in the development of hydrometallurgical processes is widely being adopted [17, 18, 23, 32–41]. Hydrometallurgical processes have the advantage of effectively processing low-grade ores because of comprehensive metal recovery and shorter retention times [23]. Hydrometallurgical processes such as high-

pressure leaching technology allow for better control and separation of co-products and produce solid waste residues with a lower environmental impact [23, 39].

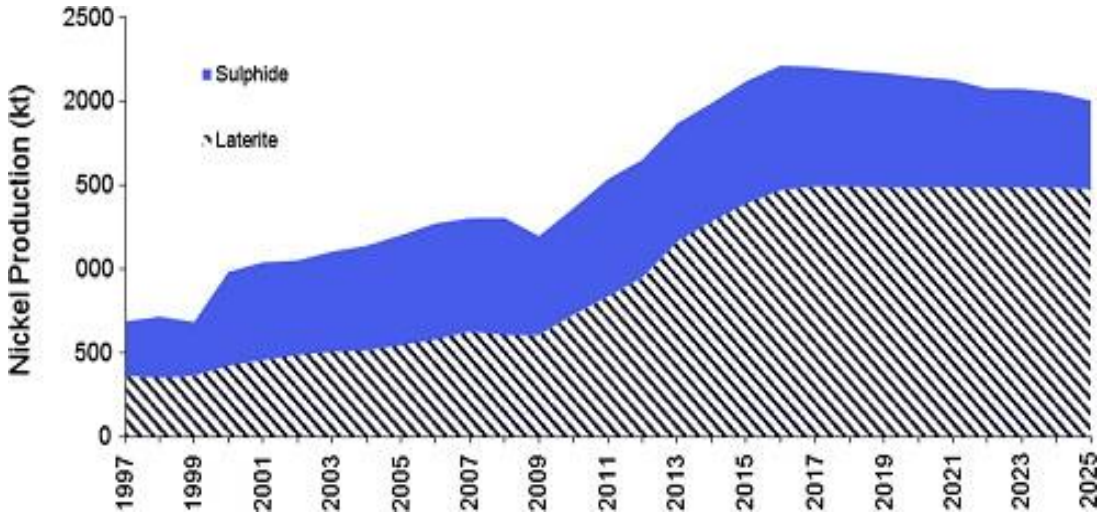

Figure 1.9: Nickel production from sulfide and laterite ores, past and future predictions [29].

1.4 Previous research on the re-processing of slag for metal recovery

The characteristics of valuable minerals in different slags differ. They may be in the form of oxides, sulfides, or both. The methods or a combination of methods generally considered for metal recovery from slags include flotation, leaching, and roasting.

The application of flotation to smelter slag re-processing is somewhat limited because only metallic form and sulfide minerals can be floated successfully, but other metals in the slag such as cobalt, exist in the oxide form, making the flotation method ineffective for the recovery of Co, Ni and oxide Cu [30]. The method of slag roasting is usually done in combination with leaching, such as roasting with ferric sulfate and subsequently leaching the obtained calcines with water or sulfuric acid solution. When iron sulfate is heated to temperatures exceeding 480°C it decomposes

yielding SO_3, which may cause sulphation of metal components or possibly change the structure of slag making it amendable to leaching. Altundogan and Tumen (1997) [31] did a study on the recovery of copper, cobalt, nickel, and zinc from copper converter slag by roasting with ferric sulfate followed by leaching with water. Recoveries of copper, cobalt, nickel, and zinc were about 93%; 38%; 13%, and 59%, respectively, were obtained. The limited values of cobalt and nickel recoveries obtained indicated that cobalt and nickel may exist in magnetite and fayalite matrices. Nadirov et. al (2013) [32] developed a technique to recover valuable metals from copper smelter slag by heat treatment with ammonium chloride and subjected the products to water leaching. They found that 91.5% of zinc and 89.7% of copper were converted to water-soluble form at 320 °C for 120 min.

Processing of slags, particularly iron silicate slags by hydrometallurgical means, has been increasingly attempted by various scholars. The common hydrometallurgical methods studied are atmospheric leaching and high-pressure oxidative acid leaching. Some limitations noted by some researchers during atmospheric leaching of slag include difficulty in solid-liquid separation due to silica gel formation, low metal extractions, and high iron co-extractions [6]. Therefore, the addition of an oxidant during atmospheric leaching has largely been studied.

Under atmospheric leaching conditions, lixiviants such as dichromate compounds or hydrogen peroxide have been considered oxidizing agents for dissolving the sulfide in the slag as well as minimizing iron co-dissolution and the influences resulting from silica gel. Yang et al. (2010) [33] developed a novel hydrometallurgical method that involved atmospheric leaching of copper smelter slag using sulfuric acid and sodium chlorate oxidant to selectively extract and recover 98%, 97%, and 89% of cobalt, zinc, and copper respectively, while the extraction of silicon and iron was only 3.2% and 0.02%, respectively. Dimitrijevic et. al (2017) [34] studied the leaching

of copper smelting slag in chloride media with lixiviants utilization of hydrogen peroxide and hydrochloric acid. The maximum obtained copper extraction from the slag was 73% with a high iron dissolution of 55% when using 3 M H_2O_2, at room temperature after 120 minutes of reaction. Altundogan et. al (2004) [35] investigated sulfuric acid leaching of copper converter slag in the presence of dichromate an oxidant under atmospheric conditions and found that a significant amount of Cu could be extracted along with very low iron concentrations when leaching with a lixiviant containing potassium dichromate and sulfuric acid rather than leaching with sulfuric acid alone. Boyrazli et. al (2006) [36] reported on the extraction of metals from copper converter slag by using a sulfuric acid/potassium dichromate lixiviant. The best results were obtained by the leaching of converter slag (-200 mesh, 10 g/L of slag/solution ratio) with a lixiviant containing 0.25 M H_2SO_4 and 0.1 M $K_2Cr_2O_7$ for 120 minutes at 70 °C. Under these conditions, 99.66% Cu extraction yield was achieved. Banza et. al (2002) [37] studied the leaching of an amorphous smelter slag using sulfuric acid under hydrogen peroxide at 70 °C and normal pressure and effectively extracted base metals from amorphous copper smelter slags while avoiding silica gel formation and iron co-extraction. Atmospheric leaching of slag is commonly associated with high acid-consuming behavior as per the stoichiometric requirement of the fayalite dissolution reaction (equation 14) [18], so alternative leaching media is sometimes considered. Aracena et. al (2019) [38] utilized ammonium hydroxide rather than the conventional route of sulfuric acid when studying column leaching of converter slag. High copper recoveries of about 88% were obtained using an ammonia system with almost no impurities while an acid leaching system yielded a lower copper recovery of only 50.8% and Fe recovery of over 67.0%.

$$Fe_2SiO_4 + 2H_2SO_4 \rightarrow 2FeSO_4(aq) + Si(OH)_4(aq) \quad (14)$$

High-pressure oxidative leaching has thus been used in several studies to resolve the challenge of low metal extractions and minimize iron contamination by oxidation and hydrolysis. The high-pressure oxidative acid leaching process has been noted to be a robust process in achieving very

high metal extraction levels and producing a benign residue consisting predominantly of hematite, which is most suitable for safe disposal [39]. During the high-pressure oxidative acid leaching (HPOXAL) of nickel converter slag, Huang et. al (2015) [6] found that temperature and sulfuric acid concentration are the two most important parameters as high temperature favors the selective extraction of valuable metals (Ni, Cu, and Co) over iron as well as the solid-liquid separation of the leaching slurry, while the sulfuric acid concentration maintains an appropriate final pH boundary which affects the content of iron and silicon in the solution. Under optimized leaching conditions, Huang et. al (2015) [6] achieved highly selective leaching of valuable metals with the extraction of >97% for cobalt and nickel, >95% for copper, < 4% for iron, and <2% silicon, with the residue containing mostly hematite and silica. Baghalha *et al.* (2007) [21] investigated an oxidative pressure acid leaching process for the extraction of nickel, cobalt, copper, and zinc from smelter slags to produce an environmentally benign residue. When utilizing the pressure acid leaching at 250 °C with an oxygen overpressure of 520 kPa, sulfuric acid to slag ratio at 0.3, more than 90% extractions of the nickel, cobalt, copper, and zinc were achieved, with a very low concentration of Fe and Al impurity metals in leached solution. Anand *et al.* (1983) [40] studied pressure leaching of the converter slag with dilute sulfuric acid and obtained metal extractions of about 90% copper, >95% nickel, and cobalt, while only 0.8% iron was leached.

Baghalha *et al.* (2007) [21] found that slags that are quenched in water produce an amorphous structure which the resulting metal (Ni, Cu, and Co) extractions are substantially lower in the 20-30% range when subjected to high-pressure oxidative leaching as compared to crystalline (naturally cooled) slag. Banza et. al (2002) [37] mentioned that smelter slag with an amorphous structure cannot efficiently be leached with sulfuric acid as the formation of silica gel induces an increase of leach liquor viscosity, difficult pulp filtration, and crud formation during solvent extraction. Perederiy and Papangelakis (2017) [41] also confirmed low metal extractions of Ni, Cu, and Co in the 45–60% range from amorphous electric furnace slag by high-pressure oxidative

acid leaching, attributing it to the formation of a passive silica layer within slag particles hindering acid attack. Conversely, the crystalline FeO-SiO_2 slags tend to dissolve fast and almost entirely during pressure leaching because of the good spatial separation of silica (SiO_2) and fayalite (Fe_2SiO_4) induced during slow solidification [41]. Yang et. al 2010 [33] added calcium hydroxide for neutralization after atmospheric leaching with sulfuric acid and sodium chlorate oxidant. Calcium hydroxide precipitates silica and iron(III) oxides thus allowing for a faster filtration of the precipitate.

1.5 Objective

The objective of the research is to develop a process to recover copper, nickel, and cobalt from the granulated waste slag.

- In consideration of the slag characterization results, that is the low grade of the valuable metals, their locked deportment in the fayalite phase, and the majority of sulfides (75%) occurring as particles of less than 20 μm, the high-pressure oxidative acid leaching method was considered to be the most effective for the recovery of valuable metals from the slag. The influence of leaching parameters such as sulfuric acid concentration, temperature, total pressure, and pulp density will be studied and explained.
- Leachability and dissolution mechanism of amorphous slag investigated and explained.
- Enrichment and separation of copper, nickel, cobalt, and iron from the pregnant leach solution by exploring other hydrometallurgical methods such as solvent extraction and selective precipitation.
- Assess the environmental loading reduction of slag by evaluating the stability of the leach residues produced from the proposed hydrometallurgical process.

1.6 Advantages of hydrometallurgical methods

Hydrometallurgical methods were used in the process development of extracting valuable metals from the granulated copper-nickel smelter slag, flotation tailings, and complex carbonaceous sulfide ore. Hydrometallurgical processing is widely being explored as an alternative route for metal extraction because of its great potential to process complex and low-grade secondary material. Below are some of the advantages of hydrometallurgical methods:

- Adaptability and easy optimization of process control to provide robust operating conditions such as different pH, strongly oxidizing, neutral or reducing conditions, elevated temperatures, and pressure. These operating conditions provide the advantages of increased reaction kinetics, enhanced metal selectivity, and recoveries.
- Hydrometallurgical methods are known to generate thermodynamically stable residues [23], that are less prone to natural weathering, therefore there is a reduced or controlled environmental impact of the waste generated from these processes. Pyrometallurgical methods, such as re-smelting of slag for metal recovery, are known to be energy-intensive and may cause further environmental harm, Perederiy, (2011) [18] noted that recycling of converter slag into the furnace causes extra fugitive emissions of sulfur dioxide to the atmosphere.
- Hydrometallurgical processes have also been noted for their comprehensive metal recovery with shorter retention times [23]. In the case of slag processing, the finely dispersed metal sulfides in the fayalite slag, are oxidized and easily dissolved [21]. Other methods such as flotation were not considered because the amount of liberated sulfides is only about 12%. This implies that to achieve about 80% liberation of the sulfides for recovery by flotation, the slag will have to be finely milled to about P_{80} of less than 20 µm which may not be economical. The flotation method was not considered moreover because only metallic form and sulfide minerals can be floated successfully, but other

metals in the slag such as cobalt, exist in the oxide form, making the flotation method ineffective for the recovery of Co and oxide Cu [30].

Therefore, the leaching method was investigated as the main extraction method of valuable metals from the smelter slag, whereby acid is required to dissolve metal oxides (e.g. cobalt) while oxygen is necessary to dissolve metal sulfides (e.g. nickel and copper) [42]. Since the leaching of valuable metals will involve the inevitable dissolution of iron from fayalite causing contamination to the pregnant leach solution, therefore the optimization of the leaching method to achieve selective extraction of valuable metals (Ni, Cu, and Co) against iron is of paramount importance.

1.7 Introduction to methodologies used

A brief introduction of the hydrometallurgical methods employed in this research is mentioned below.

1.7.1 Atmospheric acid leaching

As a preliminary study, atmospheric acid leaching (AL) was investigated as an option to extract nickel, copper, and cobalt from the smelter slag. Atmospheric acid leaching is a basic method that is cost-effective, easily employed, and if feasible can provide the possibility of heap leaching, especially when dealing with huge amounts of waste such as slag dumps. Sulfuric acid is commonly used as a leaching medium due to its effectiveness and easy availability from most smelting plants. During AL, the sample is ground to a suitable size to form a slurry with the leaching medium at a controlled slurry density. The leaching tank is equipped with an agitator for efficient solid-liquid contact by maintaining the solids in suspension to achieve leaching. During leaching, there is dissolution and transfer of valuable metals from the solid material to the leach solution, and under the selective dissolution, most of the undesirable components remain in the

solid-state and are removed as the solid residue, containing waste minerals such as alumina, silica, and insoluble iron oxides/hydroxides/sulfates [8]. The valuable metals are separated in the pregnant leach solution (PLS) as metal ions (e.g. Ni^{2+}, $Cu^{2+,}$ and Co^{2+}), however, the PLS can still contain other impurity species, such as Fe, Al, Co, Mn, Zn, Mg, Ca, etc., that were leached with the valuable metals. Since AL does not commonly involve oxygen injection, the addition of an oxidizing agent such as hydrogen peroxide is sometimes added to improve metal recoveries and generate stable residues.

1.7.2 High-pressure oxidative leaching

High-pressure oxidative acid leaching (HPOAL) is commonly preferred over atmospheric acid leaching due to the ability to operate at elevated temperatures and oxygen overpressure. These operating conditions provide the advantages of increased reaction kinetics, enhanced metal selectivity, and the generation of stable residues [23]. HPOAL is often employed to resolve the issue of low metal extractions, slow kinetics, and excessive consumption of acid [18], as in the case of atmospheric leaching of fayalite slag. HPOAL can be tailored to operate in acidic, neutral, and alkaline pH conditions including either strongly oxidizing or reducing conditions.

Industrial applications of the high-pressure leaching technology are mostly used under challenging extraction of metals from refractory ore bodies which are often encountered in the gold industry [45]. The high-pressure acid leaching method is commonly used for the extraction of nickel and cobalt from laterite ore bodies. Leading technologies such as the CESL process and the PLATSOL™ process have been developed and used worldwide in the industry. These technologies involve the utilization of efficient pressure leaching systems to selectively extract PGM group metals, gold, and base metals from complex sulfide orebodies with good separation and immobilization of impurities such as arsenic, rendering them environmentally sound technologies [46, 47].

In the leaching of fayalite slag, the utilization of HPOAL has been found to yield good results as the presence of oxygen promotes oxidation of ferrous iron and the hydrolysis of ferric iron, resulting in zero net consumption of sulfuric acid needed for fayalite dissolution (equation 2.1)[18]. This provides a possibility to carry out leaching of fayalite slag with very dilute sulfuric acid solutions under high-pressure oxidized leaching conditions.

$$Fe_2SiO_4 + 1/2O_2 + 2H_2O \rightarrow Fe_2O_3(s) + Si(OH)_4(aq) \quad 2.1$$

High operating temperatures also promote the precipitation of stable iron solids and thus provide a very good selectivity for the valuable metals over silicon and iron [18, 33]. By maintaining a high oxygen overpressure under HPOAL, the finely dispersed metal sulfides similar to the matte in the fayalite slag, are oxidized and easily dissolved [21].

The application of the high-pressure leaching methodology has extensively been done by previous research (mine tailings, arsenic, and carbonaceous material). In those studies, our team successfully applied HPL on high impurity material and successfully extracted the metals of interest while exceptionally separating and fixing the undesirable impurities (arsenic and carbonaceous matter) with the solid residue. Similarly, with the slag, a good selectivity during leaching for the valuable metals over silicon and iron is one of the primary objectives, rendering the high-pressure leaching method the most promising technique to use.

1.7.3 Solvent Extraction

To purify the pregnant leach solution and enrich the copper concentration, the solvent extraction method is commonly preferred. The solvent extraction method is used to separate compounds or metal complexes, based on their relative solubilities in two different immiscible liquids; aqueous and organic solvent. For copper extraction, the organic solvent contains an extractant that reacts

selectively with copper over other metal cations present in the PLS, resulting in the net transfer of copper ions from the aqueous phase into the organic phase (equation 2.2) [8]. The complexation of the extractant with the Cu^{2+} ion is a process known as chelation. All other species present in the PLS are left in the aqueous phase, which is often termed the raffinate or the barren aqueous solution. To recover copper from the loaded organic, it is contacted with a strong acid, and the copper is stripped into the advanced electrolyte from which copper is electrowon (equation 2.3) [8].

The stripped organic solvent is then recycled to the extraction step, while the enriched copper solution produced is now an electrolyte suitable for electrowinning of copper. A schematic summary of the solvent extraction process is shown in figure 1.10.

Extraction: $2RH_{(org)} + Cu^{2+}_{(aq)} + SO_4^{2-}{}_{(aq)} \rightarrow R_2Cu_{(org)} + 2H^+_{(aq)} + SO_4^{2-}{}_{(aq)}$ 2.2

Organic solvent *PLS* *Loaded organic* *Raffinate*

Stripping: $R_2Cu_{(org)} + 2H^+_{(aq)} + SO_4^{2-}{}_{(aq)} \rightarrow 2RH_{(org)} + Cu^{2+}_{(aq)} + SO_4^{2-}{}_{(aq)}$ 2.3

Loaded organic *Stripping solution (180-190 g/L H_2SO_4)* *Stripped organic* *Cu-rich solution (electrolyte)*

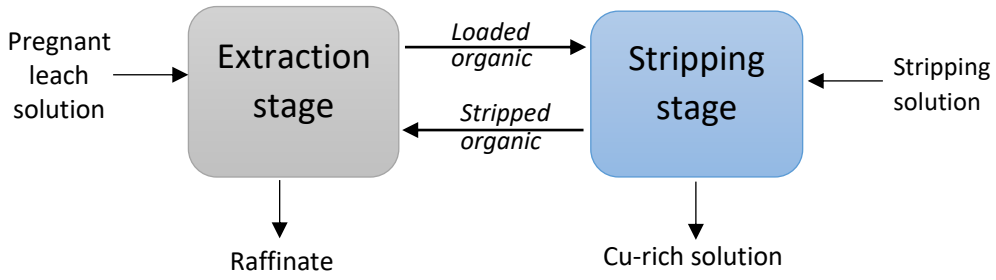

Figure 1.10: A schematic illustration of the copper solvent extraction process.

1.7.4 Selective precipitation

Selective precipitation is a technique used to separate ions of the same charge but with adequately different solubilities out of an aqueous solution by adding a dissolved reagent. Precipitation occurs when cations and anions in an aqueous solution combine to form an insoluble ionic solid called a precipitate. Solubility is defined as the maximum possible concentration of a solute in a solution at a given temperature and pressure, while the solubility product (Ksp) of the solid is the equilibrium constant for the equilibrium between a slightly soluble ionic solid and a solution of its ions [43]. When an aqueous solution contains two different cations, the lower Ksp will precipitate first, making it possible for metal ions with significantly different Ksp to be separated. The determining factors of the formation of a precipitate differ, some precipitation reactions depend on pH, and temperature, while others depend on solution concentration. The solids produced in precipitate reactions usually fall to the bottom of the solution or can be suspended throughout the solution. The precipitate can be separated from the residual solution by either filtration, centrifugation, or decantation. The principle of selective precipitation is shown in figure 1.11.

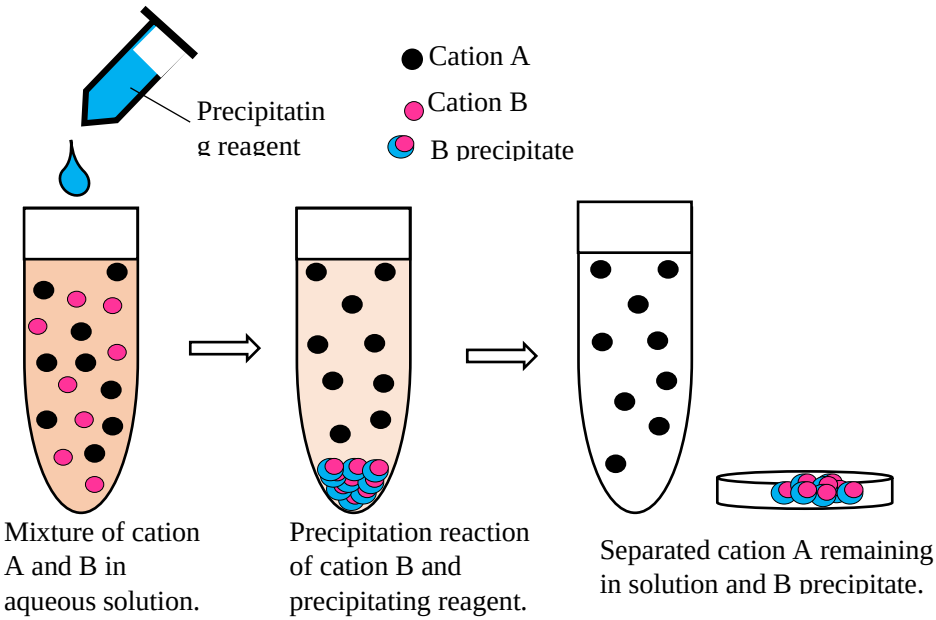

Figure 1.11: The basic principle of selective precipitation.

1.7.5 Analysis methods and formulas

All the solutions obtained, including; the PLS, the raffinate and strip solutions from the solvent extraction experiments, and the residual solutions after precipitation tests were analyzed using Agilent 4210 Microwave Plasma Atomic Emission Spectroscopy (MP-AES). About 0.3g of the solid residues were dissolved by aqua regia and also analyzed using MP-AES for residual metal content determination.

The following equations (2.4 - 2.6) were used after the leaching experiments for calculating the amount of metals extracted in the solution (equation 2.4), the metals leaching efficiency from the slag into the sulfuric acid solution (equation 2.5), and the concentration of the metals in solution (equation 2.6).

$$metal\ leached, \% = \frac{\mathrm{D.F} * \ C_M \left(\frac{mg}{L}\right) * V_L\ (L)}{m_f(g) * 1000\ \left(\frac{mg}{g}\right)} * 100 \qquad 2.4$$

$$Leaching\ efficiency, \% = \frac{\%\ \text{metal leached}}{\%\ metal\ in\ original\ sample} * 100 \qquad 2.5$$

$$Metal\ concentration\ in\ PLS, g/L = \frac{\%\ metal\ leached * \ m_f}{V_L} * 100 \qquad 2.6$$

Where D.F. is the dilution factor, C_M is the metal concentration in the PLS (mg/L), V_L is the volume of the PLS (L) and m_f is the dry mass of the slag feed (g).

For the solvent extraction and stripping experiments, equations (2.7 – 2.8) were used for calculating the amount of copper extracted into the organic solvent (equation 2.7) and the amount of copper stripped into the solution (equation 2.8).

$$Copper\ extraction\ efficiency, \% = \frac{C_{Cu_i} - C_{Cu_f}}{C_{Cu_i}} * 100 \qquad 2.7$$

Where C_{Cu_i} (g/L) is the initial concentration of copper in the PLS, while C_{Cu_f} (g/L) is the copper concentration in the raffinate solution after the extraction test.

$$Copper\ stripping\ efficiency, \% = \frac{C_{Cu-rich}}{C_{Cu-loaded}} * 100 \qquad 2.8$$

Where $C_{Cu\text{-}rich}$ (g/L) is the concentration of copper in the stripped solution (copper-rich solution), while $C_{Cu\text{-}loaded}$ (g/L) is the copper concentration in the loaded organic solution.

To calculate the precipitation efficiency, equation 2.9 was used.

$$Precipitation\ efficiency, \% = \frac{C_{sol.i} - C_{sol.f}}{C_{sol.i}} * 100 \qquad 2.9$$

Where C_{sol_i} (g/L) is the initial concentration of metal in the solution to be precipitated, while $C_{sol.f}$ (g/L) is the metal concentration in the residual solution after the precipitation test.

For solid characterization tests, that is the original slag, the solid residue obtained after leaching, and the solids obtained after precipitation tests were analyzed using an X-Ray Diffractometer (XRD, Rigaku RINT–2200V) to identify the mineral composition of the solid samples. Scanning Electron Microscope Energy Dispersive X-ray Spectrometry (SEM-EDS) was also used for the characterization of slag and the solid residues obtained after leaching.

1.8 Thesis Overview

This thesis consists of five (5) chapters, with the two main chapters being chapter 2 and 3 which fully addresses the hydrometallurgical technologies used for the process development of treating the smelter slag for metal recovery. Chapter 4 presents the important application of the developed hydrometallurgical processes to different materials for efficient metal recovery.

Chapter 1: Introduction

This chapter introduces the pyrometallurgical production of nickel, and copper from sulfide nickel ore, including the description of the smelting process that results in the generation of slag as a waste product. A worldwide current situation regarding the production statistics and predicted data is outlined. Slag is explained and how metal losses are incurred in slag. Environmental consequences due to discarded slag are demonstrated. The importance of re-processing slag is outlined, as well as the objective of this research.

Chapter 2: Direct atmospheric leaching (AL) and high-pressure oxidative acid leaching (HPOAL) of slag

This chapter mainly discusses the results of atmospheric leaching and high-pressure leaching of slag. The characterization of the electric furnace slag sample is illustrated using XRF, XRD, and SEM-EDS. The HPOAL method was extensively explored over atmospheric acid leaching due to its ability to operate at elevated temperatures and oxygen overpressure. Due to the inevitable dissolution of fayalite, high operating temperatures promote the precipitation of stable iron solids from the solution and thus provide a very good selectivity for the valuable metals (Cu, Ni, and Co) recovery in the pregnant leach solution over precipitated impurities of silicon and iron. With a

high oxygen overpressure under HPOAL, the finely dispersed metal sulfides in the fayalite slag, are oxidized and easily dissolved at a lower acid consumption. Various leaching parameters such as sulfuric acid concentration, temperature, oxidant concentration/total pressure, and leaching time were investigated. Under atmospheric leaching, the sulfuric acid concentration was investigated in the range of 0 (distilled water)–1.0 M, the leaching temperature 30–90 °C, and the leaching time 30–120 minutes. The stirring speed and pulp density were kept constant at 700 rpm and 100 g/L, respectively. The effect of oxidant addition was also investigated using hydrogen peroxide (H_2O_2) and its concentration ranged between 0.2–0.6 M. Under HPOAL, the slag particle size was investigated in the range of 45–212 µm, the sulfuric acid concentration was varied between 0.2–1.0 mol/L, and the pulp density was adjusted between 100–300 g/L. The stirring speed, leaching time, and temperature were varied in the ranges of 300–900 rpm, 0.5–2.0 hr, and 120–180 °C, respectively. The oxygen (O_2) gas was injected into the slurry vessel at a controlled total pressure of 0.6 – 1.5 MPa. From the leaching results, the leaching behavior and the dissolution mechanism of slag are discussed. Finally, leach residue elution tests were performed to understand its leaching behavior properties and evaluate its environmental stability.

Chapter 3: Selective separation of metals from leach liquor by solvent extraction, precipitation, and xanthate complexation.

The objective of this chapter is to illustrate the separation process developed to selectively separate metal ions of Ni, Cu, Co, and Fe from the pregnant leach solution (PLS) using various separation and enrichment techniques. Three hydrometallurgical processes of solvent extraction (SX), precipitation, and xanthate complexation processes are discussed in this chapter. The solvent extraction method was mainly used to separate copper from other metals (Ni, Co) and impurities (Fe, etc.) as well as upgrade the copper concentration in the PLS obtained from the HPOAL of the smelter slag. Solvent extraction is an important step in generating an electrolyte of high quality

that can be electrowon to produce pure copper. A countercurrent two-stage mixer settler extraction column was utilized. Fundamental parameters influencing the extraction process such as pH, mixing speed, H_2SO_4 concentration, and organic/aqueous (O/A) phase ratio were investigated. For copper enrichment in solution, a combination of two extraction stages and two stripping stages were employed. Furthermore, selective precipitation techniques were used to treat the raffinate solution for iron removal by the addition of calcium carbonate ($CaCO_3$) suspension followed by the addition of potassium amyl xanthate (PAX) solution for co-precipitation of Ni and Co as xanthate precipitates. Selective precipitation is known to have good selectivity for metal removal, fast reaction rates, and low solubility of the precipitated compound. Iron impurity in solution, which is known to have detrimental effects on the upstream processes and therefore was removed by selective precipitation from the solution. The xanthate complexation method displayed an effective route to separate nickel and cobalt from solution due to the strong hydrophobic properties of nickel and cobalt xanthates and the different solubility constant product (Ksp) between nickel xanthate and cobalt xanthate. Lastly, nickel was separated from cobalt by selective dissolution of nickel xanthate using ammonia solution while the remaining cobalt xanthate precipitate was roasted and Co recovered as CoO powder.

Chapter 4: Application of high-pressure leaching processes to mine tailings and complex carbonaceous sulfide ore.

This chapter presents the application of high-pressure leaching (HPL) technology to extract valuable metals from other metallurgical waste material (flotation tailings) and a complex ore of high impurity content (complex carbonaceous sulfide ore). The high-pressure leaching technology operated at high temperatures and elevated oxygen overpressure provides the possibility of high metal extractions and the generation of stable residues for sustainable mining. The HPL method was efficiently used to treat the flotation tailings to convert the AMD supporting minerals to more

stable forms, for reduction of environmental loading while simultaneously valorizing the mine tailings. A combination of other hydrometallurgical processes of solvent extraction (SX) and electrowinning (EW) was utilized to recover copper from mine tailings. On the other hand, complex carbonaceous sulfide ores are extremely difficult to treat due to their mineralogical complexity and impurities of organic carbon and carbonates. High-pressure leaching of complex carbonaceous sulfide ore in oxygenated sulfuric acid solution was performed, and the highest copper extraction achieved was 97.55%. Free acidity analysis through titration of the leaching medium and the pregnant leach solution showed that selective dissolution/separation of copper and iron can be achieved through efficient control of free acidity in the pregnant leach solution. Such a relationship is important as it allows for the determination of H_2SO_4 consumption, especially when dealing with carbonate minerals.

Chapter 5: Conclusion

This chapter provides a summary of the major findings of the previous chapters. An overall process flow chart of the developed hydrometallurgical process for recovery of valuable metals from slag is presented.

References

1. Khoday T., (2019), Nickel base metals, Accessed 2 December 2021, https://fyers.in/school-of-stocks/chapter/commodities/nickel.html
2. Geology.com, Facts About Nickel, Nickel Uses, Resources, Supply, Demand, and Production Information, Republished from USGS Fact Sheet from March 2012, Accessed 2 December 2021, https://geology.com/usgs/uses-of-nickel/
3. Metalpedia, Nickel use, Accessed 2 December 2021, http://metalpedia.asianmetal.com/metal/nickel/application.shtml
4. Handbook of Extractive Metallurgy 1997, Edited by Fathi Habashi Volume II: Primary Metals Secondary Metals Light Metals, GQ WILEY-VCH, Germany.
5. Sawe, B.E. (2018) Top 10 Nickel Consuming Countries, https://www.worldatlas.com/articles/top-10-nickel-consuming-counties.html
6. Huang, F., et al., Selective recovery of valuable metals from nickel converter slag at elevated temperature with sulfuric acid solution. Separation and Purification Technology, 2015. 156: p. 572-581.
7. Marsh, A.T.M., Yang, T., Adu-Amankwah, S., and Bernal, S.A. (2021), Utilization of metallurgical wastes as raw materials for manufacturing alkali-activated cements, Woodhead Publishing Series in Civil and Structural Engineering, Waste and Byproducts in Cement-Based Materials, Woodhead Publishing, 335-383, https://doi.org/10.1016/B978-0-12-820549-5.00009-7
8. Schlesinger, M.E., King, M.J., Sole, K.C., and Davenport, W.G., (2011), Extractive metallurgy of copper, 5th Edition, Oxford, UK: Elsevier pg. 252 – 256.
9. Muravyov, M.I., et al., Leaching of copper and zinc from copper converter slag flotation tailings using H_2SO_4 and biologically generated $Fe_2(SO_4)_3$. Hydrometallurgy, 2012. 119-120: p. 40-46.

10. Davenport, W. G., King, M., Schlesinger, M., and Biswas, A. K. (2002). Extractive Metallurgy of Copper, 4th edition: Oxford, UK: Elsevier.
11. Zhang, T., et al., Alkali Activation of Copper and Nickel Slag Composite Cementitious Materials. Materials (Basel), 2020. 13(5).
12. Gorai, B., R.K. Jana, and Premchand, Characteristics and utilization of copper slag—a review. Resources, Conservation and Recycling, 2003. 39(4): p. 299-313.
13. Desjardins, J., (2017). Cobalt: A Precarious Supply Chain, Visual Capitalist, https://www.visualcapitalist.com/cobalt-precarious-supply-chain/
14. Flanagan, D., (2021). Copper statistics and information, USGS-National Minerals Information Center, https://www.usgs.gov/centers/nmic/copper-statistics-and-information
15. Herford, S., G. (2001). Entropy production as a measure for resource use [doctoral dissertation], University of Humburg, https://www.researchgate.net/publication/33957903_Entropy_production_as_a_measure_for_resource_use_Elektronische_Ressource_method_development_and_application_to_metallurgical_processes
16. Imris, I., Sanchez, M., and Achurra, G. (2004). Copper losses to slags obtained from the El Teniente process. VII International Conference on Molten Slags Fluxes and Salts, The South African Institute of Mining and Metallurgy, 2004.
17. Potysz, A., B. Mikoda, and M. Napieraj, (Bio)dissolution of Glassy and Diopside-Bearing Metallurgical Slags: Experimental and Economic Aspects. Minerals, 2021. 11(3).
18. Perederiy, I., (2011). Dissolution of Valuable Metals from Nickel Smelter Slags by Means of High-pressure Oxidative Acid Leaching [doctoral dissertation], Graduate Department of Chemical Engineering and Applied Chemistry, University of Toronto.
19. Ettler, V., Soil contamination near non-ferrous metal smelters: A review. Applied Geochemistry, 2016. 64: p. 56-74.

20. Motswaiso, F.S., et al., Geochemical Investigation of Metals and Trace Elements around the Abandoned Cu-Ni Mine Site in Selibe Phikwe, Botswana. Journal of Geoscience and Environment Protection, 2019. 07(05): p. 275-293.
21. Baghalha, M., V.G. Papangelakis, and W. Curlook, Factors affecting the leachability of Ni/Co/Cu slags at high temperature. Hydrometallurgy, 2007. 85(1): p. 42-52.
22. M Stroud, M Bogopa, D C Keitshokile, G Dzinomwa, (2009). BCL sulphur capture options, The Southern African Institute of Mining and Metallurgy Base Metals Conference, Kasane, Botswana.
23. Godirilwe, L.L., et al., Copper Recovery and Reduction of Environmental Loading from Mine Tailings by High-Pressure Leaching and SX-EW Process. Metals, 2021. 11(9).
24. Piatak, N.M., M.B. Parsons, and R.R. Seal, Characteristics and environmental aspects of slag: A review. Applied Geochemistry, 2015. 57: p. 236-266.
25. Pollution issues, Smelting. Accessed 3 December 2021 http://www.pollutionissues.com/Re-Sy/Smelting.html#ixzz7DysWPUAS
26. Mudd, G.M., Global trends, and environmental issues in nickel mining: Sulfides versus laterites. Ore Geology Reviews, 2010. 38(1-2): p. 9-26.
27. Henckens, M.L.C.M. and E. Worrell, Reviewing the availability of copper and nickel for future generations. The balance between production growth, sustainability and recycling rates. Journal of Cleaner Production, 2020. 264.
28. Zhang, H., et al., Recovery of Iron from Copper Slag Using Coal-Based Direct Reduction: Reduction Characteristics and Kinetics. Minerals, 2020. 10(11).
29. Oxley, A., M.E. Smith, and O. Caceres, Why heap leach nickel laterites? Minerals Engineering, 2016. 88: p. 53-60.
30. Bulut, G., et al., Recovery of metal values from copper slags by flotation and roasting with pyrite. Mining, Metallurgy & Exploration, 2007. 24(1): p. 13-18.

31. Altundogan, H.S., Tiimen, F., 1997. Metal recovery from copper converter slag by roasting with ferric sulfate. Hydrometallurgy 44, 26 l-267. https://doi.org/10.1016/S0304-386X(96)00038-2
32. Nadirov, R.K., et al., Recovery of value metals from copper smelter slag by ammonium chloride treatment. International Journal of Mineral Processing, 2013. 124: p. 145-149.
33. Yang, Z., Rui-lin, M., Wang-dong, N., Hui, W., 2010. Selective leaching of base metals from copper smelter slag. Hydrometallurgy 103, 25–29. https://doi.org/10.1016/j.hydromet.2010.02.009
34. Dimitrijevic, M., et al., Dissolution of copper from smelting slag by leaching in chloride media. Journal of Mining and Metallurgy, Section B: Metallurgy, 2017. 53(3): p. 407-412.
35. Altundogan, H.S., M. Boyrazli, and F. Tumen, A study on the sulfuric acid leaching of copper converter slag in the presence of dichromate. Minerals Engineering, 2004. 17(3): p. 465-467.
36. Boyrazli, M., H.S. Altundogan, and F. Tumen. Recovery of metals from copper converter slag by leaching with $K_2Cr_2O_7$-H_2SO_4. Canadian Metallurgical Quarterly, 2006. 45(2): p. 145-152.
37. Banza, A.N., Gock, E., Kongolo, K., 2002. Base metals recovery from copper smelter slag by oxidizing leaching and solvent extraction. Hydrometallurgy 67, 63–69.
38. Aracena, A., et al., Converter slag leaching in ammonia medium/column system with subsequent crystallization with NaSH. Hydrometallurgy, 2019. 188: p. 31-37.
39. Li, Y., V.G. Papangelakis, and I. Perederiy, High-pressure oxidative acid leaching of nickel smelter slag: Characterization of feed and residue. Hydrometallurgy, 2009. 97(3-4): p. 185-193.
40. Anand, S., Sarveswara Rao, K., Jena, P.K., 1983. Pressure leaching of copper converter slag using dilute sulfuric acid for the extraction of cobalt, nickel, and copper values. Hydrometallurgy 10 (3), 305–312. https://doi.org/10.1016/0304-386X(83)90061-0

41. Perederiy, I. and V.G. Papangelakis, Why amorphous FeO-SiO_2 slags do not acid-leach at high temperatures. J Hazard Mater, 2017. 321: p. 737-744.
42. Li, Y., I. Perederiy, and V.G. Papangelakis, Cleaning of waste smelter slags and recovery of valuable metals by pressure oxidative leaching. J Hazard Mater, 2008. 152(2): p. 607-15.
43. Chemistry-LibreTexts. Precipitation and the Solubility Product. (2020, August 15). https://chem.libretexts.org/@go/page/41632
44. Malema M.T. and Legg A.C., Recent Improvements at the BCL Smelter, Southern African Pyrometallurgy 2006, Edited by R.T. Jones, South African Institute of Mining and Metallurgy, Johannesburg, 5-8 March 2006.
45. Sikka, P. SNC-Lavalin Group (2022). Under Pressure and Feeling the Heat: Autoclave Technology at the Heart of the Metal Extraction Process. Accessed 14 May 2022. https://www.snclavalin.com/en/beyond-engineering/underpressure-and-feeling-the-heat
46. Mayhew, K., McCoy, T., and Mean, R. Teck's CESL Copper Process: A Commercial Ready Concentrate Leach Alternative, Teck Resources Limited, Canada. Accessed 14 May 2022. https://www.teck.com/media/CESL-Publication-Copper-teck-cesl-process.pdf
47. SGS. (2013). Pressure Leaching Capabilities. SGS Minerals Services – T3 SGS 174, Accessed 14 May 2022. https://www.sgs.com/-/media/global/documents/flyers-and-leaflets/sgs-min-wa053-pressure-leaching-en-11.pdf

Chapter 2. Direct atmospheric leaching (AL) and high-pressure oxidative acid leaching (HPOAL) of slag

This chapter mainly discusses the results of atmospheric leaching and high-pressure leaching of slag. The characterization of the electric furnace slag sample is firstly illustrated. From the leaching results, the leaching behavior and the dissolution mechanism of slag are discussed. The HPOAL method was extensively explored over atmospheric acid leaching due to its ability to operate at elevated temperatures and oxygen overpressure. Due to the inevitable dissolution of fayalite, high operating temperatures promote the precipitation of stable iron solids from the solution and thus provide a very good selectivity for the valuable metals (Cu, Ni, and Co) recovery in the pregnant leach solution over precipitated impurities of silicon and iron. By maintaining a high oxygen overpressure under HPOAL, the finely dispersed metal sulfides in the fayalite slag, are oxidized and easily dissolved at a lower acid consumption. Finally, leach residue elution tests were performed to understand its leaching behavior properties and evaluate its environmental stability.

2.1 Slag Characterization

The slag sample was obtained from the copper-nickel mine in Botswana. The sample was formed through granulation of the electric arc furnace slag melt in water resulting in a glassy material. The slag characterization studies and mineralogical analysis included methods such as X-ray diffraction (XRD) to identify crystalline phases present in slag sample, XRF (X-ray fluorescence) spectrometry (Rigaku ZSX Primus II), and Agilent 4210 MP-AES (Microwave Plasma Atomic Emission Spectroscopy) was used to determine the elemental and chemical composition of the

slag. Additionally, SEM-EDS (Scanning Electron Microscope-Energy Dispersion Spectroscopy) was used to characterize slag.

2.1.1 Size Analysis

The size analysis was done on the original slag sample and the particle size distribution curve is shown in figure 2.1. The size screening was done using a sieve shaker (AS200 digit, Retsch Japan Co., Ltd) in six size fractions: -250 µm, +250 –500 µm, +500 –850 µm, +850 –1000 µm, +1000 –1700 µm, and +1700 µm. The slag particle size ranged from 0.25 to 3.0 mm and the cumulative percentage passing at 80% (P_{80}) was about 2.3 mm.

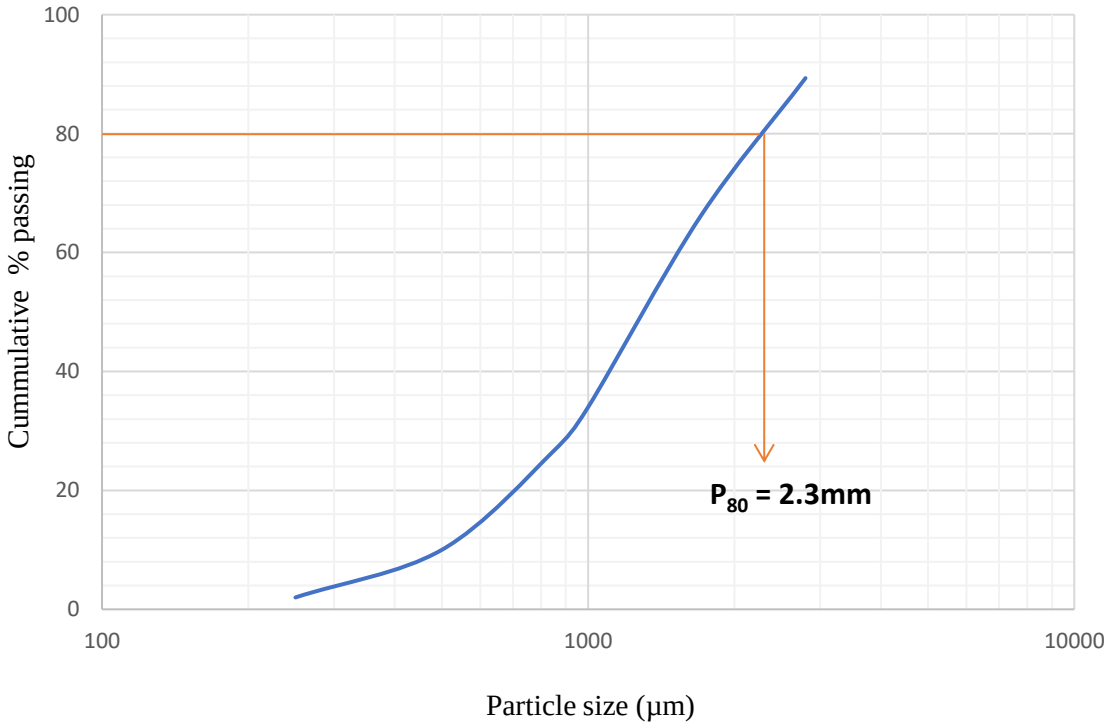

Figure 2.1: The size distribution curve of the electric furnace slag sample.

2.1.2 XRD Analysis

The slag sample was analyzed using XRD (Rigaku Miniflex) (figure 2.2), which showed that the dominant mineral composition of the slag is fayalite. The slag sample is amorphous, as demonstrated by a very high background of the XRD pattern. The presence of the glass phase is known to raise the background in the XRD pattern [11]. Several authors also confirmed that molten slags which are quenched in water produce an amorphous structure [5, 6, 9, 11]. Gabasiane et. al (2021) [12] did mineralogical characterization studies on the BCL mine's copper-nickel slag sample and quantified that more than 80% content is of amorphous structure, through the addition of an internal standard. The sulfide phase could not be detected by the XRD analysis.

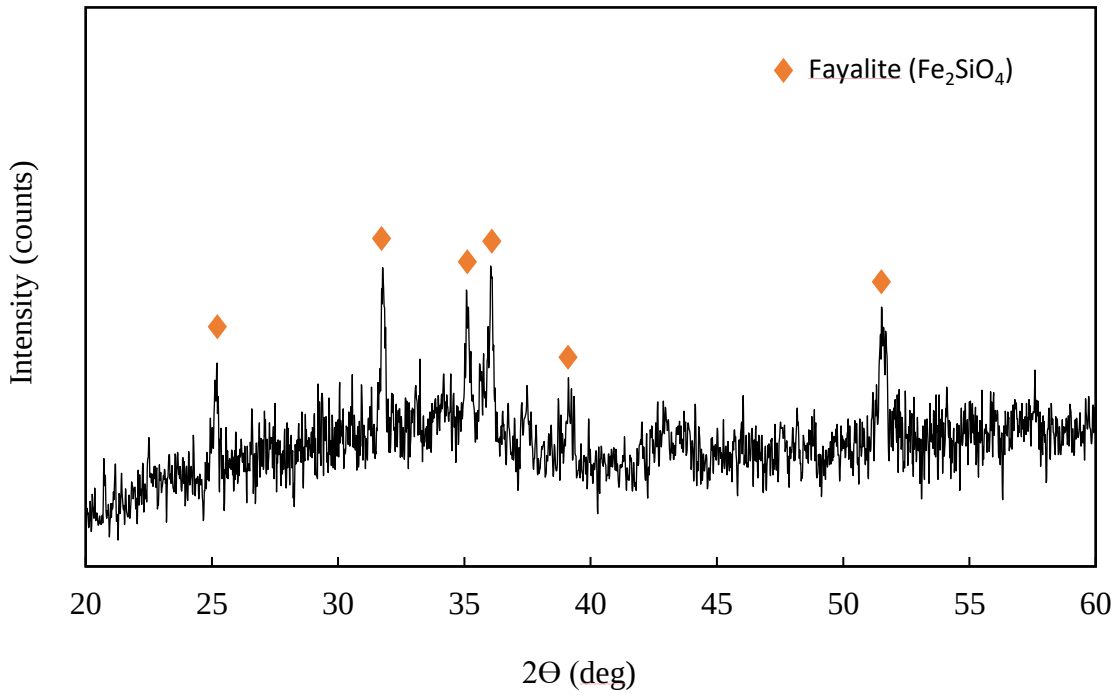

Figure 2.2: XRD pattern of the slag sample

2.1.3 XRF Analysis

Table 2.1. shows the slag composition as determined by XRF. The chemical composition of slag was further confirmed by aqua regia followed by analysis with MP-AES for Fe, Cu, Ni, and Co content, and the results are displayed in Table 2.2. The XRF results show that the most abundant element is iron at 38.7 wt.% followed by silicon at 13.3 wt.%, while the content of valuable metals of interest (nickel, copper, and cobalt) was measured to be 0.36, 0.36, and 0.17 wt.% respectively. Piatak et. al 2015 [11] also noted that the composition of non-ferrous slag, especially from base-metal production, is dominated by Fe and Si with significant but lesser amounts of Al and Ca. The slag does not contain high concentrations of potentially toxic elements such as As, Cd, Pb, and Zn, the only detected toxic elements were Zn and Pb at concentrations of 0.05 and 0.01 wt.% respectively.

Table 2.1: XRF analysis of slag composition (wt.%)

Fe	Si	Ni	Cu	Co	Al	Mg	Ca	S	Cr	Na	K
38.7	13.3	0.36	0.36	0.17	3.26	1.96	1.98	0.64	0.18	0.63	0.72

Table 2.2: Chemical composition of slag by MP-AES analysis (wt.%)

Fe	Ni	Cu	Co
32.14	0.29	0.288	0.109

2.1.4 SEM Observation

Figure 2.3 shows SEM micrographs of the slag particles, showing entrapped matte (MeSx) where Me can either be Ni, Cu, and/or Co. The matte which is the sulfide phase appears as visible bright dots (light grey), occurring as fine occlusions in the fayalite phase (dark grey). The majority of the matte spots appear to be locked in the fayalite phase, numerous sulfide dots are less than 10 μm in diameter and only a few about 50 μm. Bimodal size distribution of the sulfide spots on the slag

sample showed that about 75% of the sulfides occur as particles of less than 20 μm while about 15% occur as particles of greater than 60 μm [13]. According to Letswalo and Martin (2018) [13], the amount of liberated sulfides in the slag is approximately 12%, so more than 80% is locked in the fayalite phase, suggesting that concentration by flotation may not be an efficient method due to fine milling (<20 μm) of the slag that will be required to achieve a good sulfides liberation.

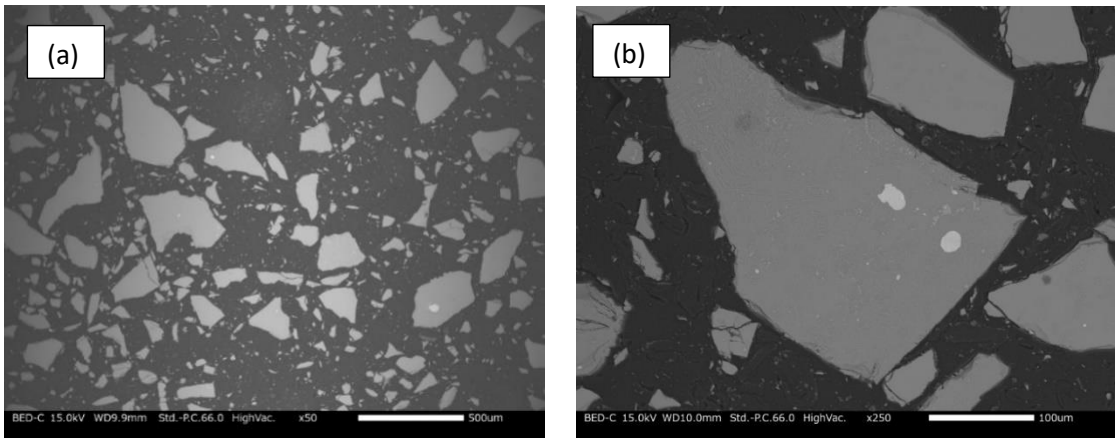

Figure 2.3: SEM images of the granulated slag sample from a copper-nickel smelter. The images show the sulfide spots (bright grey), hosted in the fayalite phase (dark grey) mounted in epoxy resin (black).

Figure 2.4 shows the SEM image (a) and EDX spectrums (b)-(d) at different areas of the slag sample. The four main mineral phases detected in the slag were; fayalite (Fe_2SiO_4), chromite ($FeCr_2O_4$), matte (MeS_x), and magnetite (Fe_3O_4). The large dark grey area is fayalite. The bright grey spot around 60 μm in diameter and other similar small dots 2-5 μm in diameter were identified as entrapped matte droplets as confirmed by the EDX spectrum in Fig. 2.4 (c). The matte phase was predominantly rich in nickel as compared to copper and cobalt as seen by very strong peaks of nickel and small peaks for copper and cobalt as seen on the EDX spectrum for matte Fig. 2.4 (c). Iron was also detected in the EDX spectrum of the matte phase, confirming the findings of Gabasiane et. al (2021) [12] that the sulfide occurs as Fe–Ni–sulfide and Fe–Cu sulfide. The gray

structures forming a texture on the fayalite phase were identified as chromite phases. Significant counts of aluminum and magnesium appeared in the fayalite and chromite phases as shown in the EDX spectrum in Fig. 2.4 (a) and (d). Magnetite was identified with the EDX spectrum, appearing as light-grey dots in figure 2.4 (a).

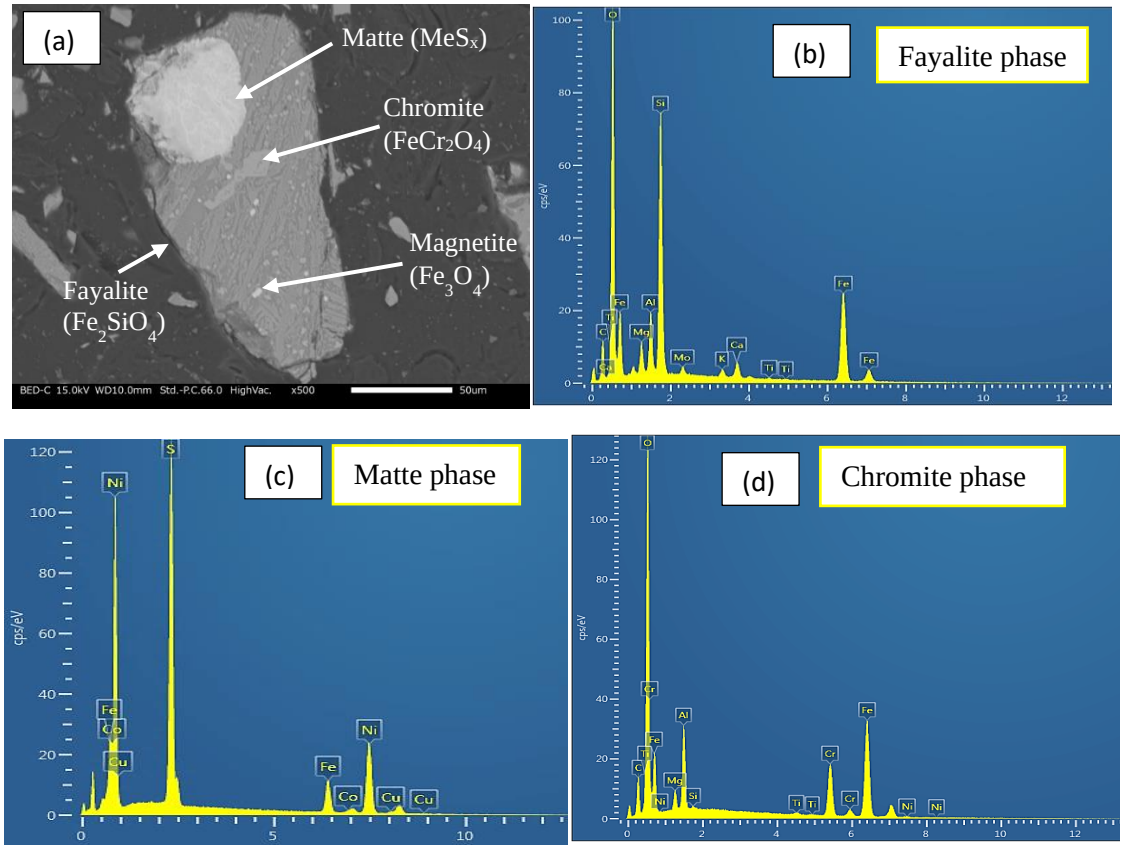

Figure 2.4: SEM image of the granulated slag sample from a copper-nickel mine, with the respective EDX spectrums.

Elemental mapping of SEM-EDS observation of granulated electric furnace slag is shown in figure 2.5. Nickel and copper exist in the slag as sulfides and occur as dispersed spherical matte inclusions while cobalt exists predominantly in the oxide form and is in the homogenous distribution in the fayalite phase. Several authors also found that typical slags from nickel and

copper smelters contain Ni and Cu mostly in the form of sulfide while Co exists in the oxide form [1, 6, 12, 14]. Magnesium and calcium are mostly associated with oxygen while aluminum is very dilute in the oxide phase with a few intensified spots liberated from the fayalite. Perederiy (2011) [1] concluded that aluminum may exist as aluminum silicate rather than dissolved oxide. An average of four spot analyses on the sample using EDX generated information showed that the elemental compositions of sulfide areas were estimated to be; 50 wt.% S, 12-25 wt.% Fe, and 20-40 wt.% Ni. The Cu content was below the detection limit in the EDX summary of the sulfide spots analysis, even though figure 2.5 confirmed that Cu is present in the sulfide phase. The elemental compositions in the chromite phase were estimated to be; 45-60 wt.% Fe, 30 wt.% O, 4-15 wt.% Cr, 8 wt.% Al, and 1 wt.% Mg. The elemental compositions in the fayalite phase were estimated to be; 38 wt.% Fe, 35 wt.% O, 18 wt.% Si, 5 wt.% Al and 3 wt.% Mg, 2 wt.% Ca, and 1 wt.% K. The elemental composition of the fayalite phase was found to be homogenous at various spot analyses.

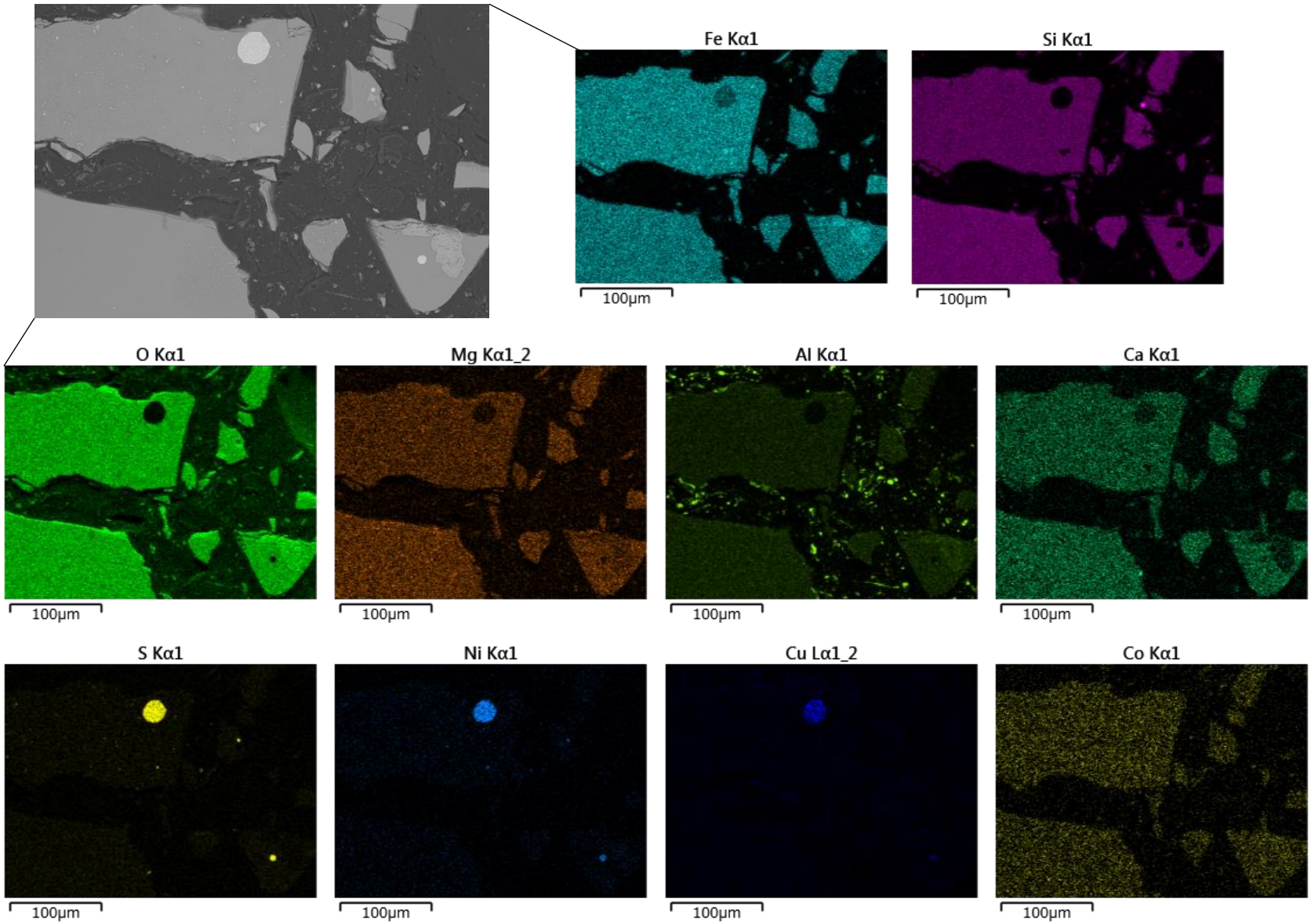

Figure 2.5: Elemental mapping of SEM-EDS observation of granulated electric furnace slag.

2.2 Atmospheric leaching

This chapter focuses on the atmospheric beaker leaching of the electric furnace granulated slag. Atmospheric leaching is an economical way and widely applicable method to explore especially in areas of low technological advancement for the extraction of valuable metals from waste materials such as slag. The effect of acid concentration, temperature, leaching time, and oxidant addition are discussed.

2.2.1 Experimental procedure

Atmospheric beaker leaching experiments were conducted in a 100 ml conical flask placed on a heating magnetic stirrer (HSH-6D, As One) using sulfuric acid. A ground slag sample (<250 µm) was mixed with distilled water and sulfuric acid solution to achieve a pulp density of 100 g/L for all the experiments. The sulfuric acid concentration was investigated in the range of 0 (distilled water) and 1.0 M, the stirring speed was kept constant at 700 rpm, the leaching temperature 30–90 ^{o}C, and the leaching time 30–120 minutes respectively. The effect of oxidant addition was also investigated using hydrogen peroxide (H_2O_2) and its concentration ranged between 0.2–0.6 M. A summary of the leaching conditions is displayed in table 2.3. The obtained slurry was filtered to separate the pregnant leach solution (PLS) from the solid residue after leaching. The PLS was analyzed using 4210 MP-AES (Agilent), while the solid residue was analyzed using X-Ray Diffractometer (XRD, Rigaku RINT–2200V) to identify the mineral composition of the solid samples. About 0.3g of the solid residue was dissolved by aqua regia and analyzed using MP-AES for residual metal content determination.

Table 2.3: A summary of the atmospheric beaker leaching conditions

Atmospheric Leaching Conditions	
Pulp density	10% solids
Temperature	30 – 90 °C
Sulfuric acid concentration	0 – 1.0 M
Leaching time	30 – 120 min
Stirring speed	700 rpm
Hydrogen peroxide concentration	0.2 – 0.6 M

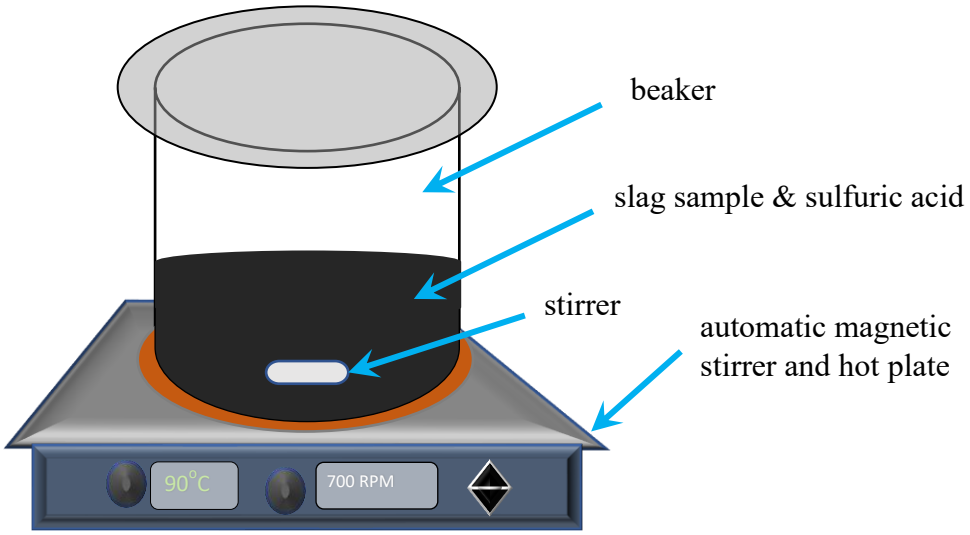

Figure 2.6: Schematic setup of atmospheric leaching of slag.

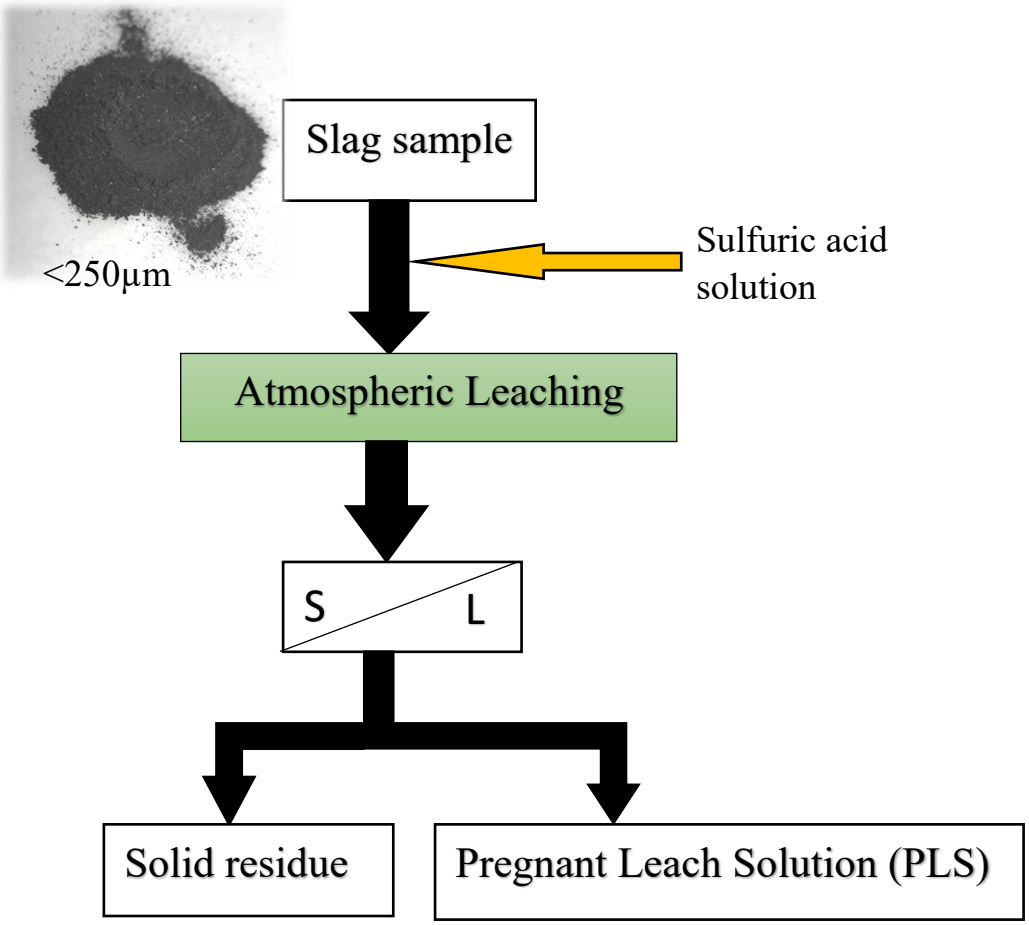

Figure 2.7: Illustrative process of atmospheric leaching.

2.2.2 Results and Discussion

2.2.2.1 Effect of sulfuric acid concentration

Figure 2.8 shows the effect of sulfuric acid concentration (0 M(water) – 1.0 M) on metal dissolution from the slag. The temperature, leaching time, pulp density, and stirring speed were kept constant at 65 °C, 60 minutes, 100 g/L, and 700 rpm respectively. As the sulfuric acid concentration increased, the metal dissolution moderately increased. Copper attained a 69% dissolution, while Ni and Co dissolutions were low at 19.5 % and 28.5% respectively. The low metal dissolutions are mostly because of their existence in sulfide form which will require oxygen to leach. Unfortunately, Fe dissolution was the highest at 85% because atmospheric

beaker leaching has poor selectivity and thus the majority of acid consumption is to dissolve the fayalite (equation 2.1), resulting in a high Fe concentration and silicic acid [4, 6].

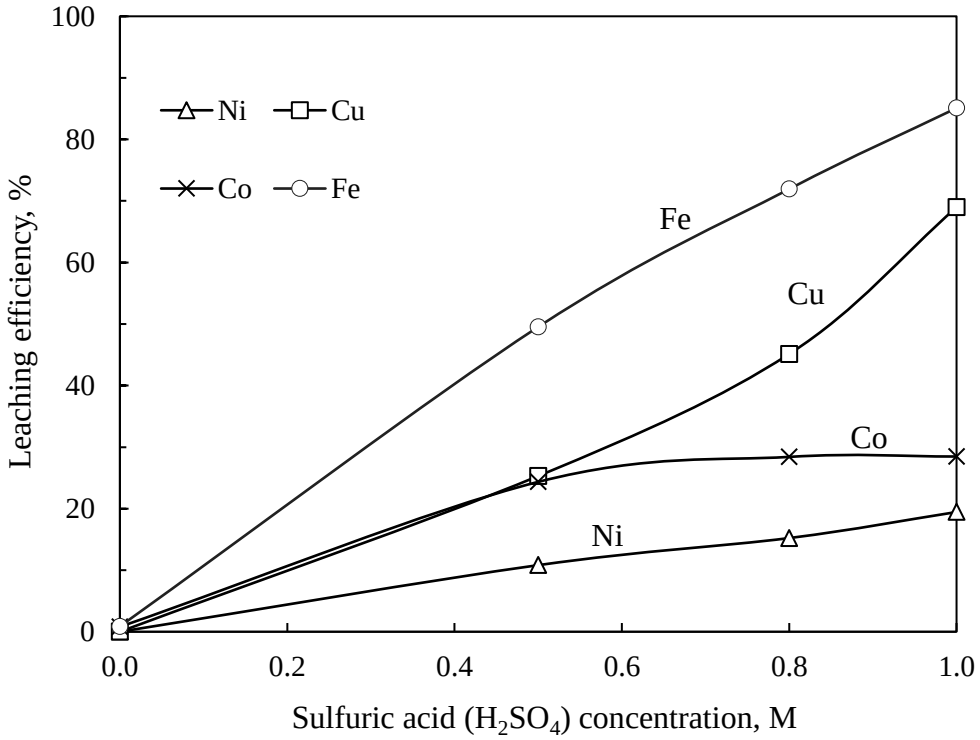

Figure 2.8: Metals dissolution profiles versus H_2SO_4 concentration: temperature 65 °C, leaching time 60 minutes, pulp density 100 g/L, and stirring speed 700 rpm.

$$Fe_2SiO_4\ (s) + 4H^+ \rightarrow 2Fe^{2+} + Si(OH)_4\ (aq) \qquad (2.1)$$

(Me = Ni, Cu or Co)

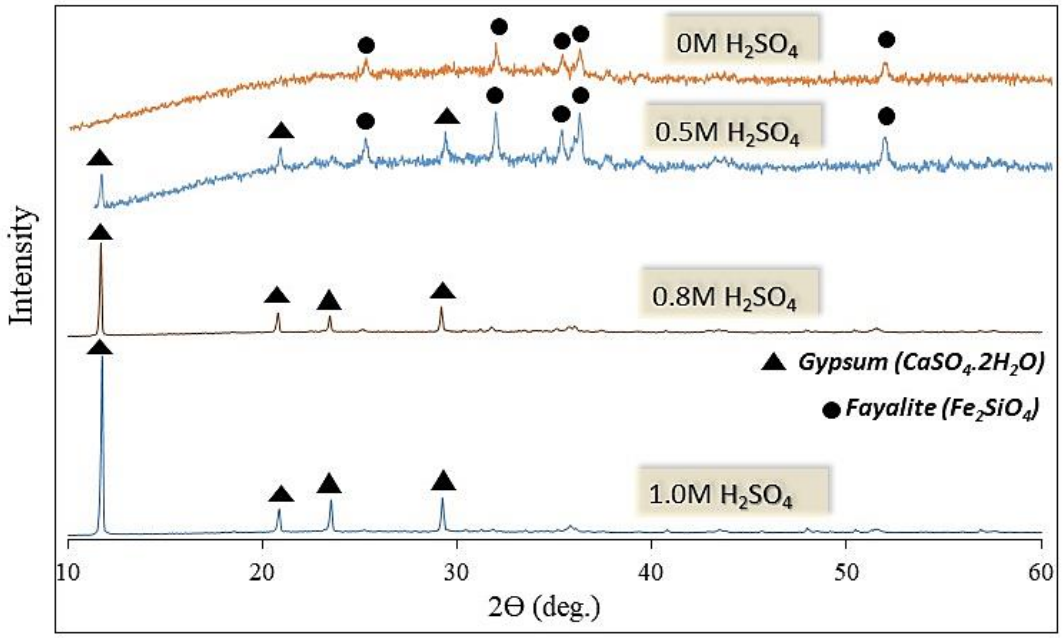

Figure 2.9: XRD patterns of residues obtained after atmospheric beaker leaching; temperature 65 °C, leaching time 60 minutes, pulp density 100 g/L, and stirring speed 700 rpm.

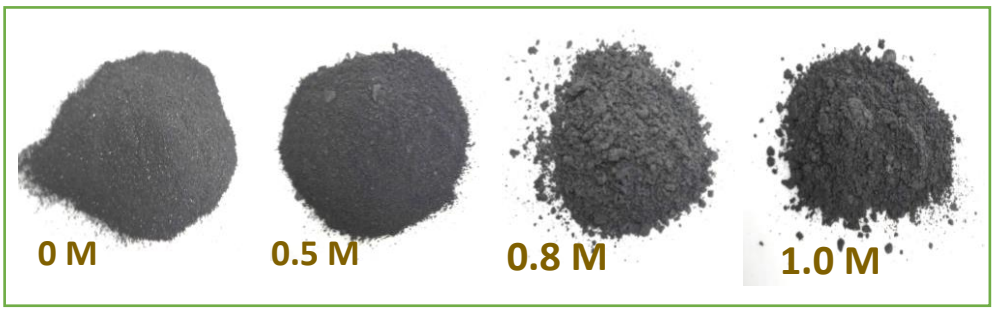

Figure 2.10: Residues obtained after atmospheric beaker leaching at different sulfuric acid concentrations.

Higher sulfuric acid concentrations above 1 M could not be effectively investigated due to increased slurry density during leaching, making it difficult to agitate or filter. The gel-like slurry which resulted has been noted by other scholars [2 – 5] as colloidal silica which forms by polymerization of silicic acid generated by equation 2.1 [4]. Banza et al. (2002) [5] noted that due to the amorphous structure of slag, the formation of silica gel hinders efficient leaching with sulfuric acid. They solved this challenge successively by leaching smelter slag with sulfuric acid under hydrogen peroxide, which simultaneously removed iron by oxidation.

Figure 2.9 shows the XRD analysis conducted on the residues obtained from leaching slag at different sulfuric acid concentrations. The main constituent in all the residues was gypsum while at low sulfuric acid concentrations (0 M(water) – 0.5 M), undissolved fayalite was observed.

2.2.2.2 Effect of temperature

The effect of temperature was investigated from 30 – 90 °C on metal dissolution from the slag and the results are shown in Figure 2.11. The H_2SO_4 concentration, leaching time, pulp density, and stirring speed were kept constant at 1 M, 60 minutes, 100 g/L, and 700 rpm respectively. The highest copper dissolution of 69% was achieved at 65 ^oC, a further increase in temperature resulted in a decreased copper leaching efficiency due to the formation of silica gel. At high temperatures, the stability of silicic acid is decreased, and there is an increased rate of re-polymerization resulting in the excess formation of silica gel [9], which closes pores and prevents further slag dissolution. Banza et. al (2002) [5] also found that filtration of the resulting pulp from the leaching at higher temperatures was very difficult due to the presence of silica gel. Therefore, the temperature is an important parameter to control during slag leaching as confirmed by other scholars [7, 8, 10]. The dissolution of nickel slightly increased as the temperature was increased but remained low with a high of 26.4% at 90 °C. On the other hand, the dissolution of cobalt sharply increased from 28.5% to 68.6% as the temperature increased from 65 °C to 90°C. A slight decrease in iron dissolution was observed as the temperature was increased, so it may be possible to minimize iron co-dissolution by leaching at high temperatures, however, this may be challenging under atmospheric conditions while maintaining the stability of silicic acid to prevent its re-polymerization into silica gel.

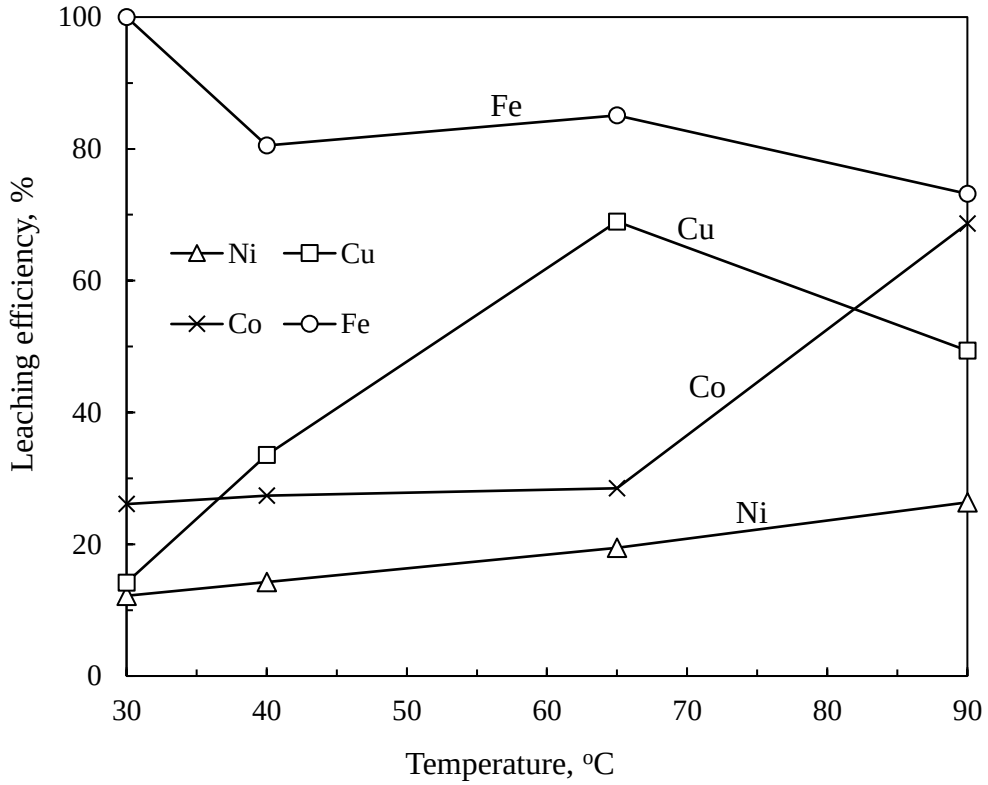

Figure 2.11: Metals dissolution profiles versus temperature: H_2SO_4 concentration 1 M, leaching time 60 minutes, pulp density 100 g/L, and stirring speed 700 rpm.

2.2.2.3 Effect of leaching time

The effect of leaching time was investigated on the dissolution of metals from the slag (figure 2.12). The sulfuric acid concentration was kept constant at 1 M, while temperature, pulp density, and stirring speed were 65 °C, 100 g/L, and 700 rpm respectively. Copper dissolution gradually increased with the increase in leaching time showing the known slow kinetics of copper conversion. Ni and Co dissolution constantly remained low (Ni below 20%, Co below 30%), and showed no effect when the leaching time was increased. The easy leachability of Fe in an acidic medium was confirmed by a high dissolution of Fe well above 80% irrespective of the leaching time.

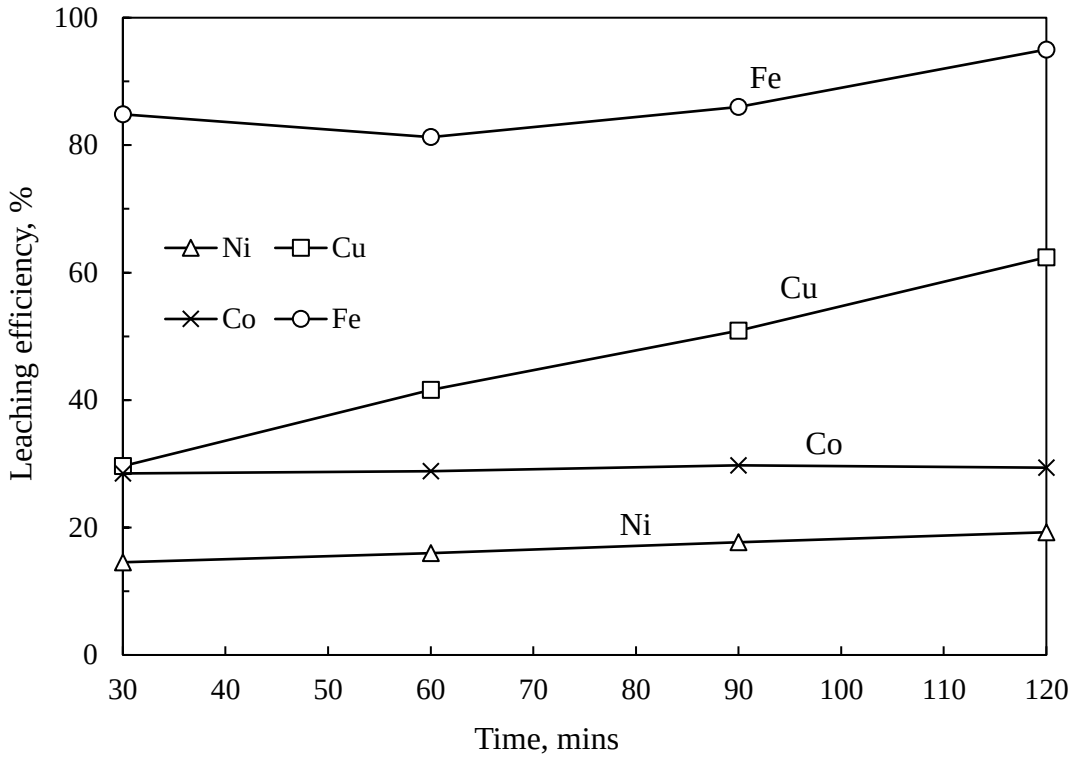

Figure 2.12: Metals dissolution profiles versus time: H_2SO_4 concentration 1 M, temperature 65 °C, pulp density 100 g/L, and stirring speed 500 rpm.

2.2.2.4 Effect of hydrogen peroxide (H_2O_2) oxidant addition

The effect of hydrogen peroxide concentration (0 M – 0.6 M) was investigated on the dissolution of metals from the slag (figure 2.13). The sulfuric acid concentration was kept constant at 1 M, temperature, with leaching time, pulp density, and stirring speed at 65 ^oC, 60 minutes, 100 g/L, and 500 rpm respectively. Copper dissolution slightly improved from 71.5% to 83%, and Ni dissolution remained low but increased from 18.5% to 39.1%. There was a significant improvement in Co dissolution, from 50.3% to 77.5%, so possibly Co largely reports in sulfide form, and therefore dissolution is favored by the presence of an oxidant. Iron dissolution slightly decreased from 89.2% to 80% possibly by being precipitated out of the solution due to oxidation of ferrous iron and hydrolysis of ferric iron [1]. Though only a slight decrease in Fe dissolution was obtained, Banza et. al (2002) [5] achieved only 5% Fe extraction when using the H_2SO_4 and H_2O_2 reagent suite. Therefore, with further experimental

optimization, the use of an oxidant may provide a way to achieve very low iron contamination to leach solution under atmospheric leaching.

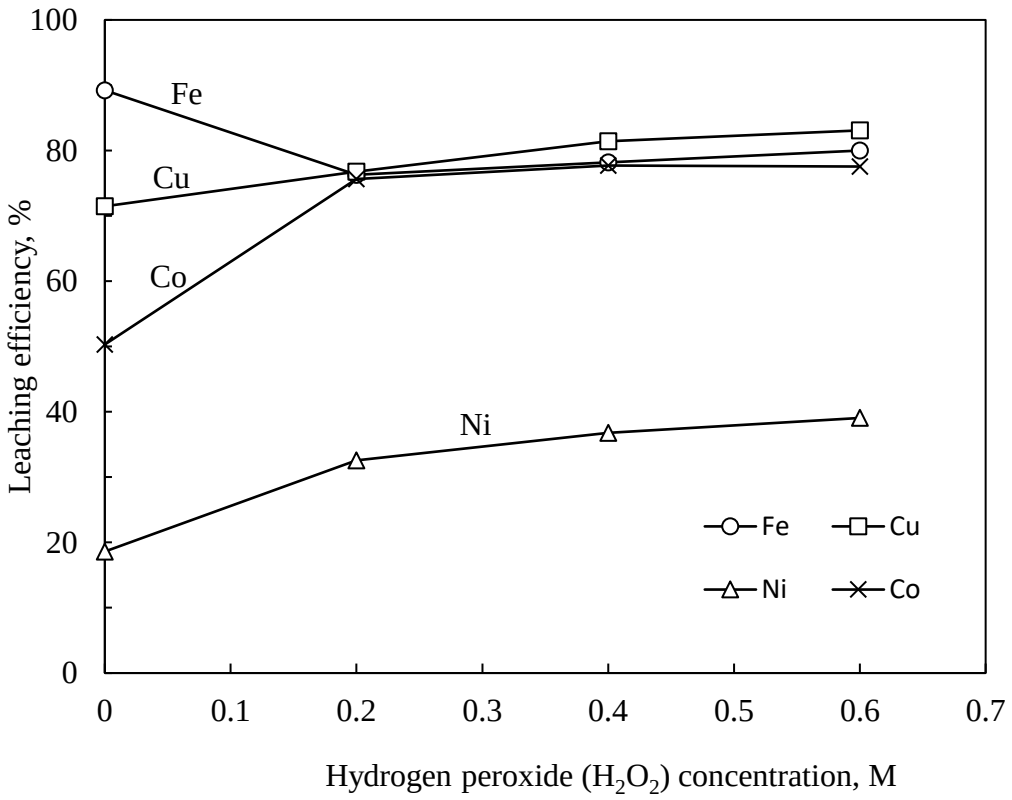

Figure 2.13: Metals dissolution profiles versus oxidant (H_2O_2) concentration: temperature 65 °C, sulfuric acid concentration 1 M, leaching time 60 minutes, pulp density 100 g/L, and stirring speed 500 rpm.

Figure 2.14 shows the XRD analysis conducted on the residues obtained from the leaching experiments. The main constituent in all the atmospheric beaker leaching experiments was gypsum which was possibly formed by equation 2.2.

$$Ca^{2+}(aq) + SO_4^{2-}(aq) + 2H_2O \rightarrow CaSO_4.2H_2O(s) \qquad (2.2)$$

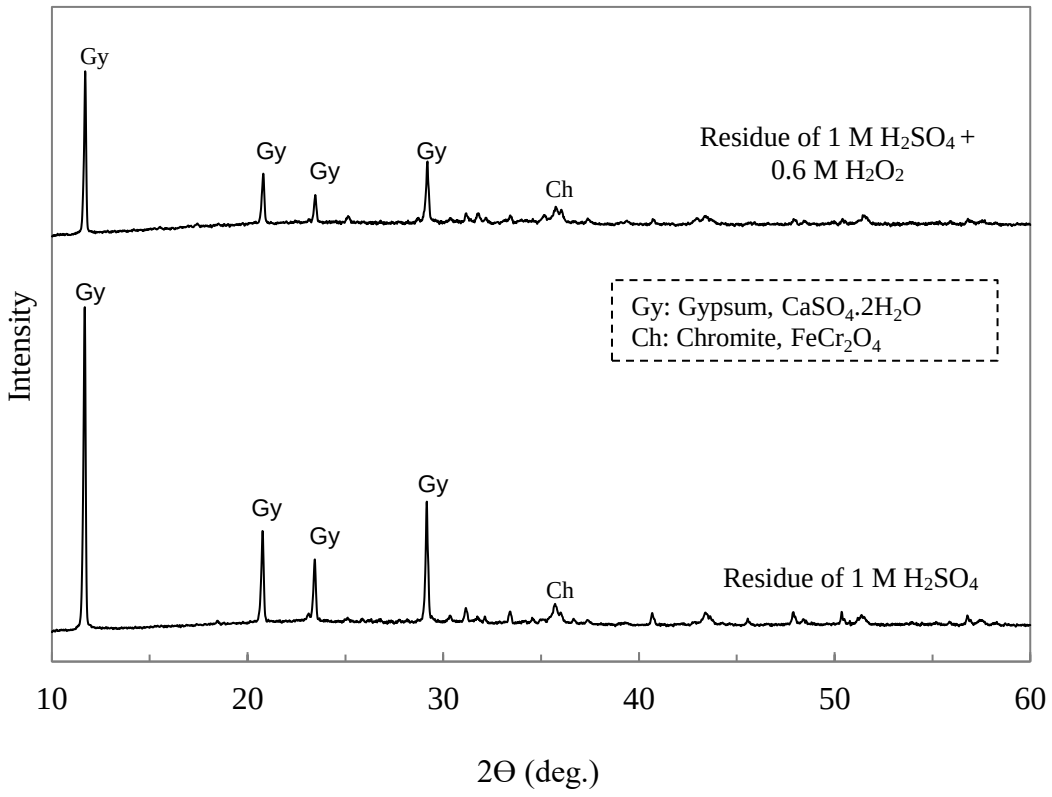

Figure 2.14: XRD patterns of residues obtained after atmospheric beaker leaching; temperature 65 °C, leaching time 60 minutes, pulp density 100 g/L, and stirring speed 500 rpm.

2.2.3 Summary of atmospheric leaching

Atmospheric beaker leaching of slag was investigated for extraction of copper, nickel, and cobalt. The findings are summarized below;

a) Under these conditions; 1.0 M sulfuric acid, 0.6 M hydrogen peroxide, 65 °C, stirring speed 700 rpm, and 100 g/L pulp density, the percentage extraction of Ni was below 40%, while those of Cu and Co were 83% and 77% respectively. The dissolved Fe was 80%, and the high dissolution of Fe has been consistently noted under all the atmospheric leaching conditions.

b) Temperature and acidity are the most important parameters to control during slag leaching. At high temperatures and acid concentrations, there is excessive formation of silica gel which hinders slag dissolution resulting in marginal metal extraction values. The stability of silicic acid generated during fayalite dissolution has been noted to decrease at high temperatures and acidity, resulting in re-polymerization resulting in silica gel.

2.3 High-pressure oxidative acid (HPOAL) leaching

This chapter focuses on the high-pressure oxidative acid leaching of the electric furnace granulated slag. HPOAL was done to improve the leaching efficiencies of metal sulfides (Ni and Cu) as well as reduce the high contamination of Fe incurred under the atmospheric leaching. High-pressure leaching is known to have a high dissolution rate, short retention time, good control of leaching conditions (oxygen pressurization, high temperature), good metal selectivity, and stable residues. The effect of particle size, stirring speed, acid concentration, temperature, leaching time, total pressure, and pulp density are discussed. The leaching mechanism of slag under high-pressure leaching conditions is deduced.

2.3.1 Experimental procedure

2.3.1.1 High-pressure leaching

Leaching experiments were conducted on a ground slag sample using a sulfuric acid solution. A stainless-steel autoclave reactor (Nitto Koastu, Japan) comprising of a 200 ml capacity reaction vessel, heating mantle, temperature controller, and a variable speed stirrer was utilized (figure 2.15). To obtain optimal leaching conditions, the slag particle size was investigated in the range of 45–212 µm, the sulfuric acid concentration was varied between 0.2–1.0 mol/L, and the pulp density was adjusted between 100–300 g/L. The stirring speed, leaching time, and temperature were varied in the ranges of 300–900 rpm, 0.5–2.0 hr, and 120–180 °C, respectively. Once the intended temperature was reached, oxygen (O_2) gas was injected into the slurry vessel at a controlled total pressure ($P_{total} = P_{vapor} + P_{oxygen}$) of 0.6 – 1.5 MPa. The slurry pH was recorded before and after leaching. A summary of the leaching conditions is displayed in table 2.4. The obtained slurry was filtered to separate the pregnant leach solution (PLS) from the solid residue after leaching. The PLS was analyzed using 4210 MP-AES (Agilent), while the solid residue was analyzed using X-Ray Diffractometer (XRD, Rigaku RINT–2200V) to identify the mineral composition of the solid samples. About 0.3g of the

solid residue was dissolved by aqua regia and analyzed using MP-AES for residual metal content determination.

Table 2.4: A summary of the High-pressure oxidative acid leaching (HPOAL) conditions.

Leaching Experiments	Investigated parameters
Particle size, µm	-45, -90, -125, -212
Stirring speed, rpm	300, 500, 700, 900
Sulfuric acid concentration, mol/L	0.2, 0.4, 0.6, 0.8, 1.0
Temperature, °C	120, 135, 150, 160, 180
Total Pressure, MPa	0.6, 1.0, 1.6
Leaching time, hr.	0.5, 1.0, 1.5
Pulp density, g/L	100, 150, 180, 200, 300

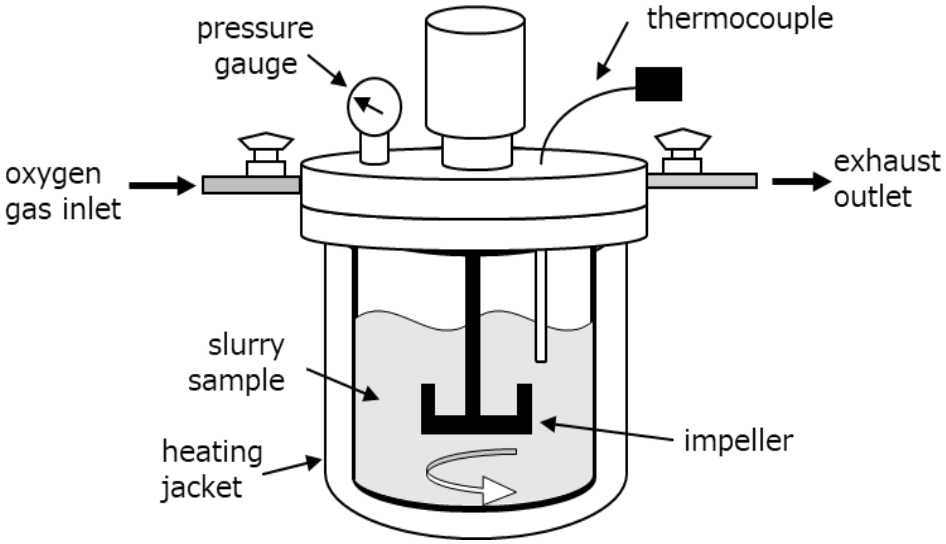

Figure 2.15: Schematic setup of autoclave used for high-pressure oxidative acid leaching.

2.3.1.2 Metals elution tests

Elution properties of the smelter slag and the solid residue obtained after HPOL were evaluated. A sample weight of 0.4 g was placed in a sample tube (capacity: 5 mL) together with 4 mL of different pH solutions (pH 2 (adjusted with H_2SO_4), pH 4 (distilled water), and pH 7 (adjusted with $Ca(OH)_2$)). The solutions were shaken for 6 hours at 200 rpm, using a shaker (MMS-4020, EYELA). Afterward, the slurry was subjected to solid-liquid separation by centrifugation. Chemical analysis of each metal in the solution was determined using MP-AES.

2.3.2 Results and Discussion

2.3.2.1 Effect of particle size

The effect of particle size of slag was studied with different feed sizes. The initial metal content of each size fraction was determined by XRF before leaching as shown in table 2.5. The slag shows a homogenous distribution of metals in the coarser size fractions as compared to a fine size fraction of less than 45 μm. Figure 2.16 shows the leaching results obtained at different particle sizes. The leaching efficiency of Ni, Cu, and Co showed no significant effect as the particle size was varied, mainly due to the homogeneity of fayalite, and the known abrupt dissolution of Fe in an acidic medium.

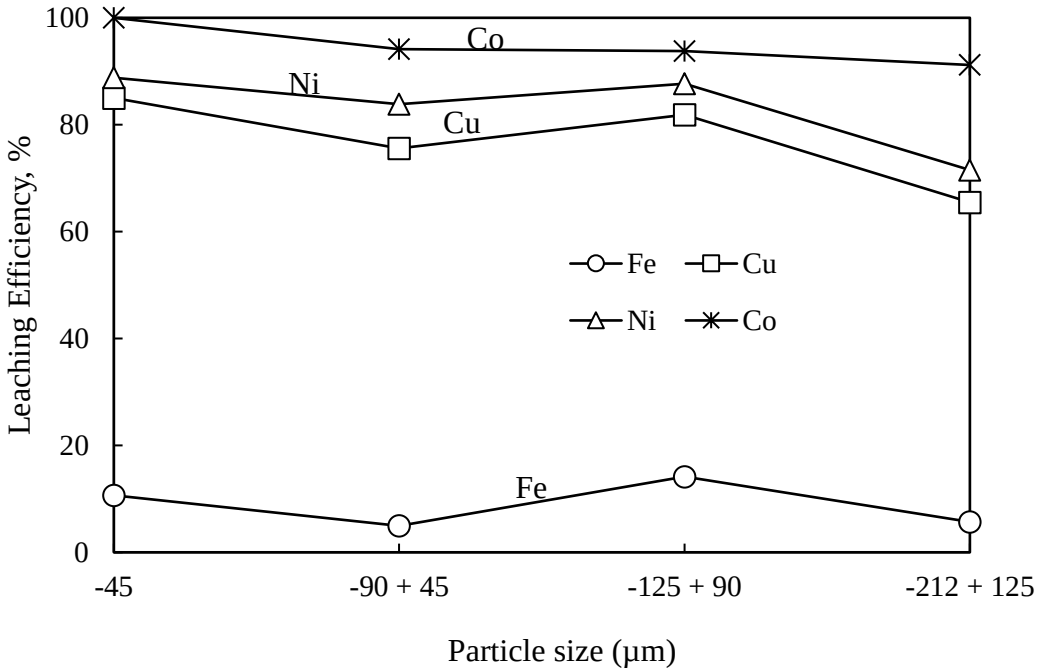

Figure 2.16: Metals dissolution profiles at different particle sizes. Conditions; H_2SO_4 0.6 mol/L, leaching time 1 hr., pulp density 100 g/L, temperature 150 ^oC, and total pressure 0.6 MPa.

Residue observation using XRD (figure 2.17), showed that a fine particle size favors the precipitation of hematite, over jarosite, which could be due to the increased contact of oxygen to the vast released Fe ions after the rapid dissolution of fayalite due to the smaller particle

size. The solid residues obtained from leaching larger particle sizes (≤90 – ≤212 µm) showed the presence of mainly jarosite and goethite mineral compositions.

Table 2.5: XRF elemental analysis of the different size fractions of slag.

Feed size µm	Fe	Cu	Ni	Co
	%			
-45	34.72	0.27	0.28	0.09
-90	42.76	0.30	0.31	0.13
-125	44.35	0.32	0.30	0.13
-212	41.98	0.34	0.31	0.13

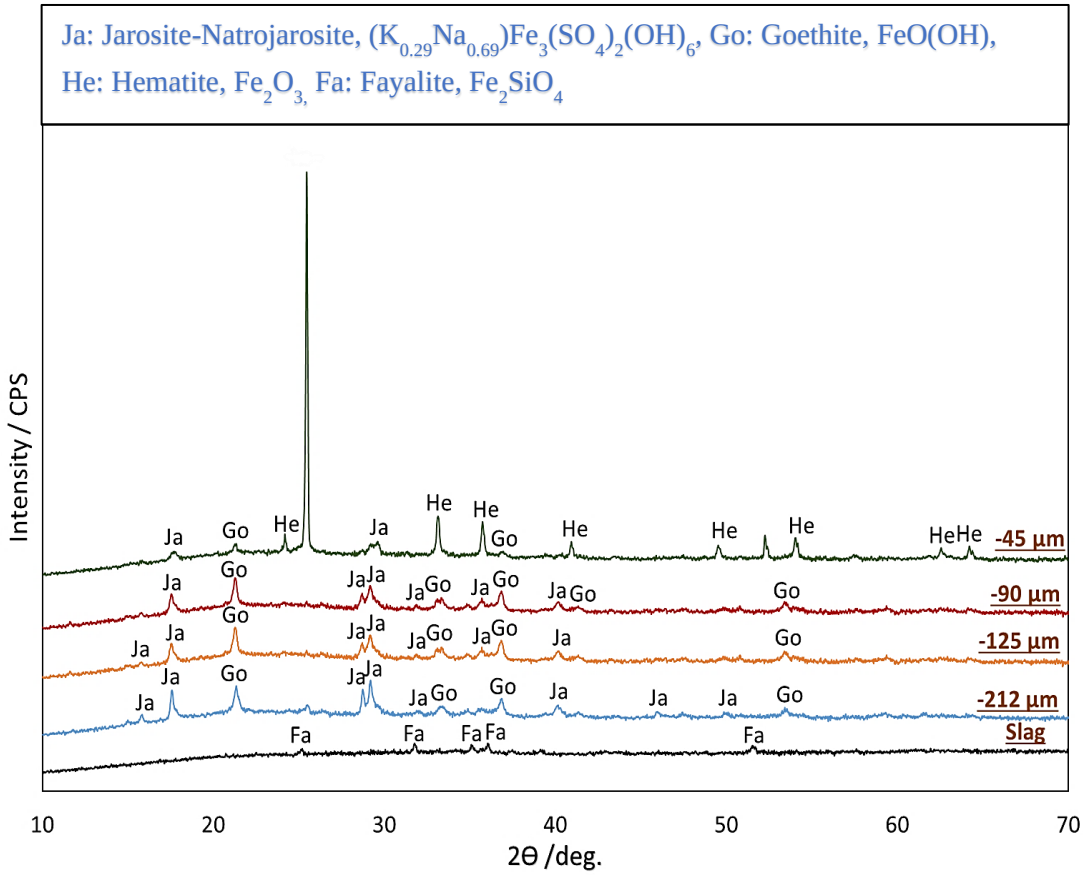

Figure 2.17: XRD patterns of residues obtained after HPOAL at different particle sizes. Conditions; H_2SO_4 0.6 mol/L, leaching time 1 hr., pulp density 100 g/L, temperature 150 °C, and total pressure 0.6 MPa.

2.3.2.2 Effect of stirring speed

The stirring speed was investigated from 300 – 900 rpm, and the results are shown in figure 2.18. The metal dissolutions of Ni, Cu, and Co from fayalite slag did not show any significant effect when the stirring speed was varied, indicating that the dissolution mechanism of slag may not be diffusion controlled [10,15]. Conversely, the low dissolution of Fe seems to be favored at 500 - 700 rpm, therefore 700 rpm was used for further optimization tests.

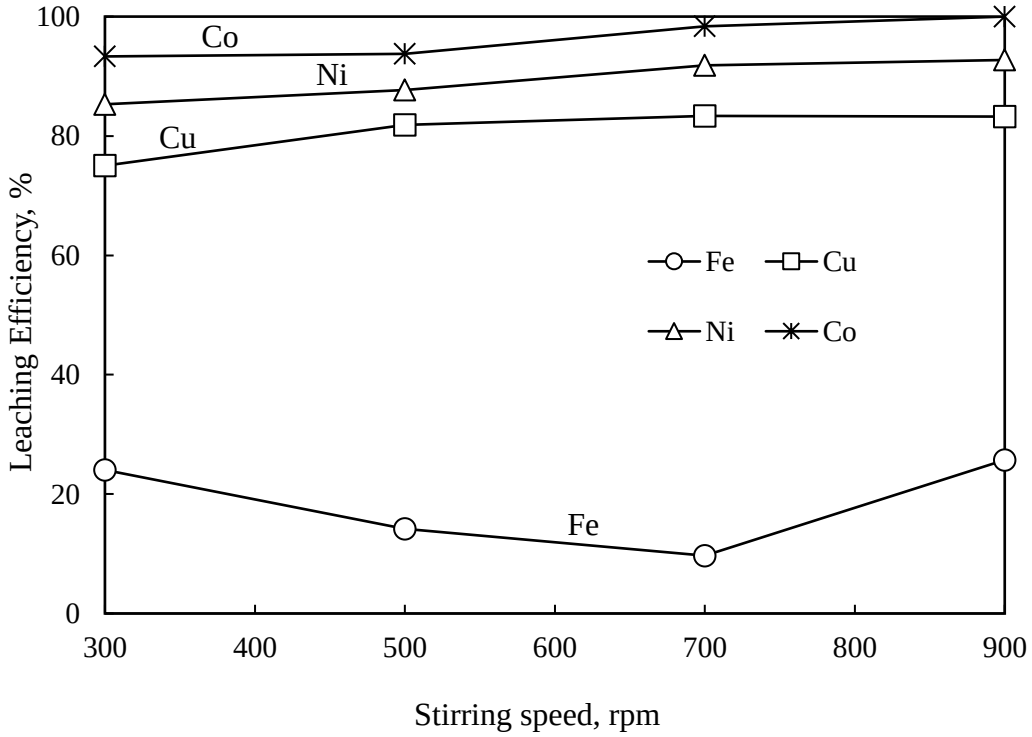

Figure 2.18: Metals dissolution profiles versus the stirring speed. Conditions: H_2SO_4 concentration 0.6 mol/L, temperature 150 °C, total pressure 0.6 MPa, leaching time 1 hr., and pulp density 100 g/L.

Figure 2.19 shows the leach residues obtained after leaching the slag at different stirring speeds. At a lower stirring speed of 300 rpm, Fe is mostly removed as hematite, while at medium stirring speed (500 rpm), goethite is mostly precipitated alongside jarosite. At higher stirring speeds, (700 – 900 rpm), Fe in solution is preferentially removed as jarosite with small amounts of goethite.

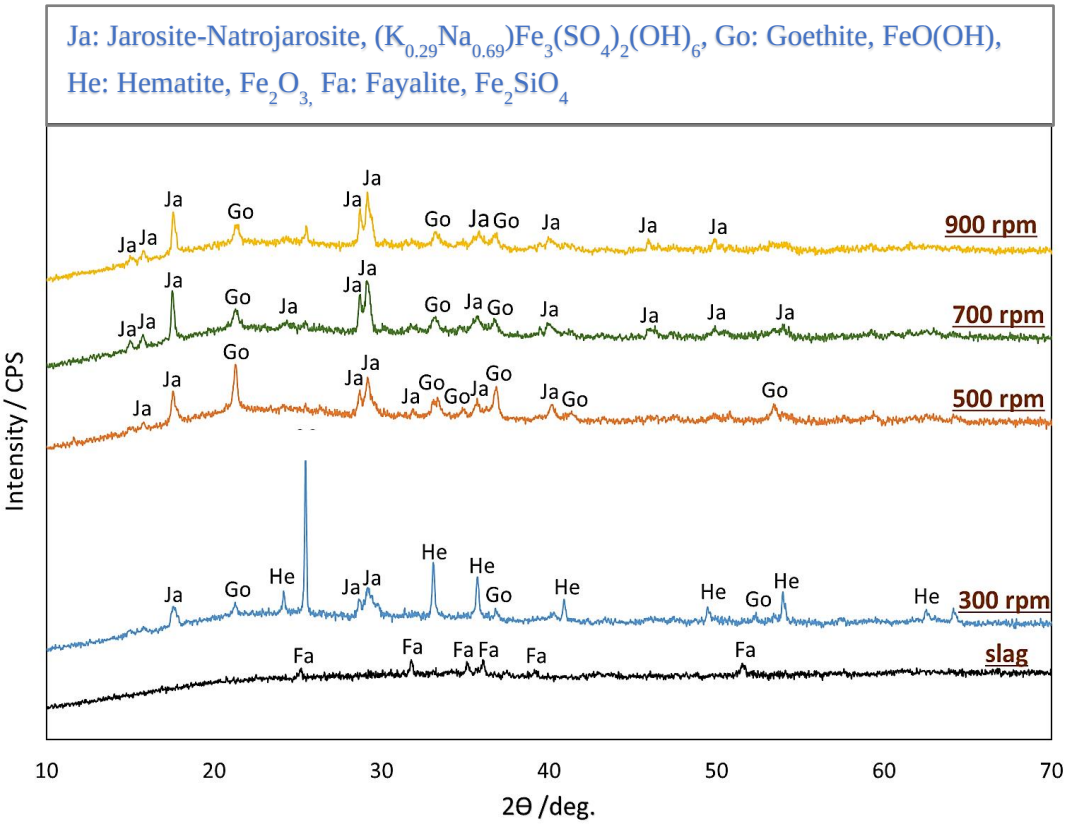

Figure 2.19: XRD patterns of residues obtained after HPOAL at different stirring speeds. Conditions; H_2SO_4 0.6 mol/L, leaching time 1 hr., pulp density 100 g/L, temperature 150 °C, and total pressure 0.6 MPa.

2.3.2.3 Effect of acid concentration

The sulfuric acid concentration was varied between 0 mol/L (distilled water) and 1.0 mol/L under 0.6 MPa total pressure, 150 °C temperature, 1hr leaching time, 100 g/L pulp density, and stirring speed of 700 rpm (figure 2.20). The metal extractions of Ni, Cu, and Co significantly increased with an increase in sulfuric acid concentration. The optimum leaching conditions were observed at 0.6 mol/L sulfuric acid concentration with Ni, Cu, and Co metal dissolutions of 91.81%, 83.36, and 98.36% respectively, beyond which there was no significant improvement in metal dissolution. Iron tenors in the PLS remained low at 9.67, however, the extent of Fe reporting to the PLS seems to increase above 0.6 mol/L H_2SO_4 concentration. At lower oxidized acid concentrations, Ni is preferentially leached over Cu and Co, while at increasing acid concentrations, almost all the Co is extracted from the slag. At the optimal conditions, the obtained Ni, Cu, Co, and Fe concentrations in the PLS were 0.30, 0.25,

0.11, and 7.22 g/L respectively (table 2.6) and it is thus crucial to further investigate operating at higher pulp densities to improve the low metal concentrations.

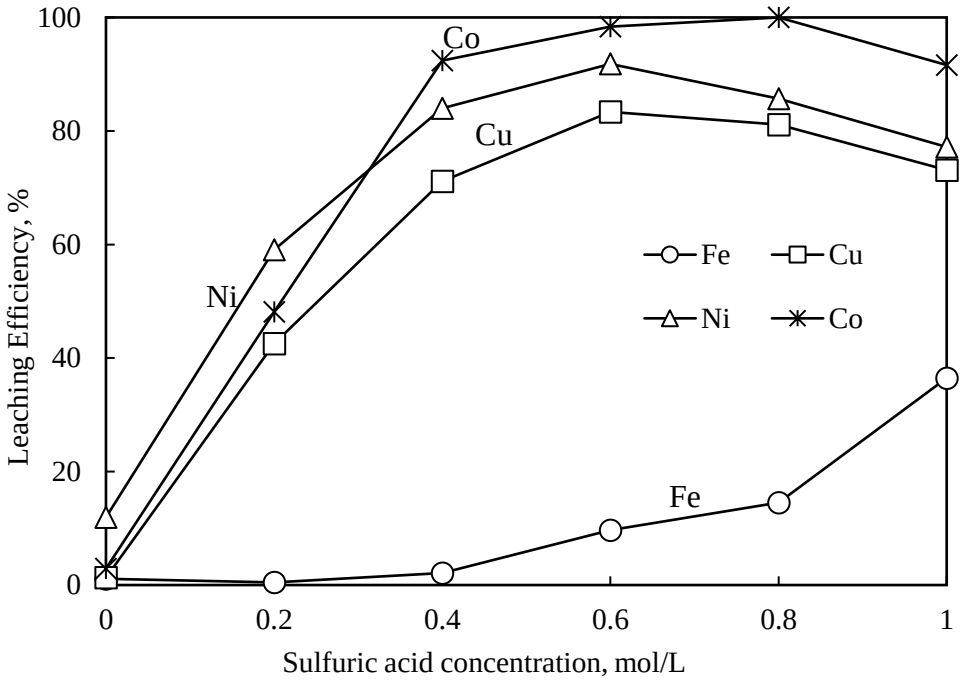

Figure 2.20: Metals dissolution profiles versus H_2SO_4 concentration: temperature 150 °C, leaching time 1 hr., pulp density 100 g/L and stirring speed 700 rpm, total pressure 0.6 MPa.

Table 2.6: A summary of the metal concentration and the pH of the pregnant leach solution (PLS) obtained after HPOAL at different H_2SO_4 concentrations.

H_2SO (mol/L)		**0.2**	**0.4**	**0.6**	**0.8**	**1.0**
	Fe	0.36	2.0	7.22	13.6	36.2
	Ni	0.21	0.28	0.30	0.27	0.25
	Cu	0.16	0.23	0.25	0.25	0.23
	Co	0.06	0.10	0.11	0.1	0.09
pH of PLS		1.36	1.25	1.02	0.98	0.83

The dissolution of Ni and Cu sulfides and Co oxide from the fayalite slag under acidic oxygenated conditions can be represented as follows:

$$NiS(s) + 2O_2 \rightarrow Ni^{2+} + SO_4^{2-} \quad (2.3)$$

$$CuS(s) + 2O_2 \rightarrow Cu^{2+} + SO_4^{2-} \quad (2.4)$$

$$CoO(s) + H_2SO_4 \rightarrow CoSO_4 + H_2O \quad (2.5)$$

The following reactions are considered for the general formations of hematite, goethite and jarosite-natrojarosite in all the leaching experiments:

$$2Fe_2(SO4)_3 + 0.5O_2 + H_2SO_4 \rightarrow Fe_2(SO4)_3 + H_2O \quad (2.6)$$

$$3Fe_2(SO_4)_3 + (K_{0.29}Na_{0.69})_2SO_4 + 12H_2O \rightarrow 2(K_{0.29}Na_{0.69})Fe_3(SO_4)_2(OH)_6 + 6H_2SO_4 \quad (2.7)$$

$$Fe_2(SO4)_3 + 4H_2O \rightarrow 2FeO(OH) + 3H_2SO_4 \quad (2.8)$$

$$2Fe_2(SO4)_3 + 6H_2O \rightarrow 2Fe_2O_3 + 6H_2SO_4 \quad (2.9)$$

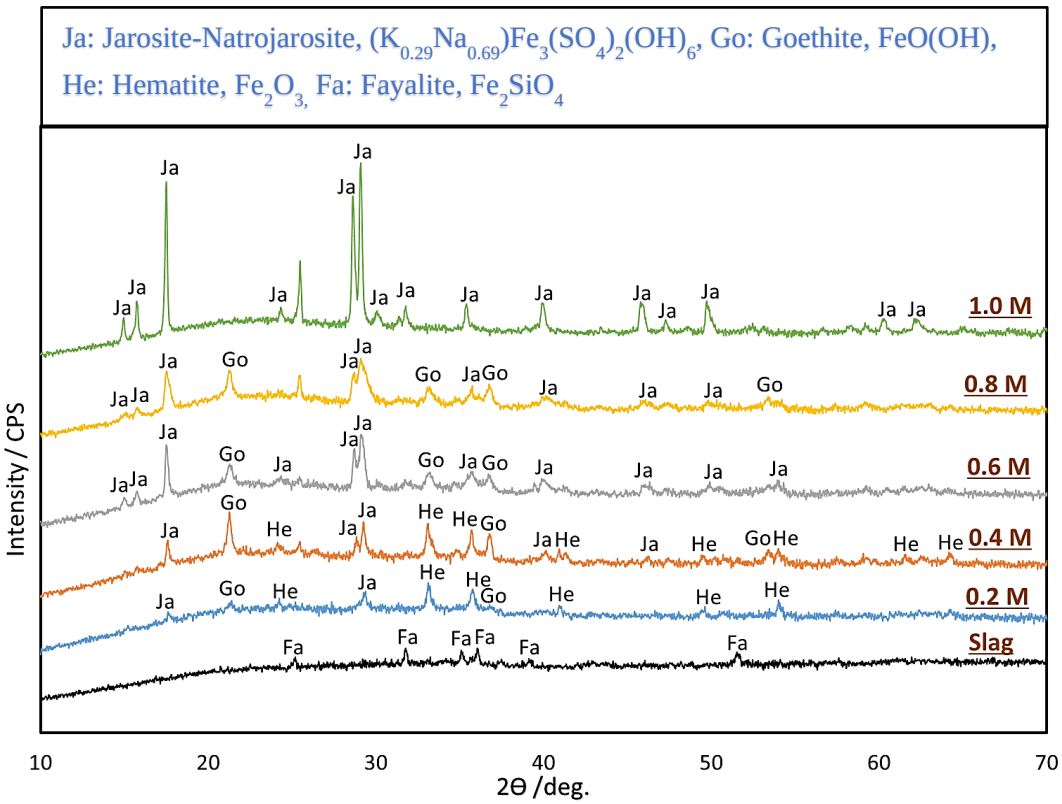

Figure 2.21: XRD patterns of residues obtained after HPOAL at different H_2SO_4 concentrations. Conditions: temperature 150 °C, leaching time 1 hr., pulp density 100 g/L, stirring speed 700 rpm, and total pressure 0.6 MPa.

The residues obtained after leaching were analyzed using XRD (figure 2.21), the main components observed were hematite, jarosite-natrojarosite, and goethite. Unreacted fayalite was mostly noted in the residue of the water-leached sample, indicating that metal dissolution is dependent on acid concentration. At lower acid concentrations (0.2 – 0.4 mol/L), hematite and goethite are preferentially precipitated, while at increasing acid concentrations (0.6 – 1.0 mol/L), jarosite is preferentially precipitated alongside goethite. Therefore, the formation of iron phases is dependent on pH and/or free acidity. McDonald and Muir, (2007), and Hans et. al., (2017) also observed that upon increasing the acid and sulfate concentrations, the predominant iron-containing residue formed was jarosite [16,17]. The silica phase was not detected by XRD, even though XRF analysis (table 2.7) indicates more than 90% silica removal in all the solid residues, thus, this implies that silica exists as amorphous silica, not in crystalline form.

Table 2.7: XRF elemental analysis of the leach residues obtained after HPOAL at different H_2SO_4 concentration

	Residue, wt.%					
	1.0 M	**0.8 M**	**0.6 M**	**0.4 M**	**0.2 M**	**slag**
Si	14.76	13.04	13.01	13.27	11.66	13.34
Fe	19.28	22.89	26.65	27.66	32.15	38.73
S	8.37	6.47	4.70	3.17	2.49	0.64
Ca	0.92	0.78	0.34	0.48	1.02	1.98
K	0.65	0.59	0.60	0.61	0.63	0.72
Na	0.57	0.66	0.50	0.36	0.26	0.63
Cr	0.14	0.14	0.14	0.15	0.18	0.18
Mg	0.13	0.18	0.07	0.11	0.34	1.96
Ni	0.06	0.05	0.03	0.05	0.11	0.36
Cu	0.05	0.04	0.04	0.06	0.14	0.36
Co	0.02	0.01	0.02	0.02	0.07	0.17

Figure 2.22: Residues obtained after HPOAL under different H_2SO_4 concentrations.

2.3.2.4 Effect of temperature

Figure 2.23 shows the metal dissolution profiles with respect to temperature. At lower temperatures (<150 °C) slag is amendable for leaching, but at high temperatures (180 °C), a negative effect on the metal dissolution of Ni, Cu, and Co is observed. This is attributed to the stability of silicic acid during fayalite dissolution. At high temperatures, silicic acid is less stable and re-polymerizes rapidly forming silica gel, which closes pores and prevents further slag dissolution [9].

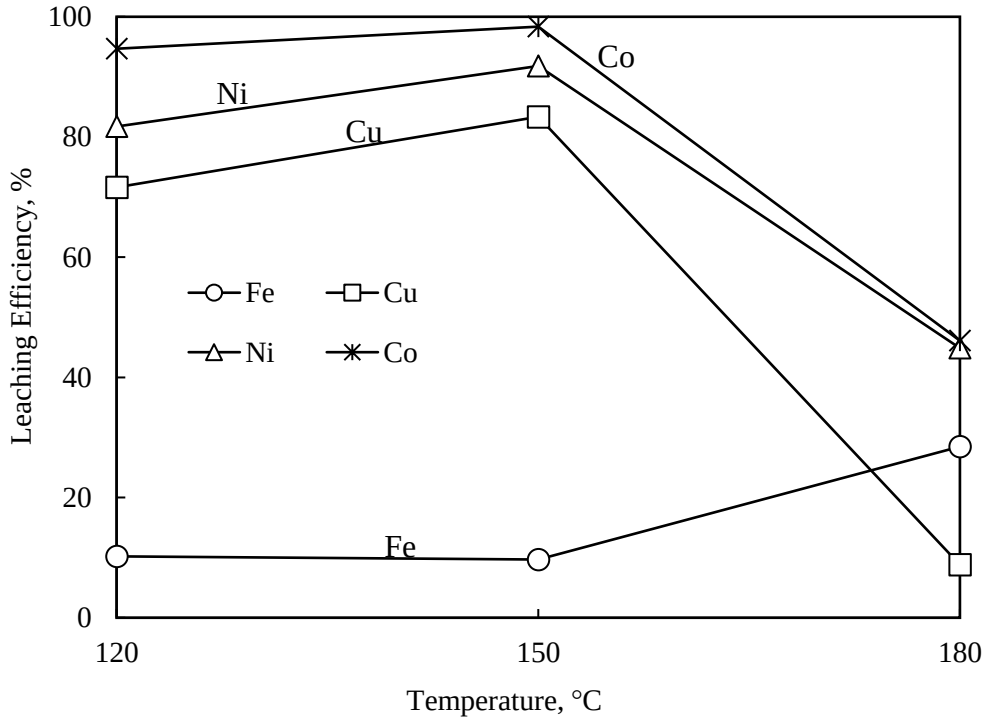

Figure 2.23: Metals dissolution profiles versus temperature. Conditions; H_2SO_4 concentration 0.6 mol/L, leaching time 1 hr., pulp density 100 g/L and stirring speed 700 rpm, total pressure 0.6 MPa.

At all investigated conditions, cobalt is preferentially leached from the slag when compared to Ni and Cu, mainly because cobalt exists in the oxide form as shown in the mineralogical analysis (figure 2.5), and thus can easily be dissolved by acid, unlike copper and nickel which exist in the slag as sulfides. Huang et. al (2015) also found that the fine dispersion of sulfides in the slag phase required high temperature and oxygen for leaching [7]. Figure 2.24 displays the observation of residues obtained after leaching at different temperatures. At lower leaching temperatures (120 – 150 °C), the main component in the solid residue is jarosite, while at high temperatures (180 °C) hematite was observed as the only iron precipitate.

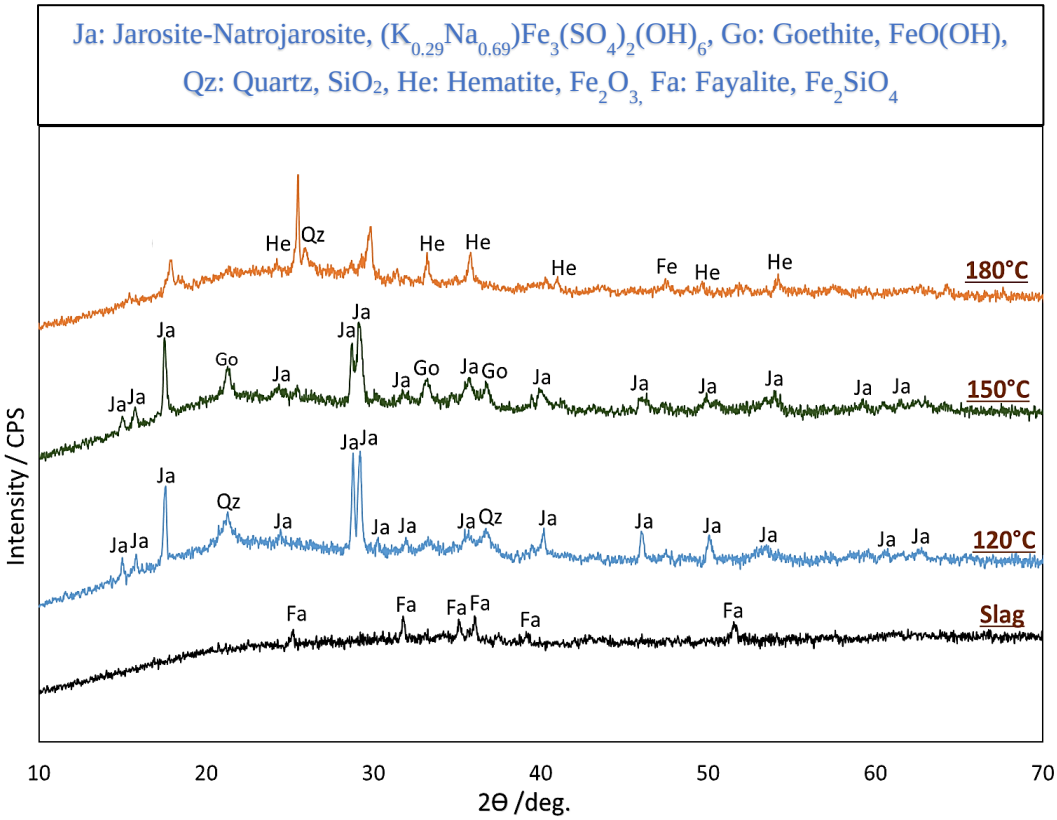

Figure 2.24: XRD patterns of residues obtained after HPOAL at different temperatures. Conditions: H_2SO_4 0.6 mol/L, temperature 150 °C, leaching time 1 hr., pulp density 100 g/L, stirring speed 700 rpm, and total pressure 0.6 MPa.

2.3.2.5 Effect of total pressure

Figure 2.25 shows the effect of total pressure which was controlled by oxygen injection. The leaching efficiency of Ni, Cu, and Co did not show a significant change when the total pressure

of the leaching system was increased. The low total pressure of 0.6 MPa was able to yield good leaching efficiency results of 91.81%, 83.36, and 98.36% for Ni, Cu, and Co, respectively, comparable to a higher total pressure of 1.6 MPa which yielded a similar leaching efficiency of 94.02%, 84.56 and 99.99% for Ni, Cu, and Co, respectively. The dissolved iron in the PLS remained low at all the investigated total pressures. Dissolved iron is mostly removed through precipitation into hematite, jarosite, and/or goethite. The presence of oxygen is mainly consumed to oxidize ferrous irons released by the dissolution of fayalite as in equations 2.1 and 2.6, while the subsequent iron removal reactions can be explained by the hydrolysis of the ferric iron as in equations 2.7 – 2.9. The total pressure of 1.0 MPa showed the highest leaching efficiency of Ni, Cu, and Co at 99.99%, 90.61%, and 99.99% Co while Fe was the lowest at 6.06%. The solid residue at these optimal conditions (1.0 MPa) showed the formation of hematite alongside jarosite and goethite (figure 2.26), unlike other residues which only showed jarosite and goethite.

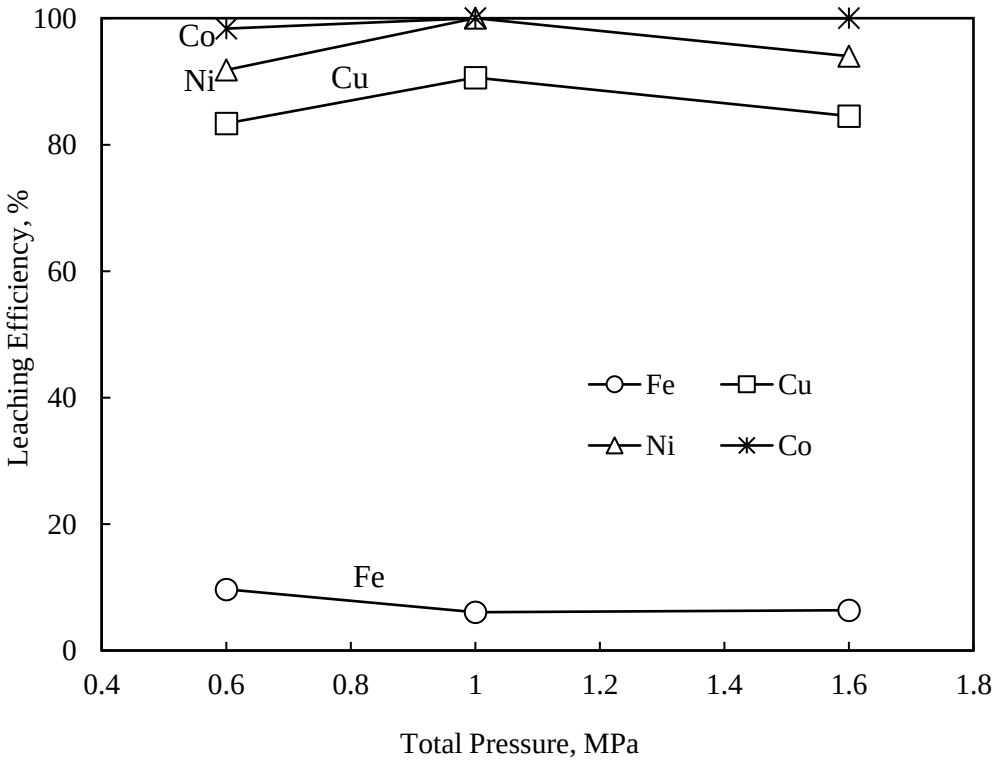

Figure 2.25: Metals dissolution profiles versus total pressure. Conditions; H_2SO_4 concentration 0.6 mol/L, leaching time 1 hr., temperature 150 °C, pulp density 100 g/L, and stirring speed 700 rpm.

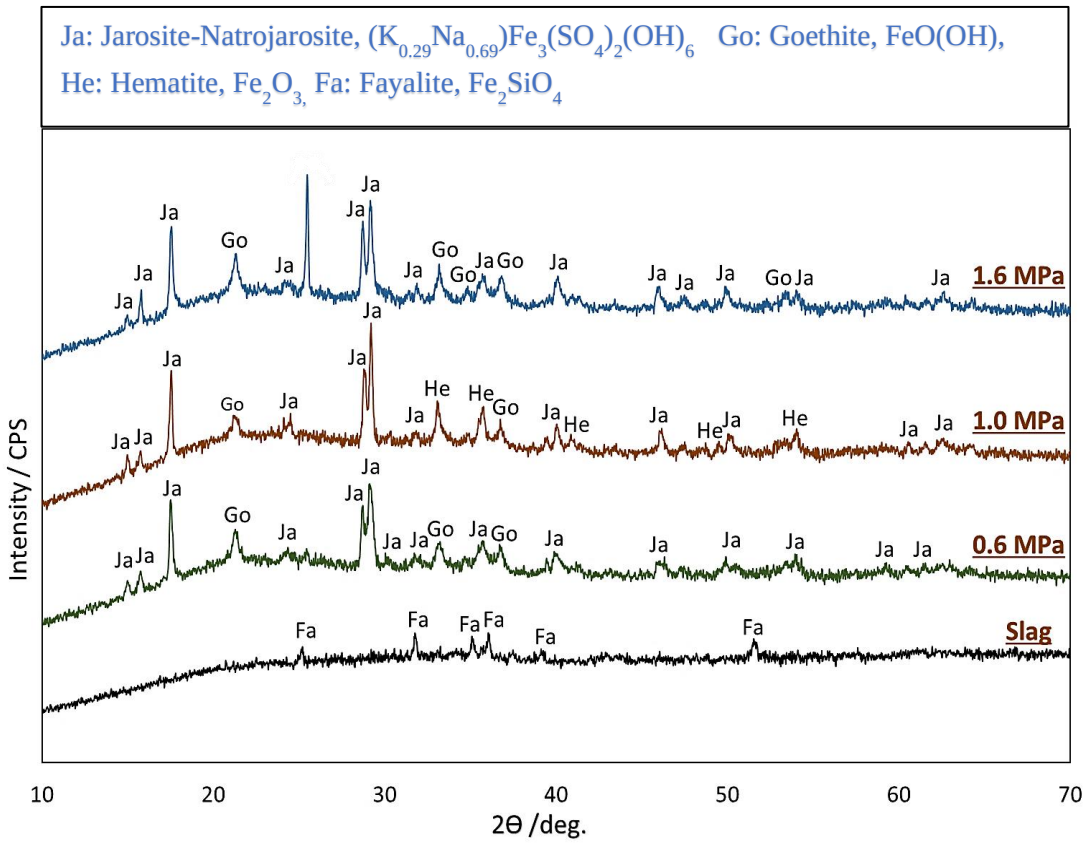

Figure 2.26: XRD patterns of residues obtained after HPOAL at different total pressures. Conditions; H_2SO_4 concentration 0.6 mol/L, leaching time 1 hr., temperature 150 °C, pulp density 100 g/L, and stirring speed 700 rpm.

2.3.2.6 Effect of leaching time

The effect of leaching time on slag dissolution was investigated at different time intervals from 0.5 – 2.0 hrs. The results are displayed in figure 2.27, showing that the dissolution of cobalt reached completion after 1.0 hr of leaching, while nickel dissolution reached completion after 1.5 hrs. The fast leaching rate of cobalt is attributed to its existence in oxide form in fayalite as compared to nickel and copper which exists in sulfide form. On the other hand, the leaching rate of copper was slower than that of Ni and Co, and reached a high of 89.42 % after 1.5 hrs, after which did not show any significant improvement in dissolution, and never reached completion in the investigated time frame. The Fe tenors to the PLS remained around 10% after 1.0 hr leaching time.

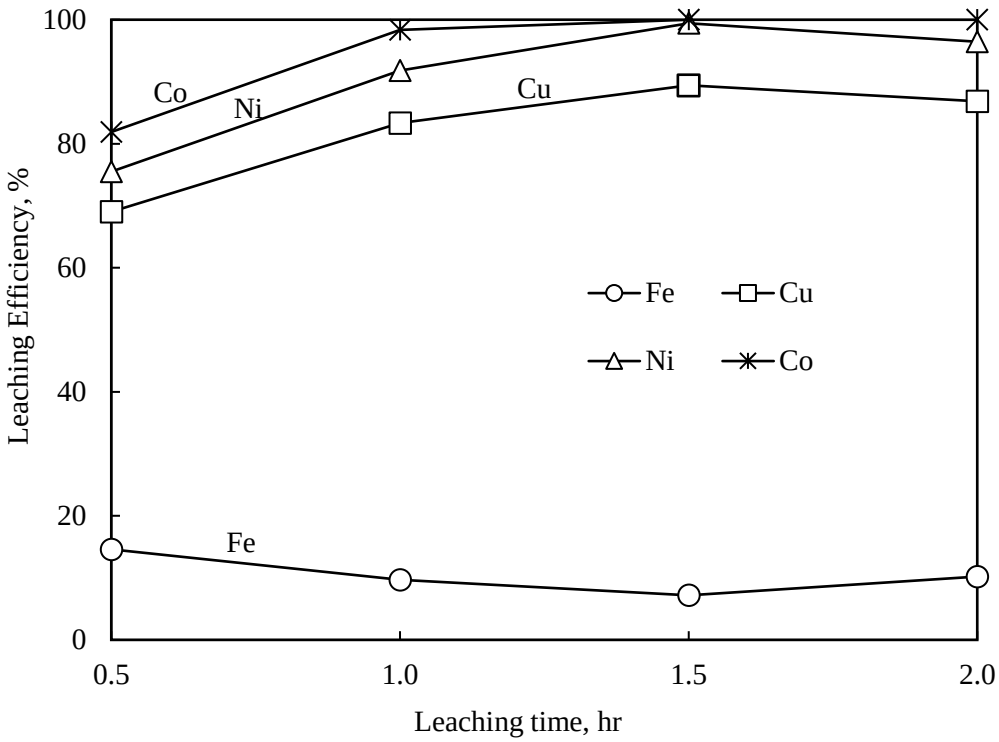

Figure 2.27: Metals dissolution profiles versus leaching time. Conditions; H_2SO_4 concentration 0.6 mol/L, total pressure 0.6 MPa, temperature 150 °C, pulp density 100 g/L, and stirring speed 700 rpm.

Figure 2.28 shows the XRD patterns of residues obtained after high-pressure leaching at different leaching times. Hematite was only noted in the leach residue obtained after 0.5 hr leaching time, alongside goethite and jarosite-natrojarosite. The leach residue obtained after 1.0 – 2.0 hrs. of leaching, had a similar mineralogical composition, comprising mainly of jarosite-natrojarosite and goethite. Crystalline silica was observed in the leach residue obtained after 2.0 hrs. of leaching, indicating a structural change from amorphous silica to crystalline silica as a function of time.

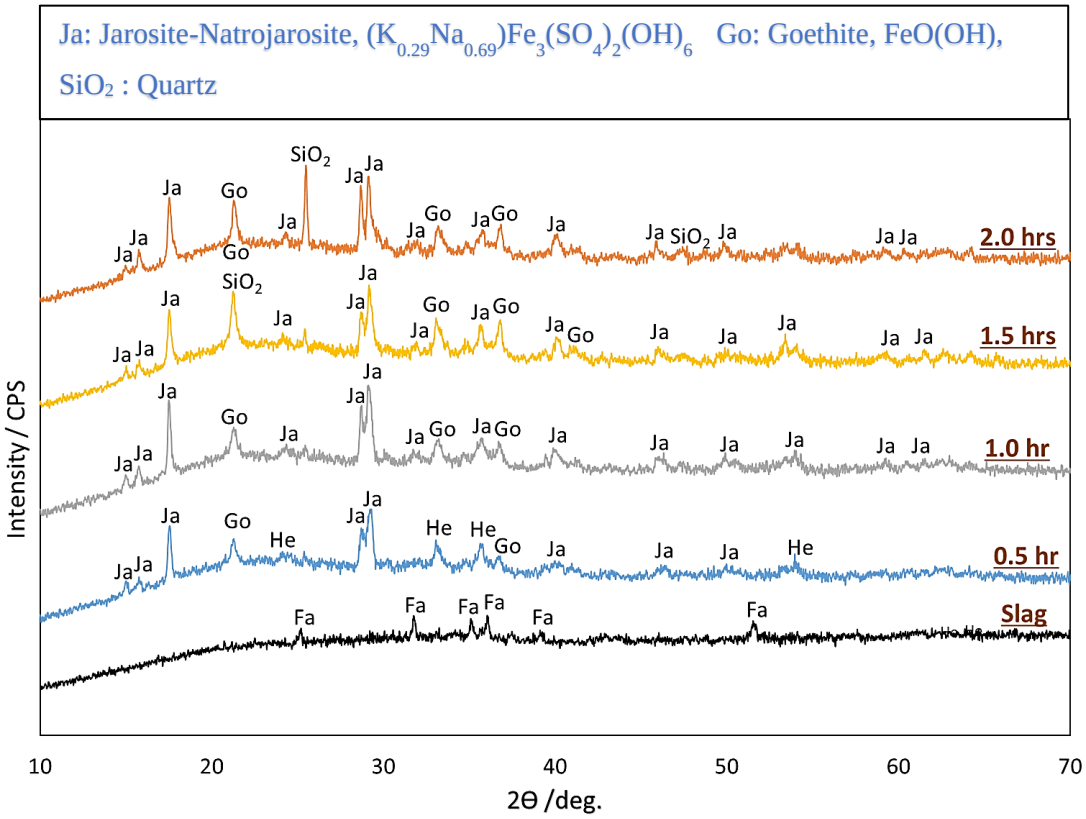

Figure 2.28: XRD patterns of residues obtained after HPOAL at different leaching times. Conditions; H_2SO_4 concentration 0.6 mol/L, total pressure 0.6 MPa, temperature 150 °C, pulp density 100 g/L, and stirring speed 700 rpm.

2.3.2.7 Effect of pulp density

Figure 2.29 shows the metal dissolution profiles with respect to pulp density (100–200 g/L), temperature 150 °C, sulfuric acid concentration 600 kg/ton, leaching time 1hr, oxygen pressure 1.0 MPa, and agitation speed 700 rpm. Increasing the pulp density beyond 180 g/L seems to have a negative effect on the metal dissolution of Ni, Cu, and Co which significantly dropped from 94.59% to 52.31%, 83.76% to 36.15%, and 99.99% to 64.44% respectively when the pulp density was increased from 180 g/L to 200 g/L. Conversely, the dissolved Fe in the solution increased from 6.40% to 29.97% due to an increased amount of fayalite in the slurry sample. It is noted that the metal dissolution rate is directly linked to the acid to solid ratio, A/S; increasing the slurry density thus decreases the A/S ratio, reducing the metal dissolution. Perederiy (2011) found that fayalite dissolution is a very fast reaction, while acid generation

due to hydrolysis of ferric iron is a slow process [1]. Therefore, acid is consumed faster for fayalite dissolution than it can be generated to encourage the dissolution of Ni, Cu, and Co. In this investigation, the sulfuric acid dosage was adjusted per weight of the sample, which was calculated from the optimal conditions obtained under the effect of acid concentration (sub-section 2.5.1), which is 600kg sulfuric acid/ton of fayalite. When the pulp density was increased beyond 200 g/L, the sample solidified inside the reactor vessel during leaching, and the leaching reaction was terminated.

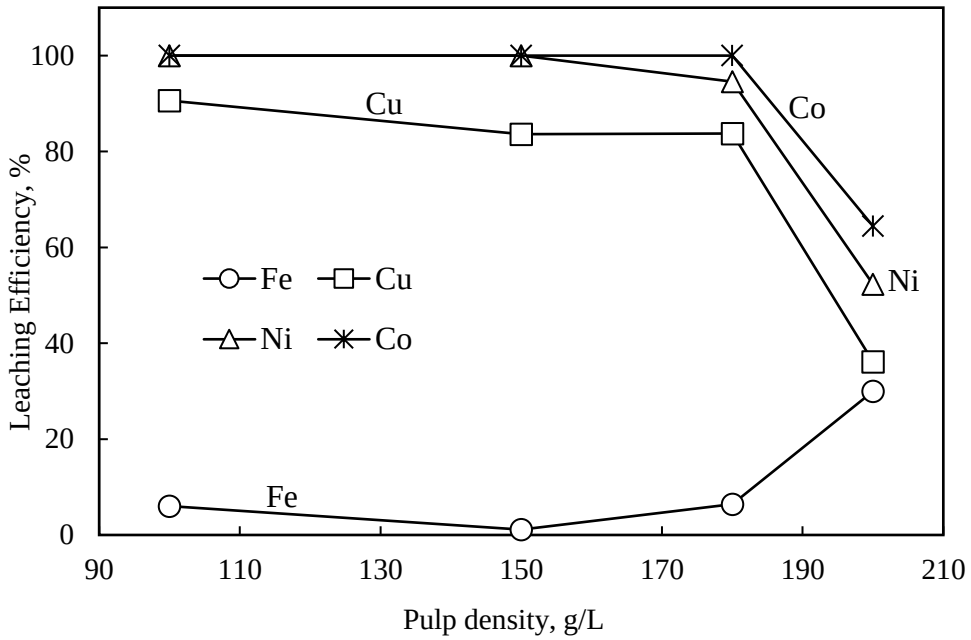

Figure 2.29: Metals dissolution profiles versus pulp density. Conditions; H_2SO_4 concentration 600 kg/ton, total pressure 1.0 MPa, temperature 150 °C, leaching time 1.5 hr., and stirring speed 700 rpm.

Observation of the solid residues obtained after leaching at different pulp densities was observed using XRD and the patterns are displayed in figure 2.30. At a high pulp density of 200 g/L, a new diffraction peak of gypsum was observed alongside jarosite-natrojarosite and goethite. The formation of gypsum (equation 2.2) possibly absorbed water from the slurry resulting in sample solidification during leaching. At 150 g/L pulp density, the resulting solid residue was mainly composed of hematite and some amounts of goethite and jarosite-

natrojarosite. While at 100 g/L, the main residue composition was jarosite-natrojarosite and goethite.

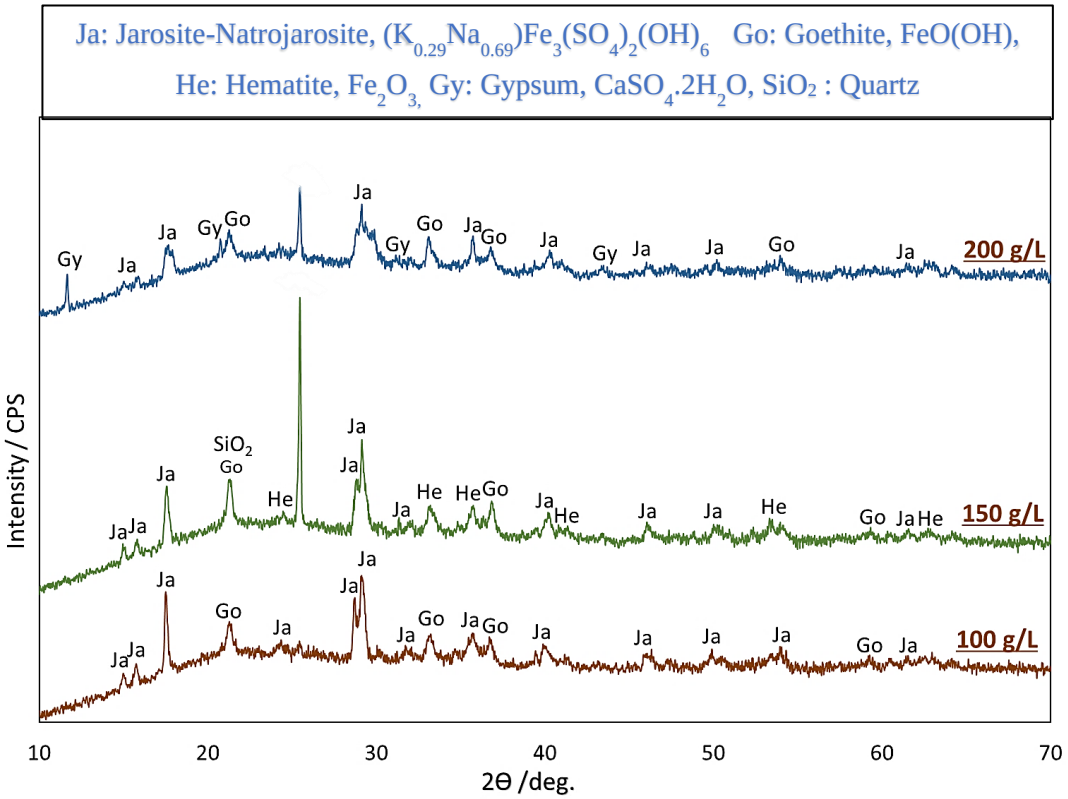

Figure 2.30: XRD patterns of residues obtained after HPOAL at different pulp densities. Conditions; H_2SO_4 concentration 0.6 mol/L, total pressure 1.0 MPa, temperature 150 °C, leaching time 1.5 hr., and stirring speed 700 rpm.

2.3.2.8 Leaching mechanism of slag under HPOAL

From the leaching results and the SEM-EDS observation images shown in figures 2.31 and 2.32, the leaching mechanism of slag under high-pressure leaching conditions is proposed and illustrated in figure 2.33. Iron abruptly dissolves from fayalite in an acidic medium, along with other metal oxides (magnesium and calcium) noted in the elemental mapping of slag in figure 2.5. The SEM-EDS observation of the leach residue in figure 2.31, shows zone A, the Fe depleted zone, created as Fe dissolves from fayalite. The ferrous ions generated are then oxidized to ferric ions when coming in contact with oxidizing high-pressure conditions. The ferric ions are then easily precipitated as jarosite natro-jarosite, goethite, or hematite (equation 2.7 – 2.9). The matte phase is exposed as fayalite dissolves and is thus oxidized and dissolved

as per equations 2.3 – 2.4. The dissolution of Fe from fayalite generates silicic acid (equation 2.1), which becomes saturated and precipitates into colloidal silica by equations 2.10 – 2.11 [18], filling the vacant pores left behind by iron, metal oxides, and matte, forming a silica-rich zone indicated by zone B. The abrupt filling of pores by silica can happen rather rapidly, prematurely ceasing any further dissolution of fayalite as observed in figure 2.32. Zone C indicated in the sulfur mapping of figure 2.31, shows a surrounding layer that was presumed to be precipitated jarosite. As Fe dissolves away from the fayalite particle, it reaches a high acidity zone, and its solubility drops and it precipitates. Peredirily (2011) noted that iron precipitates are porous and do not hinder the dissolution of ions through [1], however, this jarosite natro-jarosite layer may slow down the diffusion of ions away from the slag particle and consequently, slow down the leaching kinetics of the system.

$$H_4SiO_4 \rightarrow H_2SiO_3 + H_2O \qquad (2.10)$$

$$H_2SiO_3 \rightarrow SiO_2 + H_2O \qquad (2.11)$$

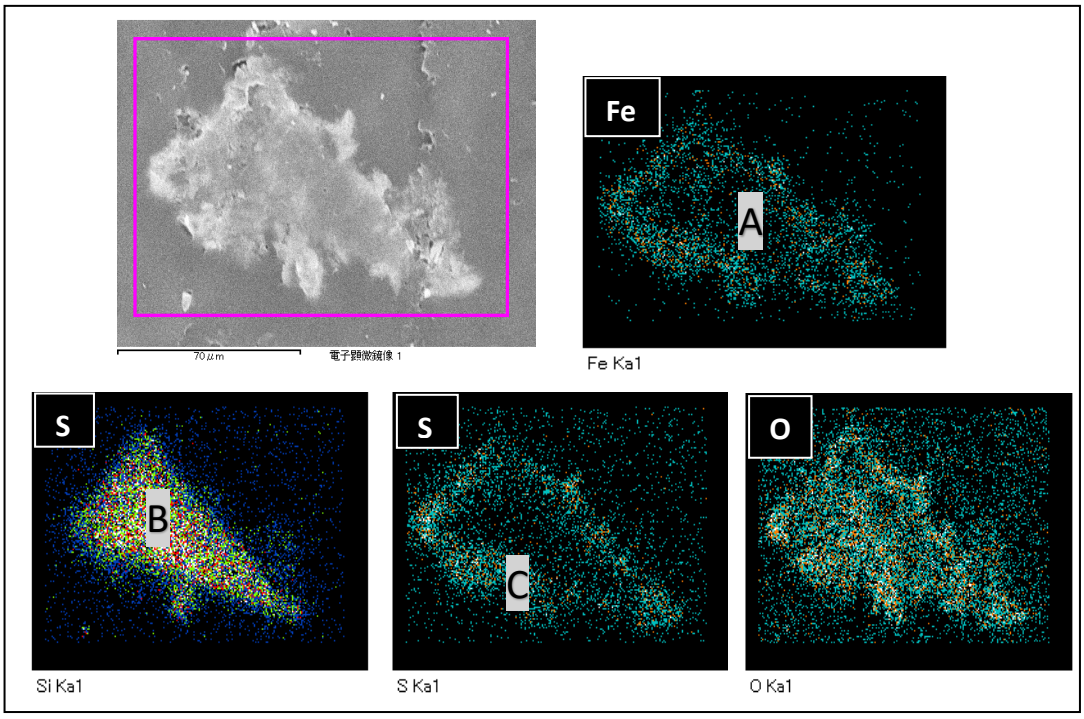

Figure 2.31: A SEM-EDS observation of the leach residue particle. Conditions: 0.6 mol/L H_2SO_4, 0.6 MPa, 150 °C, 1hr, 700 rpm, 100 g/L pulp density.

A= Fe-depleted zone, **B**= Silica-rich zone filling the Fe depleted zone, and **C**= Jarosite-natrojarosite passivation layer surrounding the particle.

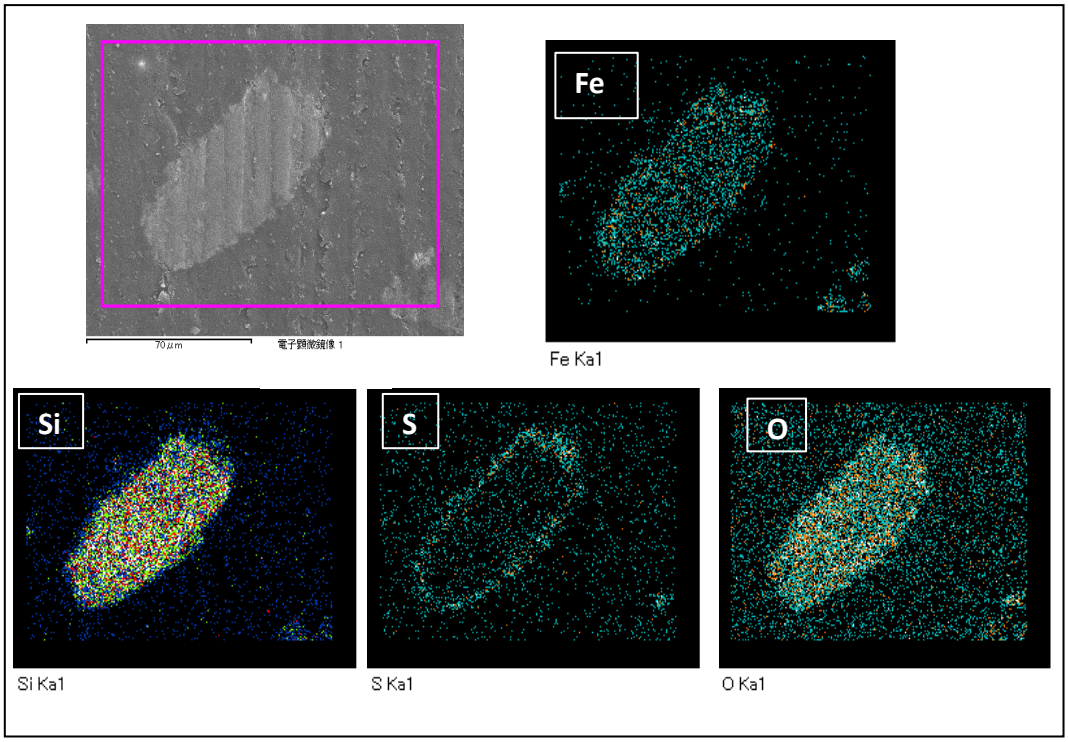

Figure 2.32: A SEM-EDS observation of the leach residue particle.
(0.6 mol/L H_2SO_4, 0.6 MPa, 150 °C, 1 hr., 700 rpm, 100 g/L pulp density)

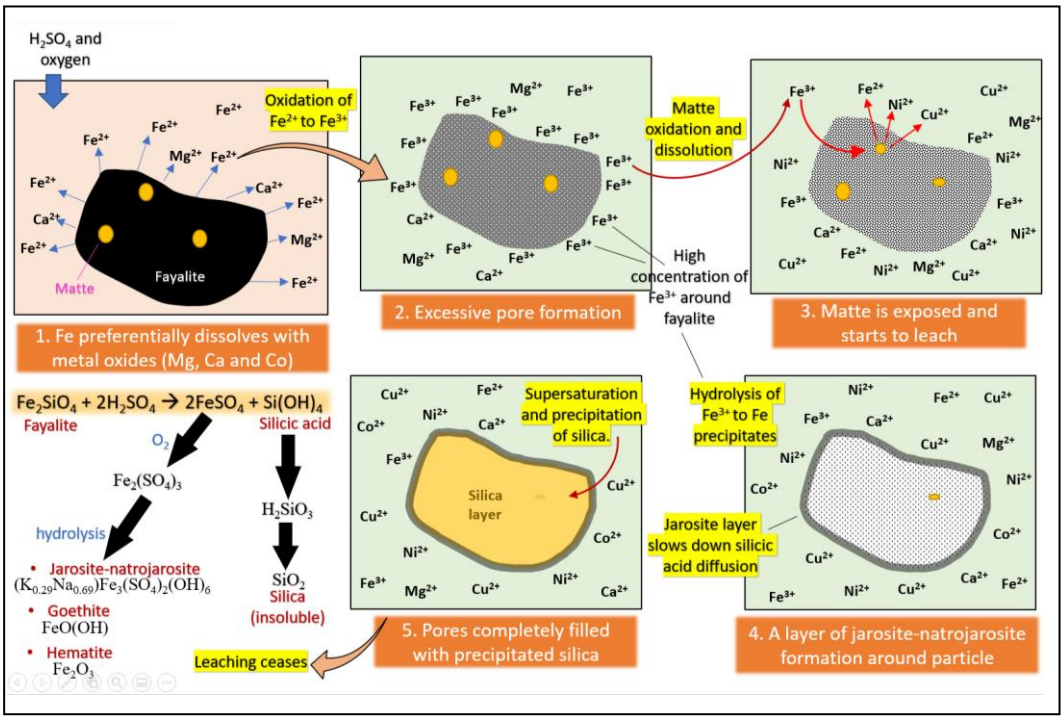

Figure 2.33: An illustration of slag dissolution mechanism.

2.3.2.9 Residue analysis

The metal elution test results of the slag and the solid residue obtained after leaching slag are displayed in figure 2.34. The metal concentrations of the eluded sample solution were compared to the wastewater discharge standards specified by the Ministry of the Environment in Japan. Under acidic conditions of pH 2, the Fe elution was extremely high from the slag sample (156 ppm) as compared to the solid residue (72 ppm), however, both samples exceeded the set limit of 10 ppm. Similarly, at pH 2, Cu elution from the slag (7.9 ppm) exceeded the set limit of 3 ppm, while the solid residue was below the set limit at 2.98 ppm. At all investigated pH conditions of 2, 5, and 7, Ni elution from the residue exceeded the set limitation of 1ppm with nickel concentrations of 4.7, 6.4, and 5.3 ppm, respectively. The limitation of cobalt concentration in the solution could not be established, however, cobalt elution from the residue was higher than from the slag at all the investigated pH conditions. Chromite and zinc elutions from both the slag and the solid residue were within their specified limits of 2 ppm.

Generally, at acidic pH conditions (pH 2), metal elution from slag is high, but at neutral pH conditions (pH 5 and 7), the slag was stable and no metal elutions were detected because of the generally stable glass phase of the granulated fayalite slag. On the contrary, the metal elutions from the leach residue were high because of the finer grain size of the residue and the reduced stability of the minerals in the residue (jarosite natro-jarosite, goethite, and hematite) as compared to the glassy fayalite mineral composition. Since the resulting solid residue has a weight composition of 25.5% Fe, it can further be utilized as a potential source of iron, especially in ferrous/steel processing operations.

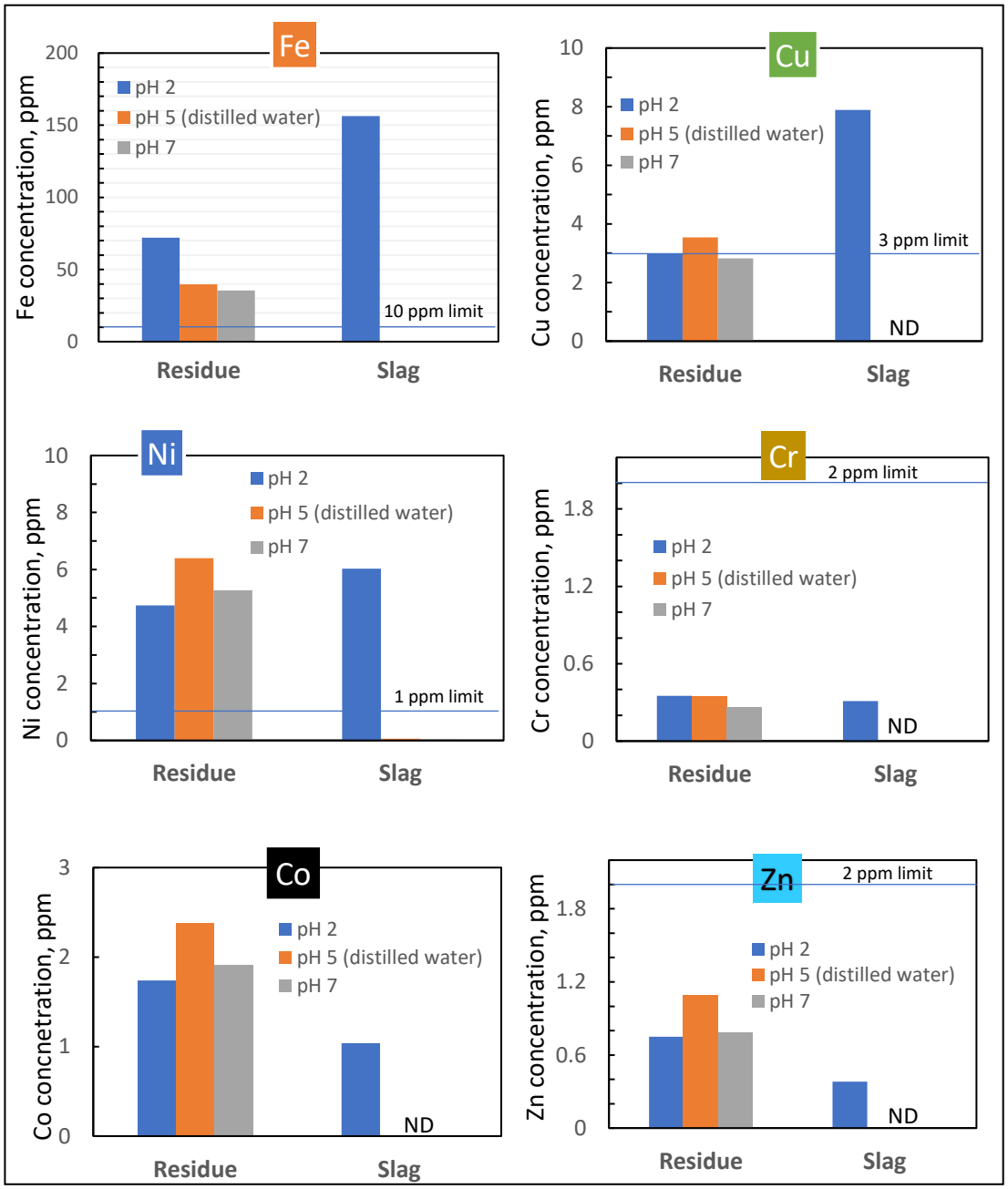

Figure 2.34: Concentration of metals in the solution obtained after the elution test of slag (before leaching) and solid residue (after leaching). ND= not detected.

2.3.3 Summary of HPOAL

High-pressure oxidative acid leaching (HPOAL) of slag was investigated for extraction of copper, nickel, and cobalt. The findings are summarized below;

a) Under these optimized leaching conditions; sulfuric acid 0.6 mol/L, total pressure 1.0 MPa, temperature 150 °C, leaching time 1.5 hr., stirring speed 700 rpm, and 150 g/L pulp density,

excellent extractions of Ni, Cu, and Co from slag were obtained. The highest metal recoveries were Ni = 99%, Cu = 84% and Co = 99% and low Fe extraction of less than 2%. The resulting solid residue was mainly composed of hematite, and some amounts of goethite and jarosite-natrojarosite, with a weight composition of 25.5% Fe and 12.9% Si.

b) Acidity and temperature are important parameters to be controlled during the high-pressure leaching of slag to achieve optimum dissolution of valuable metals.

c) Characterization of the solid residues using SEM-EDS, showed excessive precipitated colloidal silica filling the dissolution pores of corroded fayalite, thus may be the limiting factor towards the dissolution of fayalite.

2.4 Conclusion

This chapter discussed atmospheric leaching and the high-pressure leaching of slag. The characterization of the electric furnace slag sample showed a highly amorphous glassy structure with the dominant mineral phase being fayalite. The matte phase is dispersed and mostly locked in the fayalite phase. The valuable metals content of Ni, Cu, and Co were 0.36%, 0.36%, and 0.17%. Various leaching parameters such as sulfuric acid concentration, temperature, oxidant concentration/total pressure, and leaching time were investigated during the leaching of slag. The atmospheric leaching results showed poor extractions of Ni below 40%, with high Fe dissolution of about 80% when utilizing 1.0 M sulfuric acid and 0.6 M hydrogen peroxide reagent suite. The formation of a passive layer of amorphous silica and gypsum was suspected to hinder oxidant access for sulfides dissolution and/or Fe precipitation. On the other hand, under optimized leaching conditions, high-pressure oxidative acid leaching yielded excellent extractions of Ni, Cu, and Co from slag with the highest metal recoveries of Ni, Cu, and Co of 99%, 84%, and 99%, respectively with low Fe extraction of less than 2%. Acidity and temperature are important parameters for optimum dissolution of valuable metals from slag and control the stability of silicic acid to prevent polymerization to silica gel which hinders slag leaching.

References

1. Perederiy, I., 2011. Dissolution of Valuable Metals from Nickel Smelter Slags by Means of High-pressure Oxidative Acid Leaching [doctoral dissertation], Graduate Department of Chemical Engineering and Applied Chemistry, University of Toronto.
2. Matthew, I.G., Elsner, D., 1977. The hydrometallurgical treatment of zinc silicate ores. Metallurgical Transactions B 8B, 73-83. https://doi.org/10.1007/BF02656354
3. Bodas, M.G., 1996. Hydrometallurgical treatment of zinc silicate ore from Thailand. Hydrometallurgy 40, 37–49. https://doi.org/10.1016/0304-386X(94)00076-F
4. Yang, Z., Rui-lin, M., Wang-dong, N., Hui, W., 2010. Selective leaching of base metals from copper smelter slag. Hydrometallurgy 103, 25–29. https://doi.org/10.1016/j.hydromet.2010.02.009
5. Banza, A.N., Gock, E., Kongolo, K., 2002. Base metals recovery from copper smelter slag by oxidizing leaching and solvent extraction. Hydrometallurgy 67, 63–69.
6. Baghalha, M., V.G. Papangelakis, and W. Curlook, Factors affecting the leachability of Ni/Co/Cu slags at high temperature. Hydrometallurgy, 2007. 85(1): p. 42-52.
7. Huang, F., et al., Selective recovery of valuable metals from nickel converter slag at elevated temperature with sulfuric acid solution. Separation and Purification Technology, 2015. 156: p. 572-581.
8. Li, Y., V.G. Papangelakis, and I. Perederiy, High-pressure oxidative acid leaching of nickel smelter slag: Characterization of feed and residue. Hydrometallurgy, 2009. 97(3-4): p. 185-193.
9. Perederiy, I. and V.G. Papangelakis, Why amorphous FeO-SiO2 slags do not acid-leach at high temperatures. J Hazard Mater, 2017. 321: p. 737-744.
10. Bai, S., Fu, X., Li, C., Wen, S., (2018) 'Process improvement and kinetic study on copper leaching from low-grade cuprite ores', Physicochem. Probl. Miner. Process., 54(2), 300-310, doi: 10.5277/ppmp1818.

11. Piatak, N.M., M.B. Parsons, and R.R. Seal, Characteristics and environmental aspects of slag: A review. Applied Geochemistry, 2015. 57: p. 236-266.
12. Gabasiane, T.S., et al., Characterization of copper slag for beneficiation of iron and copper. Heliyon, 2021. 7(4): p. e06757.
13. Letswalo P., Martin G., 2018. Mineralogical Report: 18/021. SGS South Africa (Pty) Ltd, pg 19-24.
14. Li, Y., I. Perederiy, and V.G. Papangelakis, Cleaning of waste smelter slags and recovery of valuable metals by pressure oxidative leaching. J Hazard Mater, 2008. 152(2): p. 607-15.
15. Souza A.D., Pina P.S., Lima E.V.O., da Silva C.A., Leão V.A., (2007) 'Kinetics of sulfuric acid leaching of a zinc silicate calcine', Hydrometallurgy, 89, 337-345
16. McDonald, R. G., and Muir, D. M. (2007b) 'Pressure oxidation leaching of chalcopyrite. Part II: Comparison of medium temperature kinetics and products and effect of chloride ion', Hydrometallurgy, 86(3–4), pp. 206–220. doi: 10.1016/j.hydromet.2006.11.016.
17. Han, B. et al. (2017) 'Leaching and Kinetic Study on Pressure Oxidation of Chalcopyrite in H_2SO_4 Solution and the Effect of Pyrite on Chalcopyrite Leaching', Journal of Sustainable Metallurgy. Springer International Publishing, 3(3), pp. 528–542. doi: 10.1007/s40831-017-0135-3.
18. Tao, L., Wang, L., Yang, K., Wang, X., Chen, L., and Ninga, P., (2021). Leaching of iron from copper tailings by sulfuric acid: behavior, kinetics and mechanism. RSC Adv., 2021, 11, 5741. Doi: 10.1039/d0ra08865j.

Chapter 3. Selective separation of metals from leach liquor by solvent extraction, precipitation, and xanthate complexation

The objective of this chapter is to illustrate the separation process developed to selectively separate metal ions of Ni, Cu, Co, and Fe from the pregnant leach solution (PLS) using various separation and enrichment techniques. Three hydrometallurgical processes of solvent extraction (SX), precipitation, and xanthate complexation processes are discussed in this chapter. The solvent extraction method was mainly used to separate copper from other metals (Ni, Co) and impurities (Fe, etc.) as well as to upgrade the copper concentration in the PLS. Solvent extraction is an important step in generating an electrolyte of high quality that can be electrowon to produce pure copper. Selective precipitation is known to have good selectivity for metal removal, fast reaction rates, and low solubility of the precipitated compound. Iron impurity in the solution, which is known to have detrimental effects on the upstream processes, was removed by precipitation from the solution. The xanthate complexation method displayed an effective route to separate nickel and cobalt from solution due to the strong hydrophobic properties of nickel and cobalt xanthates and the different solubility products (Ksp) between nickel xanthate and cobalt xanthate.

3.1 Solvent extraction of copper

Solvent extraction and stripping of copper were carried out using the pregnant leach solution obtained from the optimized high-pressure leaching experiment. The metal concentration in the PLS is displayed in table 3.1, showing very metal concentrations of nickel, copper, and cobalt. The solvent extraction technique provides an effective way to selectively extract copper from relatively dilute sulfuric acid leach solutions. A simulated multicomponent leach solution containing 0.3 g/L Cu^{2+}, 0.34 g/L Ni^{2+}, 0.13 g/L Co^{2+}, and 2.96 g/L Fe^{3+} was prepared and used for optimization tests during solvent extraction experiments.

Table 3.1: Metal concentration in the pregnant leach solution from HPOAL stage.

Element	Fe	Ni	Cu	Co
Concentration, g/L	2.96	0.34	0.30	0.13

3.1.1 Experimental Procedure

Batch solvent extraction tests were carried out using a countercurrent two-stage mixer settler extraction column illustrated in figure 3.1. Copper was selectively extracted using LIX 984N (10%v/v) with Isoper M as a diluent. The initial pH of the PLS was measured to be 1.0, and the pH was adjusted between 1.0 – 2.5 using a 1 M NaOH solution. For each extraction test, 400 ml of solution and 100 ml of diluted extractant (O/A = 0.25) were simultaneously fed by a pump into the extraction column at about 15 ml/s. The agitation speed was adjusted to the desired setpoint. Once the extractant has been filled into the extraction column, the respective pump was stopped to avoid air bubbles in the extraction column. The mixing and settling were allowed for 20 minutes to achieve steady-state and clear phase separation. The copper-loaded organic phase was then collected at its respective outlet leaving behind the copper barren aqueous phase (raffinate), which was collected afterward at the aqueous phase outlet. The raffinate solution was analyzed using MP-AES to determine the metal concentration and compute the extraction efficiency. Fundamental parameters influencing the extraction process such as pH and mixing speed were investigated.

The copper-loaded organic was subjected to stripping experiments using a sulfuric acid solution. The stripping column had a similar setup as the extraction column. A desired volume of the sulfuric acid solution (50 – 175 g/L H_2SO_4) and the copper loaded organic was pumped into the stripping column at 15 ml/s and mixed at an agitation speed of 400 rpm. After 20 minutes contacting, the barren organic and the stripped solution were collected separately from their respective outlets. The strip solution was analyzed using MP-AES for copper concentration and determination of the stripping efficiency. Fundamental parameters

influencing the stripping efficiency of copper such as H_2SO_4 concentration, and organic/aqueous (O/A) phase ratio were investigated. For copper enrichment in solution, a combination of two extraction stages and two stripping stages were employed. An illustration of the extraction and stripping procedure is shown in figure 3.2. In order to evaluate the possibility of re-using the extractant, the extractant was recycled a number of times in a few extraction tests, and its extraction efficiency was evaluated.

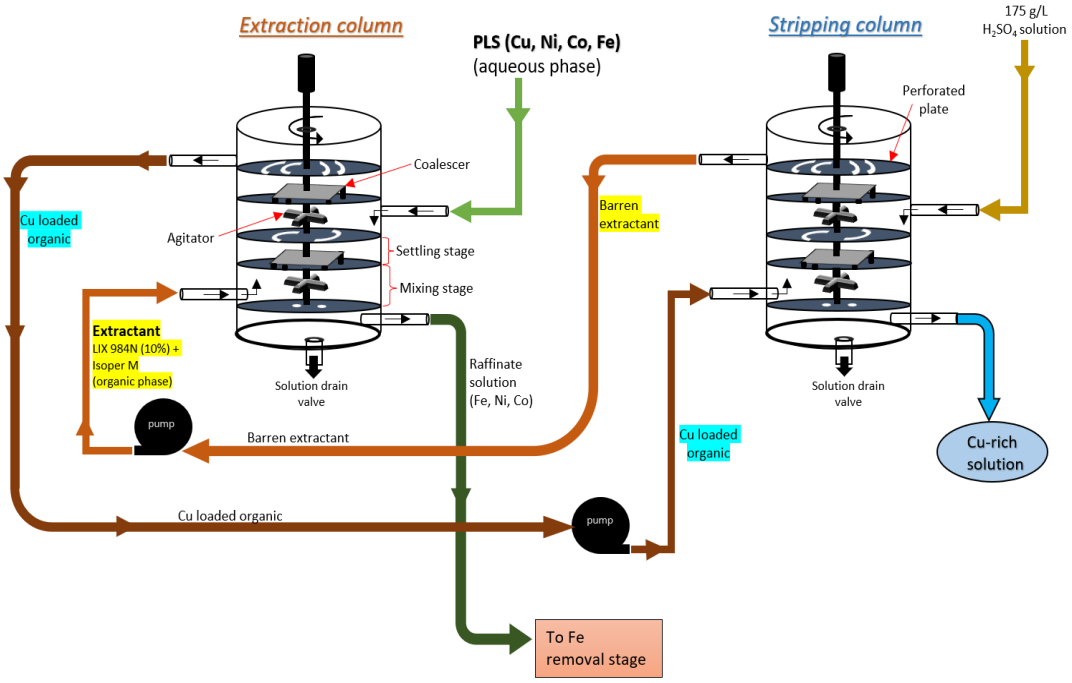

Figure 3.1: Experimental setup using a 2-stage mixer-settler extraction column

LIX 984N is a 1:1 aldoxime-ketoxime mixture of LIX 84-I (2-hydroxy-5-nonylace-tophenone ketoxime) and LIX 860-I (5-nonyl-salicyl aldoxime). Ketoximes are known to be highly stable in solvent extraction circuits and have excellent stripping ability, while aldoximes are strong and excellent selective copper extractants [1, 16]. Aldoxime-ketoxime mixtures are often preferred when Cu concentrations in the PLS are low [1]. The dissociation of oxime molecule (LIX 984N) resulting in the formation of Cu–LIX984N complex and thus enhancing the extraction of copper is illustrated in figure 3.3 [16].

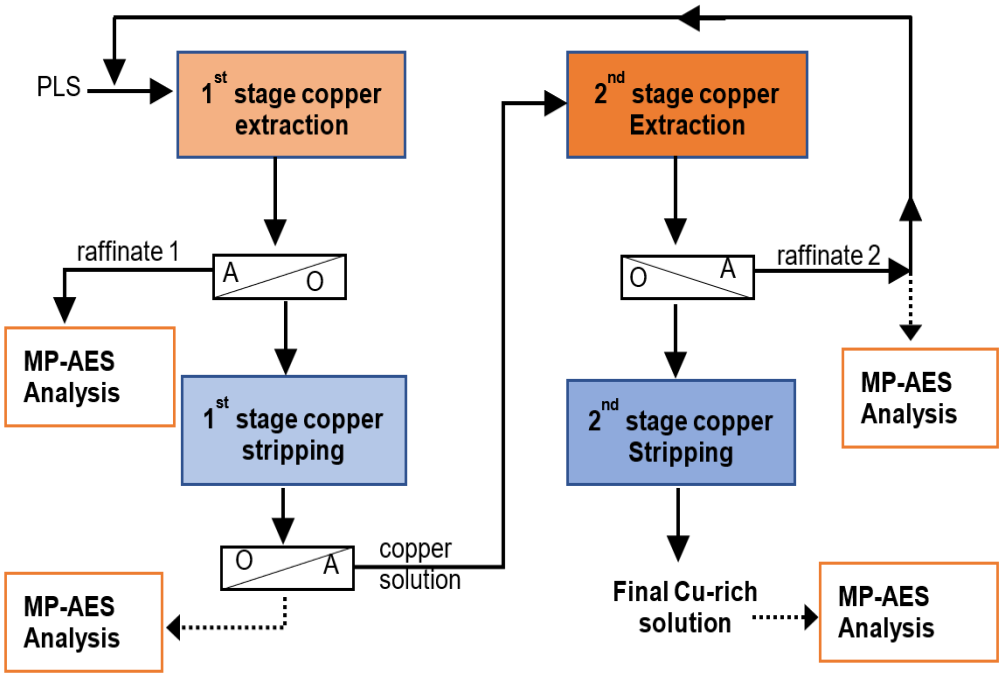

Figure 3.2: An illustration of the extraction and stripping procedure of the pregnant leach solution obtained from high–pressure oxidative acid leaching of slag.

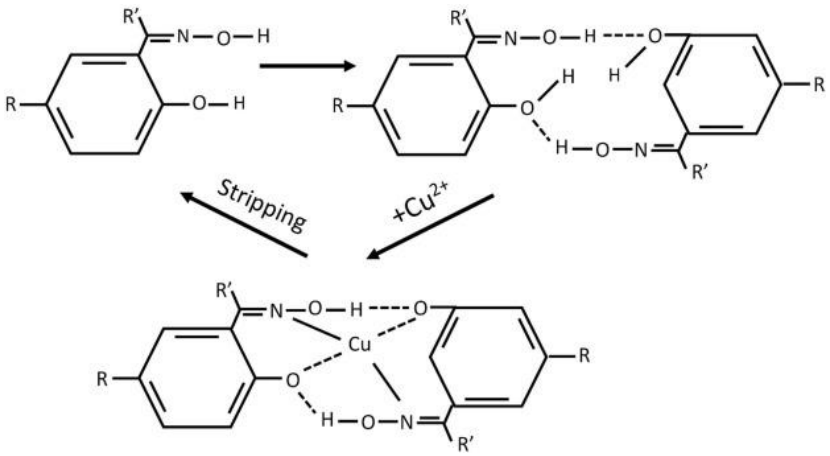

Figure 3.3: Copper extraction and stripping by ion-exchange chelation [16].

3.1.2 Results and discussions

3.1.2.1 Effect of stirring speed

The stirring speed was investigated in the range of 200 – 400 rpm to find the optimal operating conditions for the extraction of copper from the pregnant leach solution. The results are

displayed in figure 3.4, showing that as the stirring speed of the column extractor is increased, the copper extraction also increases, with the highest percentage extraction of 98.28% at 400 rpm. A high stirring speed increases the contact between the organic phase and the aqueous phase thus more copper is extracted from the leach solution. However, iron also had an increasing trend with an increase in the stirring speed, which is mostly by entrapment in the organic phase [1].

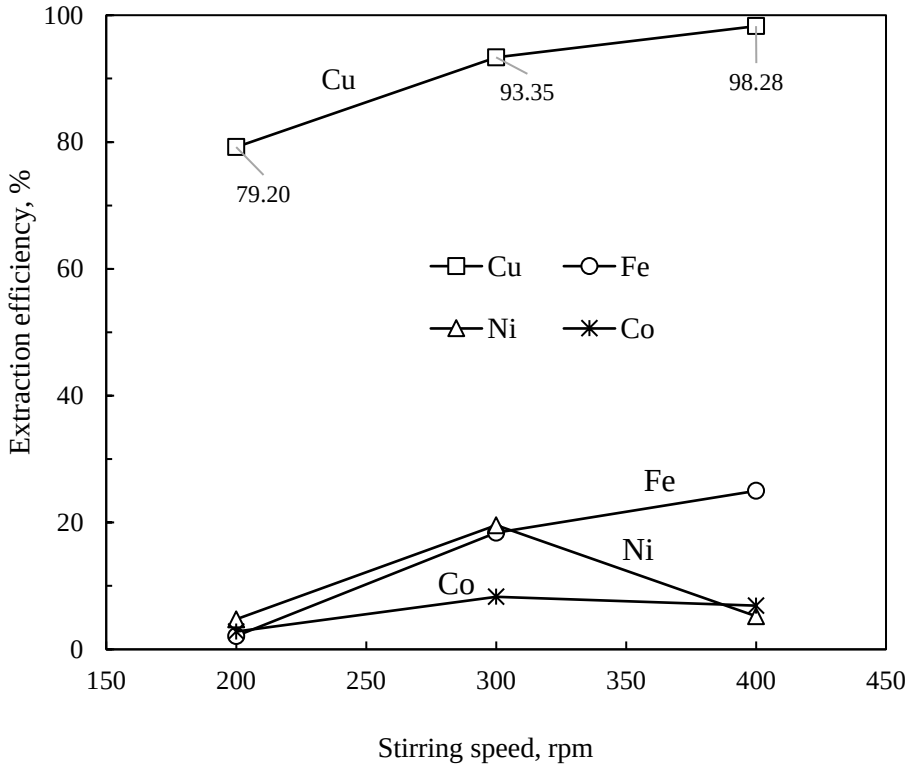

Figure 3.4: The extraction behavior of metals versus the stirring speed. Conditions: O/A ratio 0.25 (100 mL to 400 mL), pH 2.5, solutions flow rate 15 ml/s, and residence time 20 min)

3.1.2.2 Effect of pH on copper extraction

The pH was investigated in the range of 1 – 2.5 on metal extractions, and the, results are displayed in figure 3.5. As the pH increased, the amount of copper extracted from the pregnant leach solution likewise increased, reaching a high of 98.28% when the pH was 2.5. The amount

of Fe extracted with copper remained below 6% when the pH was 2 or lower, however, when the pH was increased to 2.5, the amount of Fe co-extracted with copper sharply increased to about 25% which is undesirable due to the consequential effects iron has in the upstream processes such as in the electrowinning process. Co-extractions of copper and nickel remained low at all the investigated pH values. Therefore, a pH of 2 was chosen as the optimal condition for the extraction of copper (97%) from the pregnant leach solution due to the good separation efficiency of copper from iron, nickel, and cobalt.

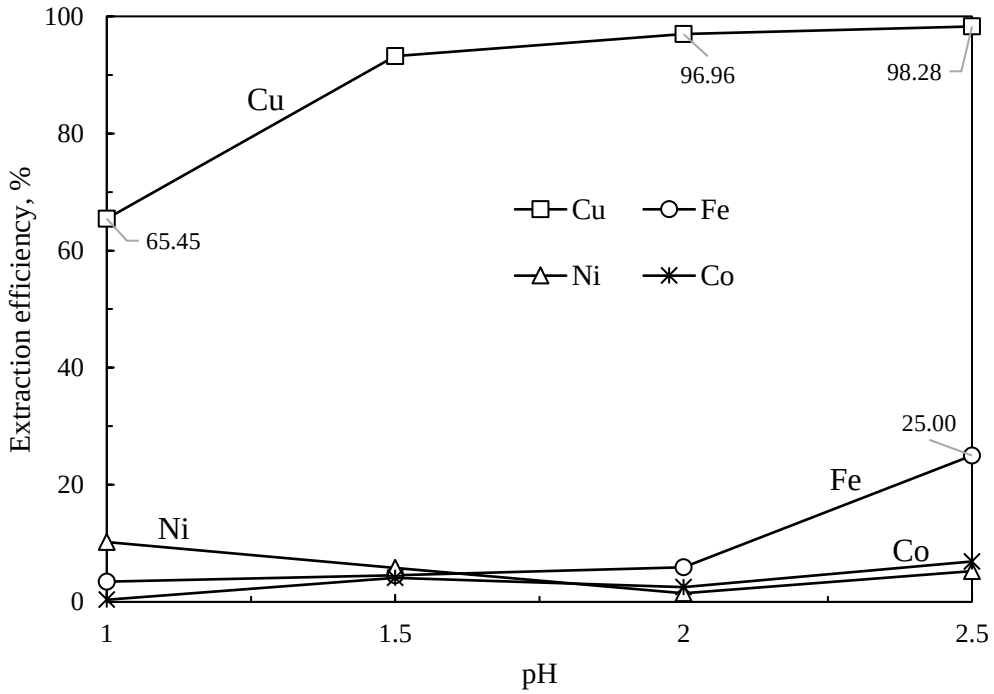

Figure 3.5: The extraction behavior of metals as a function of pH. Conditions: O/A ratio 0.25 (100 mL to 400 mL), agitating speed 400 rpm, solutions flow rate 15 ml/s, and residence time 20 min)

3.1.2.3 Effect of sulfuric acid concentration on stripping

The effect of sulfuric acid on the stripping of copper from the organic phase was investigated in the range of 50 g/L to 175 g/L H_2SO_4 concentration (figure 3.6). At lower acid concentration, 50 g/L H_2SO_4, copper stripping efficiency was low, and only 66% was recovered from the organic phase while the amount of iron stripped from the organic phase was high at 89%. As

the concentration of sulfuric acid increased, so as the separation efficiency between copper and iron. Utilizing a sulfuric acid concentration of 175 g/L, a high copper stripping efficiency of 97.28% was achieved, with a lower iron stripping efficiency at 15.63%, yielding a separation efficiency of 81.65% between copper and iron. Therefore 175 g/L sulfuric acid was selected as the optimum conditions for efficient copper stripping from the organic phase.

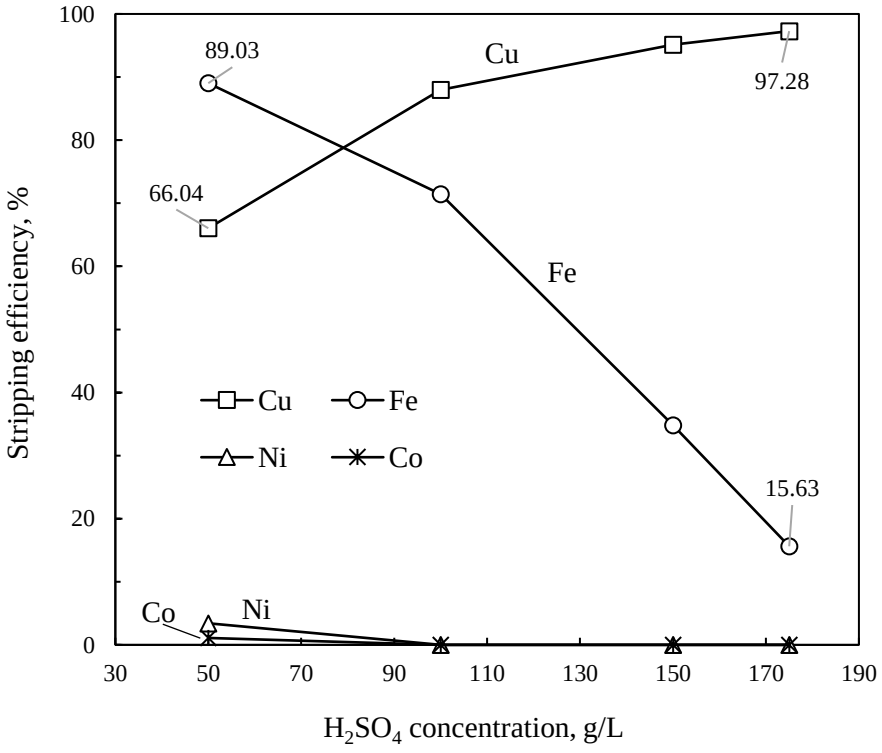

Figure 3.6: The copper stripping behavior of metals as a function of sulfuric acid concentration. Conditions: O/A ratio 0.25 (100 mL to 400 mL), stirring speed 400 rpm, solutions flow rate 15 ml/s, and residence time 20 min)

3.1.2.4 Effect of organic/aqueous (O/A) ratio

The organic/aqueous (O/A) ratio was investigated to achieve a higher copper concentration in the stripped solution. The copper concentration increased from 0.26 g/L to 4.18 g/L as the O/A ratio was increased from 1:4 to 4:1 of O:A volume ratio. The concentration of iron slightly increased as the O/A ratio was increased, reaching a high of 1.27 g/L at a 4:1 O/A ratio. The

stripping efficiency of copper was not significantly affected by the increase in the O/A ratio but maintained a stripping efficiency above 86% at the O/A ratio of 4:1 (figure 3.7).

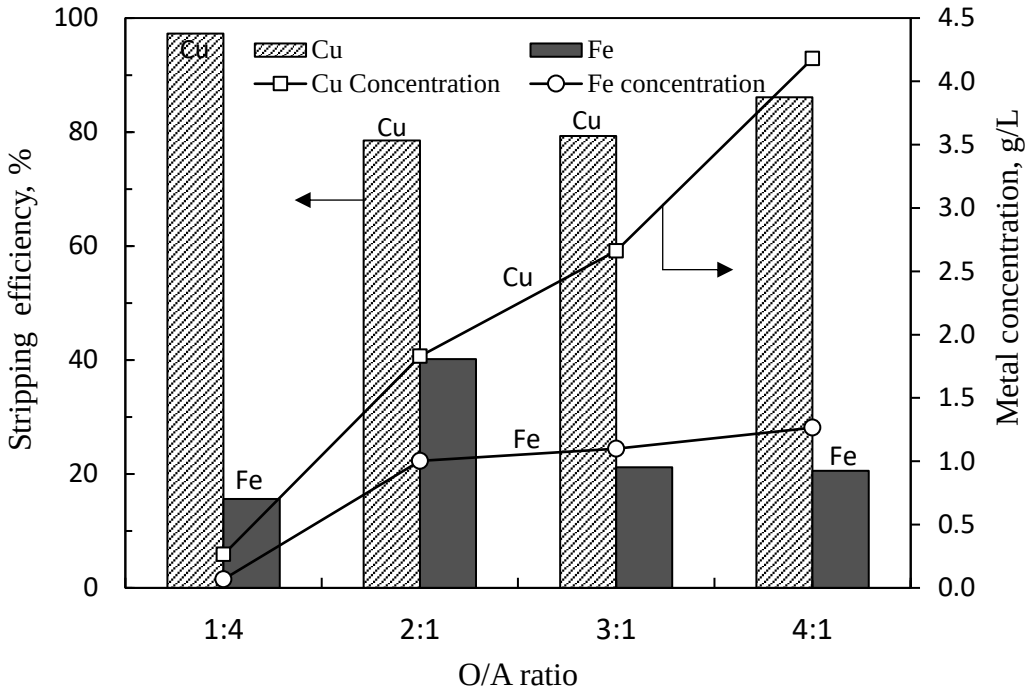

Figure 3.7: The effect of the organic/aqueous (O/A) ratio on the concentration of metals in the stripped copper solution. Conditions: H2SO4 concentration 175 g/L, stirring speed 400 rpm, solutions flow rate 15 ml/s, and residence time 20 min)

3.1.2.5 Two stages of copper extraction and stripping

The stripped solution obtained under the optimal conditions in sub-section 4.1.2.5 (O/A ratio 4:1) was further contacted with a fresh extractant to carry out the second stage of extraction and stripping stages. Figure 3.8 shows the results obtained after employing 2 stages of copper extraction and 2 stages of copper stripping to further upgrade the copper concentration in the final stripped solution. The conditions of extraction and stripping in the second stages were kept the same as in the first extraction and stripping stages. The copper concentration was successfully upgraded from 4.18 g/L in the first extraction and stripping stages to 22.9 g/L in the second extraction and stripping stages. Moreover, iron concentration was further minimized in the final stripped solution, decreasing from 1.27 g/L to 0.05 g/L in the first and second stripped solution, respectively.

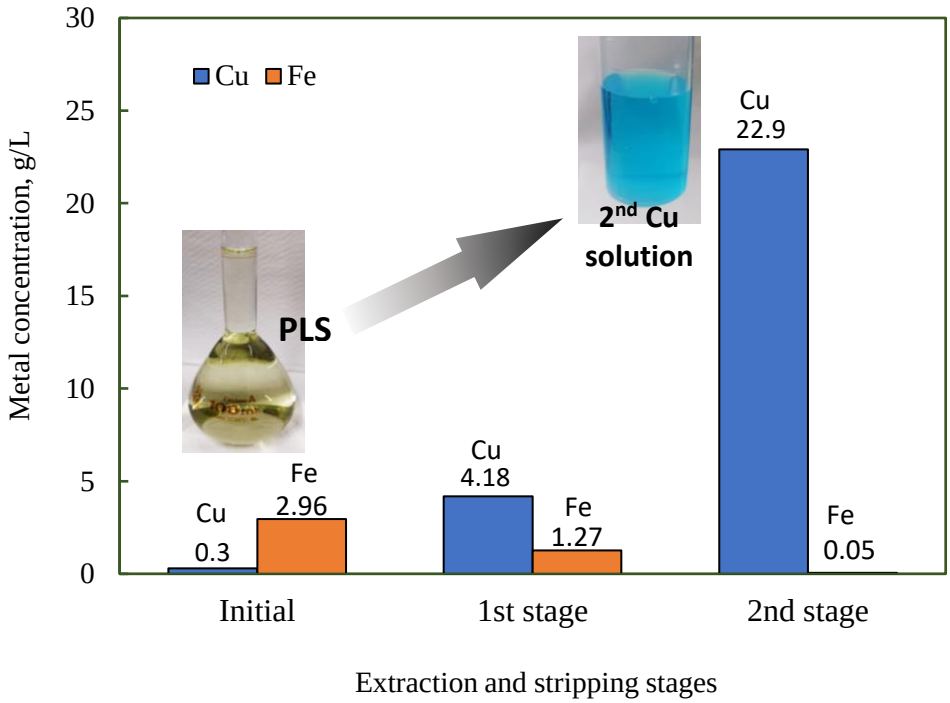

Figure 3.8: A summary of the change in concentration of metals in the stripped copper solution as the number of extraction and stripping stages increase.

3.2 Iron removal

3.2.1 Experimental procedure

The raffinate solution obtained from the first extraction stage contained 0.303 g/L nickel, 0.125 g/L cobalt, and 2.52 g/L iron and was further processed for iron removal. A prepared calcium carbonate emulsion of 200 g/L was added to the raffinate solution in a dropwise manner, to achieve a pH of 4. The raffinate solution was then heated to 65 °C using a magnetic stirrer operating at 500 rpm. Once the temperature reached 65 °C the reaction time was set to 20 minutes. A schematic of the iron removal process is illustrated in figure 3.9. The resulting precipitate and the residual solution were cooled and filtered and the solution was taken for MP-AES analysis for the elemental analysis to determine the precipitation efficiency. The Fe precipitate solids were dried and analyzed for mineral composition using XRD while part was dissolved using aqua regia for chemical analysis of the precipitated solids.

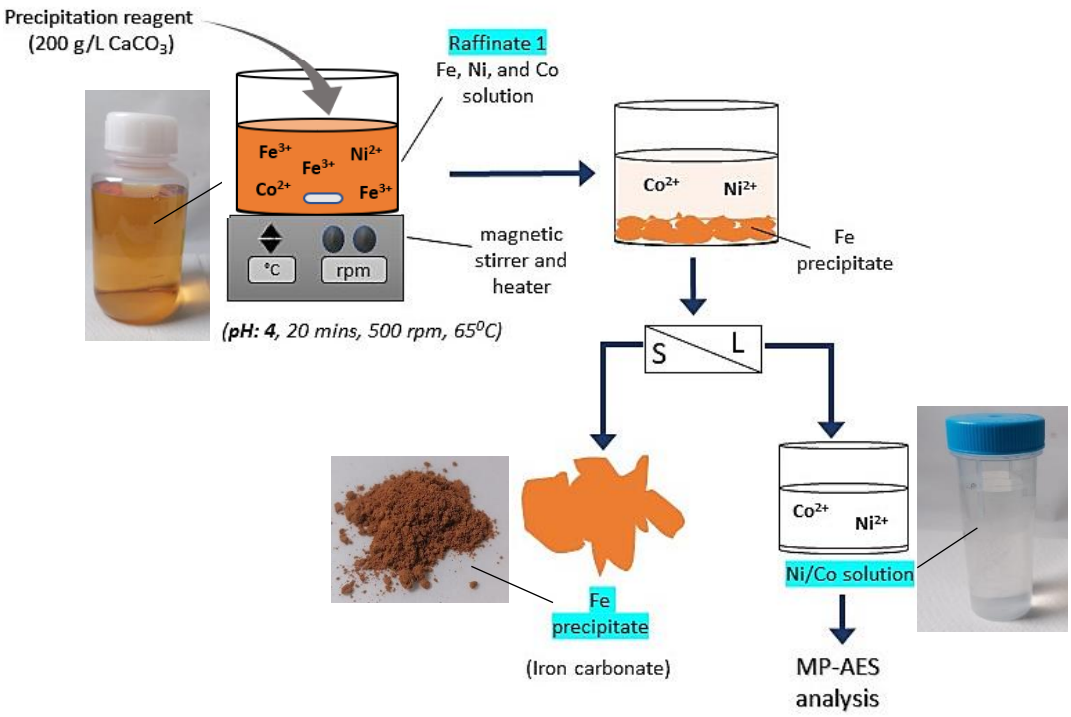

Figure 3.9: A schematic illustration of the iron removal procedure.

3.2.2 Results and discussions

Figure 3.10 shows the results obtained after iron removal using a calcium carbonate precipitating reagent. Excellent removal of iron (99.99%) from the solution was achieved at a pH of 4, with no residual iron detected by MP-AES. The post precipitation pH was measured to be about 3.5. Possible reactions during precipitation of iron from solution using $CaCO_3$ are displayed in reactions 3.1 – 3.3, which can either be in crystalline structure or colloidal form [10,18]. Bhattacharjee et al. noted that the precipitation of iron using calcium carbonate may also form a mixture of calcium-iron hydroxides ($Ca_3Fe_2(OH)_{12}$) [17]. Low co-precipitation of nickel and cobalt was obtained at 3.68% and 2.27%, respectively. An XRD analysis of the obtained precipitates was carried out and the result is displayed in figure 3.11. The main mineral component is shown to be gypsum, while the iron mineral components could not be detected by XRD, indicating that the iron precipitate formed may exist in a colloidal structure, not in a crystalline structure. The precipitate was chemically analyzed to contain about 12 wt.% Fe.

$Fe^{2+}_{(aq)} + CO_3^{2-}{}_{(aq)} \rightarrow FeCO_{3\,(s)} + 2e^-$ 3.1

$Fe^{3+}_{(aq)} + 3OH^-_{(aq)} \rightarrow Fe(OH)_{3\,(s)}$ 3.2

$Ca^{2+}\,(aq) + SO_4^{2-}\,(aq) + 2H_2O \rightarrow CaSO_4.2H_2O\,(s)$ 3.3

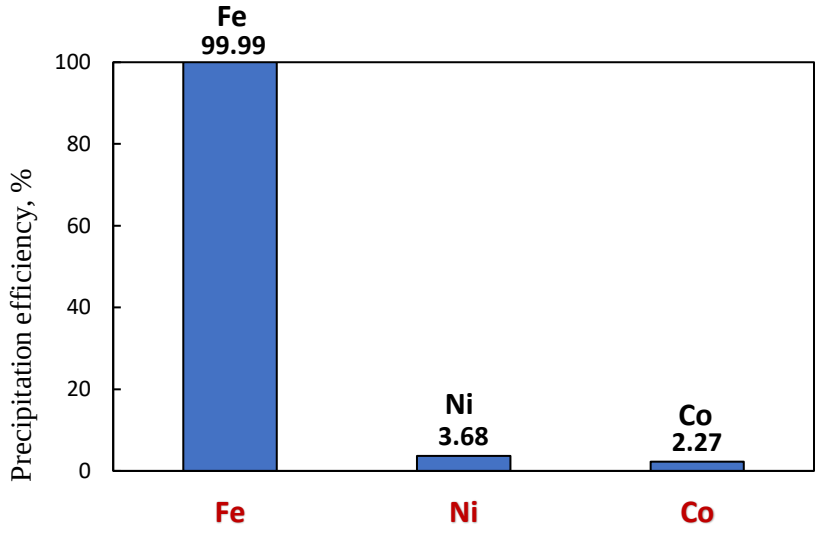

Figure 3.10: Metal precipitation efficiency from raffinate 1 using calcium carbonate emulsion.

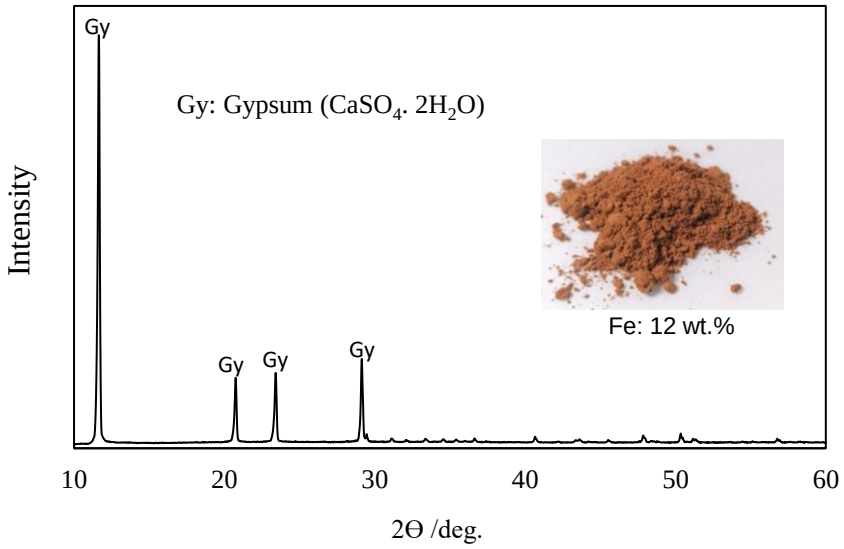

Figure 3.11: An XRD pattern of the precipitate obtained after iron removal.

3.3 Xanthate complexation of nickel and cobalt

For the recovery of nickel and cobalt from the raffinate solution obtained from the first stage of copper extraction, a xanthate complexation method was used. Nickel and cobalt xanthates form insoluble metal xanthates which are hydrophobic [15], making it possible to remove nickel and cobalt as xanthate precipitates from the solution. Potassium amyl xanthate, PAX, (potassium-O-pentyl dithiocarbonate), with a structure displayed in figure 3.12, was used to complex nickel and cobalt (equations 3.4 and 3.5). The xanthates' solubility product constant (Ksp) is an essential physicochemical parameter affecting the selective extraction of metals in hydrometallurgical methods [12]. Therefore, factors such as the solution pH significantly influence the Ksp. The nickel xanthate has a lower K_{sp} of about 12.5 compared to that of cobalt xanthate at 24.2 [11], therefore nickel and cobalt xanthates can easily be dissolved while the cobalt xanthate remains as an unaltered precipitate, which can be calcined to obtain cobalt oxide powder.

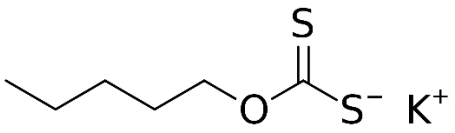

Figure 3.12: Chemical structure of potassium amyl xanthate, PAX ($C_6H_{11}KOS_2$)

The complexation of nickel and cobalt from solution using PAX is suggested to follow reactions (3.4) and (3.5), respectively [12, 13].

$$Ni^{2+} + 2CH_3(CH_2)_4OCS_2K \rightarrow Ni(CH_3(CH_2)_4OCSS)_2 + 2K^+ \quad (3.4)$$

$$Co^{2+} + 2CH_3(CH_2)_4OCS_2K \rightarrow Co(CH_3(CH_2)_4OCSS)_2 + 2K^+ \quad (3.5)$$

3.3.1 Experimental procedure

3.3.1.1 Complexation of nickel and cobalt

For the recovery of nickel and cobalt from the raffinate solution obtained from the first copper extraction stage, a potassium amyl xanthate (PAX) solution of 55 g/L was prepared and dosed

correspondingly to achieve the desired molar ratio of xanthate to nickel and cobalt. A 50 ml solution of the raffinate was utilized for each complexation test. The pH was investigated between 4 to 8, with a pH of 4 being the initial pH of the raffinate solution. A 1 mol/L NaOH solution was used to adjust the pH to the required pH. The mixture was then heated to 50 °C using a magnetic stirrer operating at 400 rpm. The complexation reaction was allowed to proceed for 2 h, after which the solution was cooled and filtered. The residual barren solution was analyzed using MP-AES to determine the amount of nickel and cobalt remaining in the solution and accordingly calculate the complexation efficiency. The Ni/Co xanthate precipitate was directly taken to the next stage without being dried.

The Ni/Co xanthate precipitate was washed with 10 ml of a 28% analytical grade ammonia solution (NH_3) and shaken at 400 rpm for 20 minutes at 30 °C. The solution was filtered and taken for MP-AES analysis to determine the amount of nickel dissolved, while the remaining cobalt xanthate was dried before the calcination process. The cobalt xanthate precipitate was roasted in a muffle furnace at 220 °C for 1.5 h. After the calcination process, the products were cooled to room temperature and analyzed using XRD for mineral identification. Part of the calcined product was dissolved using aqua regia and analyzed for elemental composition using MP-AES.

3.3.1.2 Ammoniacal dissolution of nickel

The Ni/Co xanthate precipitate was washed with 10 ml of ammonia solution and shaken for 15 minutes using a shaker at room temperature. The solution was filtered and taken for MP-AES analysis to determine the amount of nickel dissolved, while the remaining cobalt xanthate was dried before the calcination process.

3.3.1.3 Calcination of cobalt xanthate

The cobalt xanthate precipitate remaining after nickel xanthate washing was dried overnight, weighed, and roasted in a muffle furnace at 220 °C for 1.5 hrs. After the calcination process

was complete, the calcined products were removed and cooled to room temperature before being analyzed using XRD for mineral identification. Part of the calcined product was dissolved using aqua regia and analyzed for elemental composition using MP-AES.

An illustrative schematic of the metal separation processes in chapter 3 is shown in figure 3.13.

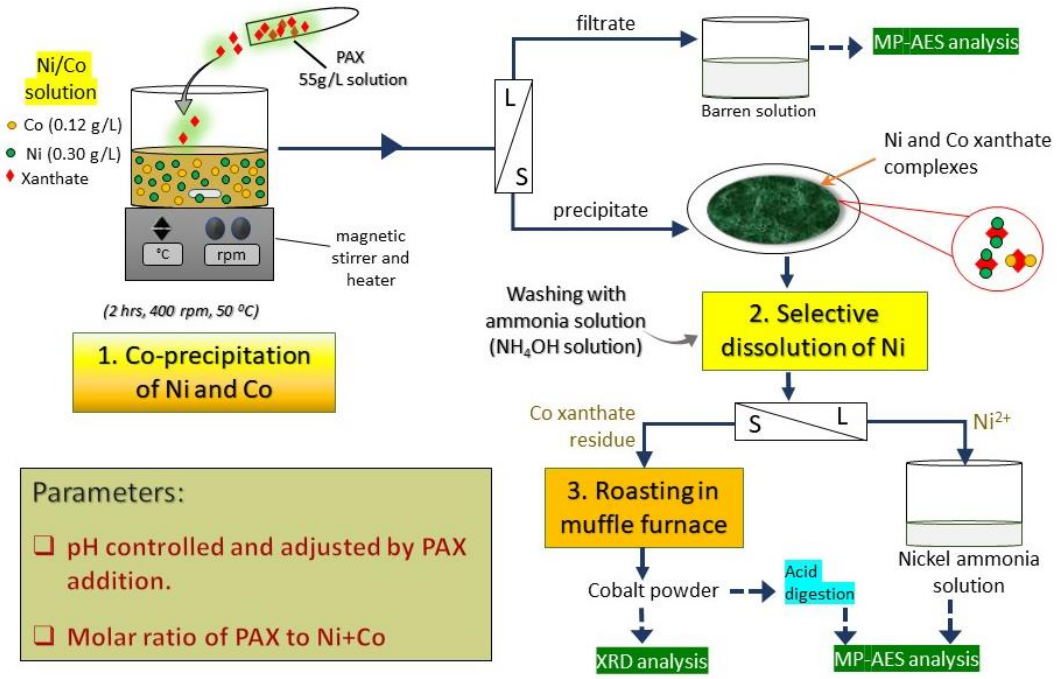

Figure 3.13: A schematic illustration of the Ni/Co separation procedure by xanthate complexation.

3.3.2 Results and discussions

3.3.2.1 Complexation of nickel and cobalt

3.3.2.1.1 Effect of pH

The solution pH is an important parameter that significantly influences the K_{sp} and the stability of xanthates [19], thus, consequently affecting the selective extraction of metals from the solution. Therefore, the effect of pH on the co-extraction of nickel and cobalt from the solution using PAX as a complexing agent was investigated. Figure 3.14 shows the complexation behavior of nickel and cobalt under different pH conditions, at 50 °C, 2 h, 400 rpm, and 1.5

molar ratio of xanthate to nickel and cobalt. The results show that a pH of about 6 is conducive for complexing Ni and Co from solution using PAX, yielding a complexation efficiency of 83.6% and 99.4% for nickel and cobalt, respectively.

At lower pH values, the xanthate complexation efficiency of nickel and cobalt is low which is attributed to the decomposition of xanthate in acidic conditions, thus resulting in insufficient xanthate ions to form nickel and cobalt complexes. A further increase in pH resulted in a decline in the formation of nickel xanthate precipitate, however, cobalt complexation efficiency was not affected by an increase in pH above 6 and maintained complete extraction from the solution. A lower complexation of Ni than Co may be attributed to a lower K_{sp} of nickel xanthate ($Ni(C_2H_5OCSS)_2$) as compared to cobalt xanthate ($Co(C_2H_5OCSS)_2$) [11], making $Ni(C_2H_5OCSS)_2$ more unstable than $Co(C_2H_5OCSS)_2$, and therefore easily re-dissolves. At high pH values, hydroxide ions have also been noted to compete with xanthates for metal ions [19], this also may have contributed to the low nickel xanthate complexation efficiency.

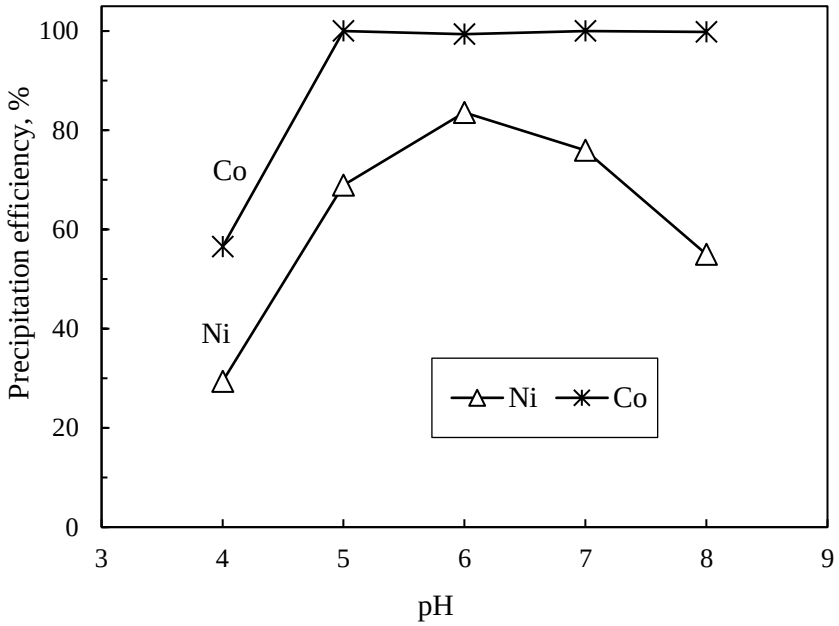

Figure 3.14: The effect of pH on the Ni/Co complexation using PAX.
Conditions: 50 °C, 2hrs, 400 rpm.

3.3.2.1.2 Effect of xanthate to Ni/Co molar ratio

The molar ratio of xanthate to nickel and cobalt ions was investigated between 1 and 2.5 by varying the PAX dosage. Other complexation conditions were kept constant at 50 °C, pH of 6, 400 rpm, and a reaction time of 2 h. The results are displayed in Figure 3.15, showing that as the xanthate/(Ni+Co) molar ratio was increased, the complexation efficiency of nickel and cobalt likewise increased. At a xanthate/(Ni+Co) molar ratio of 2, almost all the nickel (99.3 %) and the cobalt (99.9 %) were complexed out of the raffinate solution, which is in agreement with reactions (3.4) and (3.5). A xanthate/(Ni+Co) molar ratio of less than 2 results in insufficient xanthate ions required to form complexes with Ni and Co, while a molar ratio beyond 2 provides excess xanthate ions that enable complete complexation of Ni and Co from the solution. The tendency of xanthate to form metal complexes with cobalt was preferred over nickel as observed by a consistent complexation efficiency of more than 99.9% even at xanthate/(Ni+Co) molar ratios of less than 2. This indicates that cobalt may have a stronger affinity to xanthate than nickel, and thus rapidly binds and forms stable cobalt xanthate complexes.

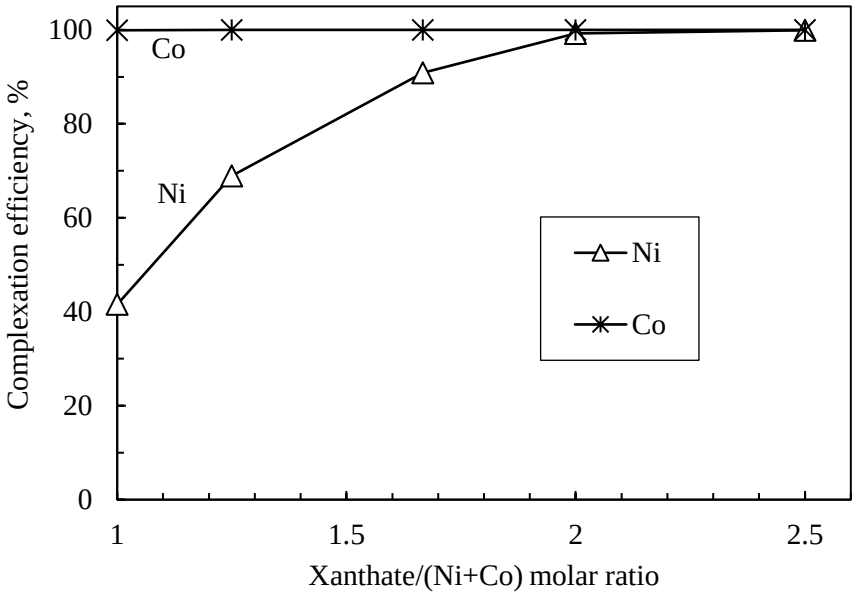

Figure 3.15: The effect of xanthate/(Ni+Co) molar ratio on the Ni/Co complexation using PAX. Conditions: 50 °C, pH 6, 2 h, 400 rpm.

3.3.2.2 Ammoniacal dissolution of nickel

For the separation of nickel and cobalt xanthate complexes, the difference in their solubility product (K_{sp}) was explored. Since nickel xanthate has a lower solubility product (K_{sp}) of 1.4×10^{-12} than cobalt xanthate (1.0×10^{-13}) [13], nickel xanthate can therefore be easily dissolved, while cobalt remains in the solid form. Additionally, nickel is known to form stable complexes with ammonia [11], therefore, an analytical grade 28% ammonia solution (NH_3) was directly used to selectively dissolve the nickel xanthate complex while cobalt xanthate remained in solid form. The dissolution of nickel xanthate complex using 10 ml ammonia solution, at 30 °C, 400 rpm for 20 min was anticipated to follow the reaction (3.5) [15]. The nickel xanthate dissolution percentage of 75.4% was obtained, yielding a nickel ammine solution of 1.2 g/L Ni, which was confirmed by the blue color. Cobalt was not detected in the wash solution by MP-AES analysis, as shown in table 3.2, confirming that almost all cobalt xanthate remained in solid form due to its higher K_{sp}. The incomplete dissolution of nickel xanthate may be attributed to the easy hydrolysis of NH_3 to NH_4^+ in an aqueous solution, resulting in insufficient ammonia to react with Ni in the solution [11].

$$Ni(CH_3(CH_2)_4OCSS)_{2\,(s)} + 6NH_{3(aq)} \rightarrow Ni(NH_3)_6^{2+}{}_{(aq)} + 2CH_3(CH_2)_4OCSS^-{}_{(aq)} \qquad 3.5$$

Table 3.2: Metal concentration in the solution after washing of Ni/Co xanthate precipitate.

Metal	Concentration, g/L	Amount washed, %
Ni	1.20	75.4
Co	0	0

3.3.2.3 Calcination of cobalt xanthate

The cobalt xanthate precipitate was thermally treated in a muffle furnace for 1.5 hrs. at 220 °C and the XRD pattern of the calcined product obtained is shown in figure 3.16. Cobalt xanthate was decomposed to form cobalt oxide powder. The chemical analysis of the CoO powder using MP-AES yielded a cobalt grade of 25.0 wt.%.

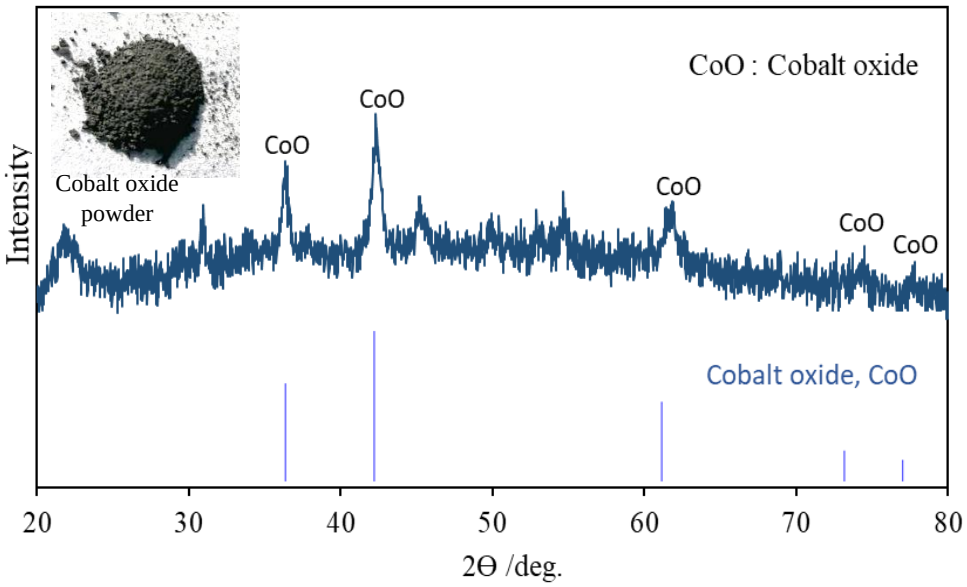

Figure 3.16: An XRD pattern of the calcined product obtained after cobalt xanthate precipitate calcination.

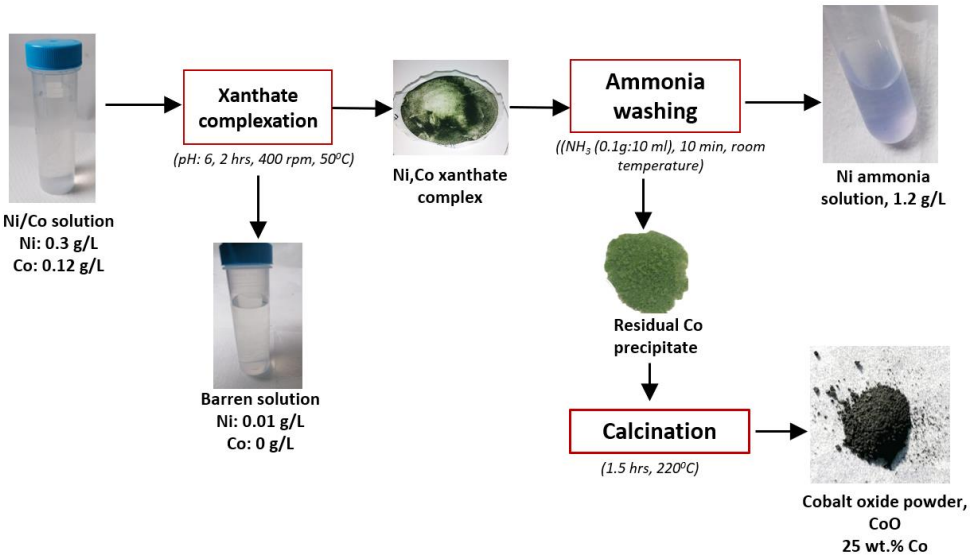

Figure 3.17: A summary of the separation process for nickel and cobalt from solution.

3.4 Summary of the separation process of Cu, Ni, and Co

The separation of metal ions from the pregnant leach solution (PLS) and the removal of impurities from the leach solution is very important in enabling efficient operation in the upstream processes to achieve high purity metals by electrowinning. Three hydrometallurgical processes of solvent extraction (SX), precipitation, and xanthate complexation processes were developed to selectively separate metal ions of Ni, Cu, and Co, and remove the Fe impurity from the pregnant leach solution (PLS). The solvent extraction method was used to separate copper from other metals (Ni, Co) and Fe impurity as well as upgrading the copper concentration in the PLS. Solvent extraction is an important step in generating an electrolyte of high quality that can be electrowon to produce pure copper. The multicomponent leach solution obtained from the high-pressure leaching of the smelter slag contained 0.3 g/L Cu, 0.34 g/L Ni, 0.13 g/L Co, and 2.96 g/L Fe. Batch solvent extraction tests were carried out using a countercurrent two-stage mixer settler extraction column. Copper was selectively extracted using LIX 984N (10%v/v) with Isoper M as a diluent and stripped with sulfuric acid (H_2SO_4) solution. Fundamental parameters influencing the extraction process such as pH, mixing speed, H_2SO_4 concentration, and organic/aqueous (O/A) phase ratio were investigated. Copper was successively separated from Fe, Ni, and Co under optimized extraction conditions (pH 2, mixing speed 400 rpm, O/A 1:4, and 20 minutes contacting time) and stripping conditions (175 g/L H_2SO_4, mixing speed 400 rpm, O/A 4:1, and 20 minutes contacting time). For copper enrichment in solution, a combination of two extraction stages and two stripping stages were employed. About 97% of copper was extracted from the simulated solution with coextraction of Fe, Ni, and Co of about 5.90%, 1.47%, and 2.53%, respectively. A final Cu-rich solution of about 23 g/L Cu was obtained with a very low Fe concentration of 0.05 g/L and no Ni and Co coextraction in the second stage.

Iron impurity in the solution, which is known to have detrimental effects on the upstream processes, was removed by selective precipitation from the Ni/Co raffinate solution. More than

99% of iron was precipitated at pH 4 by the addition of a calcium carbonate ($CaCO_3$) suspension, with low coprecipitation of nickel and cobalt of around 3.68% and 2.27%, respectively. The xanthate complexation method (figure 3.17) displayed an effective route to separate nickel and cobalt from solution due to the strong hydrophobic properties of nickel and cobalt xanthates and the different solubility products (Ksp) between nickel xanthate and cobalt xanthate. A good 99.3 % of nickel and 99.9% cobalt were co-precipitated from the solution by potassium amyl xanthate (PAX) solution (55 g/L) at pH 6 forming Ni and cobalt xanthates. Selective dissolution of nickel xanthate using ammonia solution was achieved while more than 99% Co remained as cobalt xanthate precipitate, which was roasted and recovered as CoO powder of about 25 wt.% Co.

3.5 Conclusion

This chapter presents various separation techniques to selectively separate metal ions from the pregnant leach solution (PLS) and upgrade the content of the metals from the dilute PLS. The general findings obtained from the three main processes (solvent extraction, precipitation, and xanthate complexation) investigated can be concluded as follows:

(1) Solvent extraction

- About 97% of copper was selectively extracted from the PLS obtained from the high-pressure leaching of the smelter slag using LIX 984N (10%v/v) extractant and 175 g/L sulfuric acid (H_2SO_4) strip solution.
- Utilizing a combination of two extraction stages and two stripping stages, copper concentration in the PLS was remarkably upgraded from 0.3 g/L Cu to 23 g/L Cu with a very low impurity content concentration of 0.05 g/L Fe and no Ni and Co coextraction in the second stage.

(2) Iron removal

- More than 99% of iron was precipitated at pH 4 by the addition of a calcium carbonate ($CaCO_3$) suspension, with low coprecipitation of nickel and cobalt of around 3.68% and 2.27%, respectively.

(3) Xanthate complexation

- A good 99.3 % of nickel and 99.9% cobalt were co-precipitated from the solution by potassium amyl xanthate (PAX) solution (55 g/L) at pH 6 and a xanthate/(Ni+Co) molar ratio of 2, forming Ni and cobalt xanthates.
- Selective dissolution of nickel xanthate using ammonia solution yielded 75.4% nickel xanthate dissolution at a concentration of 1.2 g/L Ni. Due to a higher solubility constant of cobalt xanthate, more than 99% Co successfully remained as cobalt xanthate precipitate.
- Cobalt xanthate precipitate was roasted and recovered as CoO powder of about 25 wt.% Co.

An efficient hydrometallurgical process for recovery of Cu, Ni, and Co from smelter slag is proposed, with the obtained total metal recoveries as follows; 94% Ni, 81% Cu, and 95% Co. Therefore, the utilization of smelter slag as a secondary source of valuable metals is viable using a combined hydrometallurgical process of HPOL, solvent extraction, selective precipitation, and xanthate complexation.

References

1. Schlesinger, M. E.; King, M. J.; Sole, K. C.; Davenport, W. G. Extractive Metallurgy of Copper, 5th ed.; Elsevier: UK, 2011; pp. 68, 356, 358, and 361.
2. Banza, A.N., Gock, E., Kongolo, K., 2002. Base metals recovery from copper smelter slag by oxidizing leaching and solvent extraction. Hydrometallurgy 67, 63–69.
3. Takahashi K., and Nii, S., Behavior of Multistage Mixer-settler Extraction Column, Memoirs of the School of Engineering, Department of Chemical Engineering, Nagoya University, Vol.51, No.1 (1999)
4. Kurniawan, et al., Simple and complete separation of copper from nickel in the ammoniacal leach solutions of metal coated ABS plastic waste by antagonistic extraction using a mixture of LIX 84-I and TBP. Separation and Purification Technology, 2021. **255**.
5. Kursunoglu, S., Z.T. Ichlas, and M. Kaya, Solvent extraction process for the recovery of nickel and cobalt from Caldag laterite leach solution: The first bench-scale study. Hydrometallurgy, 2017. **169**: p. 135-141.
6. Perez, I.D., et al., Comparative study of selective copper recovery techniques from nickel laterite leach waste towards a competitive sustainable extractive process. Cleaner Engineering and Technology, 2020. **1**.
7. Sridhar, V. and J.K. Verma, Extraction of copper, nickel, and cobalt from the leach liquor of manganese-bearing sea nodules using LIX 984N and ACORGA M5640. Minerals Engineering, 2011. **24**(8): p. 959-962.
8. Huang, K., Q.-w. Li, and J. Chen, Recovery of copper, nickel, and cobalt from acidic pressure leaching solutions of low-grade sulfide flotation concentrate. Minerals Engineering, 2007. **20**(7): p. 722-728.
9. Parhi, P. and K. Sarangi, Separation of copper, zinc, cobalt and nickel ions by supported liquid membrane technique using LIX 84I, TOPS-99, and Cyanex 272. Separation and Purification Technology, 2008. **59**(2): p. 169-174.

10. Korchef, A. and M. Touaibi, Effect of pH and temperature on calcium carbonate precipitation by CO removal from iron-rich water. Water and Environment Journal, 2019. **34**(3): p. 331-341.
11. Yang, Y., et al., Recovering valuable metals from the leaching liquor of blended cathode material of spent lithium-ion battery. Journal of Environmental Chemical Engineering, 2020. **8**(5).
12. Darezereshki, E., et al., Hydrometallurgical Synthesis of Nickel Nano-Sulfides from Spent Lithium-Ion Batteries. Minerals, 2021. **11**(4).
13. Behrad Vakylabad, A., E. Darezereshki, and A. Hassanzadeh, Selective Recovery of Cobalt and Fabrication of Nano-Co_3S_4 from Pregnant Leach Solution of Spent Lithium-Ion Batteries. Journal of Sustainable Metallurgy, 2021. **7**(3): p. 1027-1044.
14. Tarun, C. V., Synthesis of metal xanthates and their application as latent catalysts for curing of epoxy resin, Graduate School Of Life Science And System Engineering Kyushu Institute Of Technology, (Doctoral Dissertation) 2015.
15. Yamasaki, T., Shimoiizaka, J., Sasaki, H., And Ohyama, T., (2011) Utilization Of Xanthate As A Selective Precipitant For Nickel And Cobalt Ions. (2nd Report) Separation Of Nickel From Cobalt. Journal of the Mining and Metallurgical Institute of Japan, 1963, Vol. 79 No. 896 p. 97-104. https://doi.org/10.2473/shigentosozai1953.79.896_97 (In Japanese)
16. Shakibania, S., et al., The effect of the chloride ion on chemical degradation of LIX 984N extractant. Minerals Engineering, 2020. 159.
17. Werner Stumm and Fred Lee, G. Oxygenation of Ferrous Iron. Department Of Sanitary Engineering, Harvard University, Cambridge, Mass. Reprinted from Industrial and Engineering Chemistry, Vol. 53, Page 143, 1961.
18. Bhattacharjee, S, Gupta, K K, Chakravarty, S, Thakur, P & Bhattacharyya, G. Separation Of Iron, Nickel, And Cobalt From Sulphated Leach Liquor Of Low Nickel Lateritic Oxide Ore. Separation Science And Technology, 39**,** 413-429, 2005.

19. Zhang, Y. H., L. M. Wu, P.-P. Huang, Q. Shen, and Z.-X. Sun, Determination and application of the solubility product of metal xanthate in mineral flotation and heavy metal removal in wastewater treatment. Minerals Engineering, 2018. **127**: p. 67-73. DOI: 10.1016/j.mineng.2018.07.016.

Chapter 4. Application of hydrometallurgical processes to mine tailings and complex carbonaceous sulfide ore

This chapter presents the application of high-pressure leaching technology to extract valuable metals from other metallurgical waste material (flotation tailings) and a complex ore of high impurity content (complex carbonaceous sulfide ore). Thus demonstrating that the HPL method is highly adaptable to a wide range of materials and through process optimization, it is possible to extract valuable metals from low-grade secondary material and difficult-to-treat ores. The application of HPL to flotation tailings highlights the importance of high-temperature oxidation treatment of metallurgical waste to convert the reactive and AMD minerals such as pyrite, to more stable solids such as hematite (Fe_2O_3) that are environmentally friendly for disposal/storage. High-pressure leaching of complex carbonaceous sulfide ore in oxygenated sulfuric acid solution was performed and the free acidity of the solution generated from sulfide minerals dissolution and leaching medium was determined. The measurement of free acidity is of considerable importance for improved process control and understanding of the leaching reactions occurring especially when leaching complex material.

The sections in this chapter contain excerpts from the following publications:

- **Godirilwe, L.L.**, Haga, K., Altansukh, B., Takasaki, Y., Ishiyama, D., Trifunovic, V., Avramovic, L., Jonovic, R., Stevanovic, Z., Shibayama, A. (2021). Copper Recovery and Reduction of Environmental Loading from Mine Tailings by High-Pressure Leaching and SX-EW Process. *Metals*, 11, 1335. https://doi.org/10.3390/met11091335
- **Godirilwe L.L.**, Magwaneng R.S., Sagami R., Haga K, Batnasan A., Aoki S., Kawasaki T., Matsuoka H., Mitsuhashi K., Kawata M., Shibayama A. (2021). Extraction of copper from complex carbonaceous sulfide ore by direct high-pressure leaching. *Minerals Engineering*, 173, 107181. https://doi.org/10.1016/j.mineng.2021.107181

4.1 Hydrometallurgical processing of mine tailings

4.1.1 Introduction

This study evaluates the high-pressure oxidative leaching (HPOL) method as an effective way to recover copper and reduce the environmental loading from the mine tailings obtained from Bor Copper Mine, Serbia. The flotation tailings contain pyrite (FeS_2) and chalcopyrite ($CuFeS_2$), these sulfide minerals are known to promote acid mine drainage (AMD) which poses a serious threat to the environment and human health [4–6]. Pyrite is a gangue mineral that is commonly found in mine tailings, when exposed to an environment with oxygen and water, oxidation of pyrite is promoted via equation 4.1, which results in low pH conditions of less than 3 [5,7–9]. The flotation tailings from Bor Copper Mine contain pyrite and chalcopyrite, therefore, management of these mine tailings is extremely important, as well as developing effective long-term strategies to reduce their environmental footprint. This study focuses on the treatment of the mine tailings to convert the AMD supporting minerals to more stable forms, while simultaneously valorizing the mine tailings. A combination of hydrometallurgical processes of high-pressure oxidative leaching (HPOL), solvent extraction (SX), and electrowinning (EW) were utilized to recover copper from the mine tailings.

4.1.2 Methodology

4.1.2.1 Sample

The chemical compositions of the two samples utilized in this study; the mine tailings and the concentrate obtained after the flotation of the mine tailings are shown in table 4.1. XRD (X-ray Diffraction) analysis (figure 4.1) showed that the main mineral compositions of the mine tailings and concentrate of the mine tailings were quartz (SiO_2), pyrite (FeS_2), and kaolinite ($Al_2Si_2O_5(OH_4)$). The main copper mineral in the mine tailings was identified as chalcopyrite ($CuFeS_2$) using SEM-EDS (Scanning Electron Microscope-Energy Dispersion Spectroscopy).

Table 4.1: Chemical compositions of the mine tailings and concentrate.

	Grade (wt.%)				
Elements	**Cu**	**Fe**	**Al**	**S**	**SiO_2**
Mine tailings	0.24	3.51	3.45	4.88	61.7
Concentrate from mine tailings	0.65	33.20	2.63	32.72	23.41

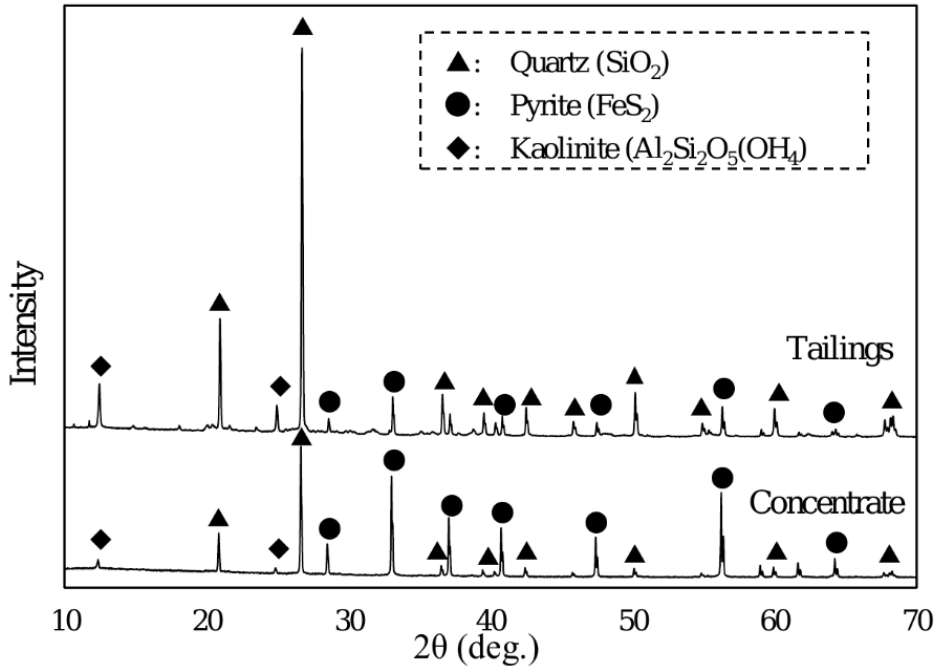

Figure 4.1: XRD patterns of mine tailings from Bor Copper Mine and concentrate of mine tailings.

4.1.2.2 Procedure

4.1.2.2.1 High-pressure leaching

An autoclave of a 200 ml teflon beaker was used as a leaching reactor in the high-pressure oxidative leaching experiment for the mine tailings and concentrate from mine tailings. A sample weight of 10 g was mixed with 0 – 1.0 M sulfuric acid (H_2SO_4) solution, where 0 M was distilled water, to obtain a pulp density of 100 g/L. The slurry was then placed inside the

autoclave and heated. After the temperature reached 180 °C, oxygen gas was injected at 2 MPa into the slurry to provide an oxidative environment. The leaching duration was set to 1 hour. After the HPOL experiment, the sample was cooled and filtered to obtain a pregnant leach solution (PLS) and a solid residue, which were taken for chemical and mineralogical analysis using ICP-OES and XRD, respectively.

4.1.2.2.2 Elution test

Elution properties of the mine tailings and the solid residue obtained after HPOL were evaluated. A sample weight of 0.4 g was placed in a sample tube (capacity: 5 mL) together with 4 mL of different pH solutions (pH 2 (adjusted with H_2SO_4), pH 4 (distilled water), and pH 7 (adjusted with $Ca(OH)_2$)). The solutions were shaken for 6 hours at 200 rpm, using a shaker (MMS-4020, EYELA). Afterward, the slurry was subjected to solid-liquid separation by centrifugation. Quantitative analysis of each metal in the solution was carried out using ICP-OES (SPS5500, SII nanotechnology). The elution rate was calculated as per equation 4.2.

$$\text{Elution rate}(\%) = \frac{C_S * V_S}{C_R * m_R} * 100 \qquad 4.2$$

Where C_S is the concentration of metal in the solution obtained from the elution test (mg/L), and C_R is the concentration of metal in the sample (leach residue/mine tailings), (mg/kg). V_S is the volume of solution (L) and m_R is the dry mass of the sample used (kg).

4.1.2.2.3 Electrowinning test

Electrowinning of copper was carried out with a simulated solution prepared in consideration of the copper and ferric ion concentrations of the stripped solution from the solvent extraction stage (44.8 g/L Cu and 1.4 g/L Fe) using distilled water, copper sulfate (II) pentahydrate ($CuSO_4 \cdot 5H_2O$) and iron (III) sulfate n-hydrate ($Fe_2(SO_4)_3 \cdot nH_2O$), where n was analyzed to be 6.33. The electrolyte also contained 170 g/L of free H_2SO_4, and no additives were used. The electrolyte temperature was maintained at 40°C with a bath heater and the volume of the electrolyte was 0.5 L. The anode and cathode were made from a platinum plate of 1 cm^2 surface area and mounted on epoxy resin with a conducting wire. The anode and cathode were

positioned in a fixed mount facing each other, the distance between the electrodes was 3 cm and the mount was placed in the preheated electrolyte cell. A regulated DC power supply (Takasago, Ltd GP025-5) was used, the operating current density was set at 250 A/m^2, and the electrolysis time was 4 hrs. To further study the effects of metal concentration in the electrolyte, the copper and iron concentrations were varied between 25 – 45 g/L and 0 – 1.5 g/L, respectively. The cathode was weighed before and after the electrolysis, test to determine the weight of the copper plated. The current efficiency was calculated as per equation 4.3. The theoretical mass of the copper deposited was calculated using equation 4.4:

$$Current\ Efficiency, (C.E) = \frac{mass\ of\ Cu\ deposited\ (actual)}{mass\ of\ Cu\ deposited\ (theoretical)} * 100 \qquad 4.3$$

$$Cu\ deposited\ (g) = \frac{mm*j*A*t}{nF} \qquad 4.4$$

Where mm is the molar mass of copper, j is the current density, A is the electrode surface area, t is the electrolysis time, n is the number of electrons and F is faradays constant.

4.1.3 Results & Discussions

4.1.3.1 High-pressure leaching of mine tailing

The effect of sulfuric acid concentration on direct pressure leaching of mine tailings was investigated using distilled water and 0.2 – 1.0 M H_2SO_4. Other optimum leaching conditions were kept the same as in Han et.al [24] at a fixed pulp density of 100 g/L, the total pressure of 2 MPa, leaching temperature of 180 ℃, and leaching time of 1 hour. As shown in figure 4.2, the highest leaching rate of Cu achieved was 98.72% when distilled water was used as a leaching medium, while the lowest leaching rate of Fe was achieved (16.31%) at the same leaching conditions. The Cu and Fe concentrations in the leachate were 0.23 g/L and 0.28 g/L. The high leaching rate of Cu can be attributed to the oxidation of pyrite which is one of the main minerals in the mine tailings. The pyrite was oxidized as per equation 1 under the total pressure of 2 MPa and leaching temperature of 180 ℃, thus generating sulfuric acid [7,9,25]. This was verified by a decline in the pH value of 3.12 before leaching to 0.8 after leaching.

The sulfuric acid generated by pyrite oxidation promoted the leaching of chalcopyrite via equation 5. Han et al. [24] confirmed that the presence of pyrite (FeS_2) in the feed has an efficient effect on copper dissolution. Antonijevic et al. [7] also found that with the increasing concentration of H^+ ions in the leach solution, the dissolution of copper increased. Figure 4.3 shows the Eh-pH diagram, where the point indicates the pH and Eh (pH: 0.8, Eh: 676 mV) of the solution obtained after leaching. The stability of Cu^{2+} in solution is favored by the leaching conditions of a high temperature and high pressure thus enabling a high leaching rate. XRD measurement of the solid residue (Figure 4.4) showed the presence of hematite (Fe_2O_3) and the absence of pyrite which was initially in the mine tailings. This indicates that the majority of ferric sulfate is hydrolyzed at a high temperature and total pressure to form hematite as shown in equation 4.6. The precipitation of Fe as hematite resulted in a high metal selectivity of dissolved copper over iron when only water was used as a leaching medium.

$$2CuFeS_2 + H_2SO_4 + 8.5O_2 \rightarrow 2CuSO_4 + Fe_2(SO_4)_3 + H_2O \quad 4.5$$

$$Fe_2(SO_4)_3 + 3H_2O \rightarrow Fe_2O_3 + 3H_2SO_4 \quad 4.6$$

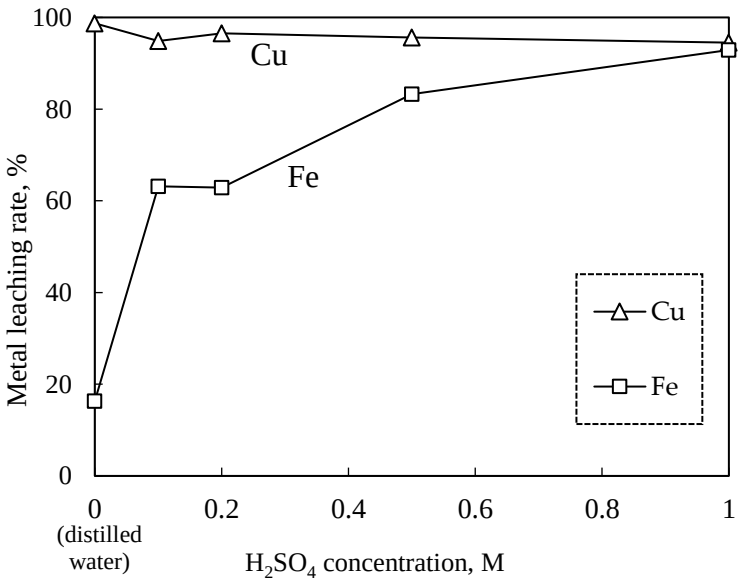

Figure 4.2: Effect of sulfuric acid concentration on the leaching rate of copper and iron. (Conditions: 100 g/L, 1 hr., 700 rpm, 180 0C, 2.0 MPa total pressure).

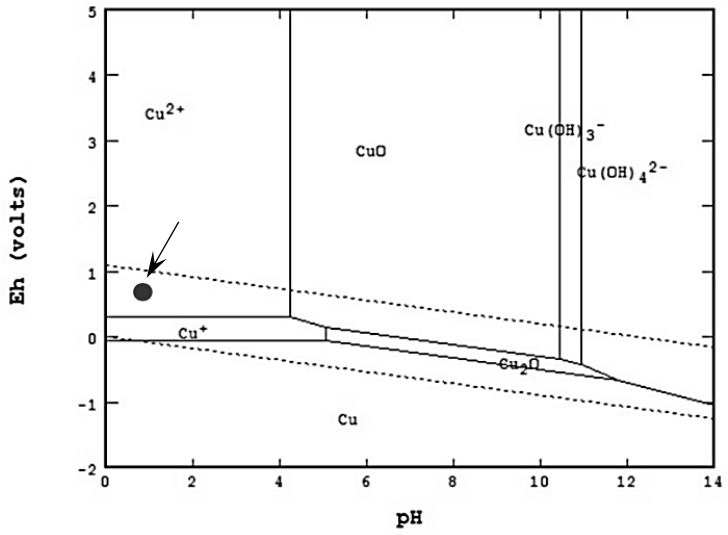

Figure 4.3: Eh-pH diagram for Cu-O system calculated by STABCAL (Condition: 180 ℃).

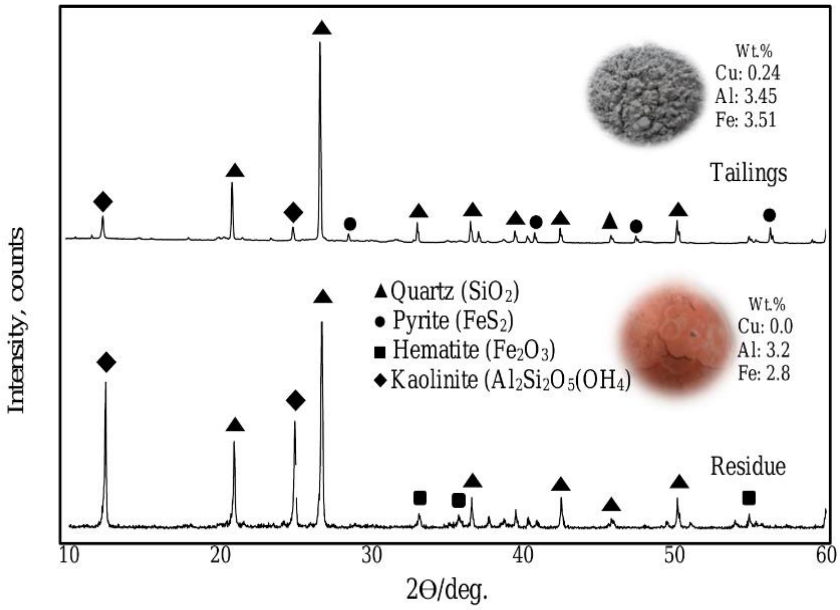

Figure 4.4: XRD patterns of the residue obtained after leaching of mine tailings with distilled water and the mine tailings.

4.1.3.2 Elution test of leaching residue obtained from high-pressure leaching

The elution test results are displayed in figure 4.5(a, b), showing copper and iron concentrations in the solution, respectively. The national effluent standards of copper and iron

in Serbia could not be identified, therefore Japan was used for comparison of the results obtained from the elution test. Based on the wastewater discharge standards specified by the Ministry of the Environment in Japan the upper limit for Cu and Fe in the wastewater discharge is 3 mg/L and 10 mg/L, respectively [26]. The concentration of copper in the solution of mine tailings exceeded this criterion at all the investigated pH values (figure 4.5(a)), while the iron concentration in solution exceeded this criterion at a low pH value of 2 (figure 4.5(b)). The elution rate of copper and iron from the mine tailings was calculated to be 4.58% and 0.46% respectively. On the other hand, the solid residue obtained from leaching the mine tailings could meet the regulatory metal criterion with a very low metal concentration below the detection limit (<0.1 ppm) of ICP-EOS. Under various pH conditions, Fe did not elude, mainly because hematite is thermodynamically stable and therefore, less soluble. Furthermore, the elution rate of copper in the solid residue remained undetectable because 98.72% of copper has been recovered in the PLS. It can thus be confirmed that the elution rate of the mine tailings can be reduced by the HPL process, generating a benign solid residue that is highly environmentally stable under various conditions. Therefore, the obtained residue after HPL treatment of mine tailings can be safely disposed of with reduced environmental loading.

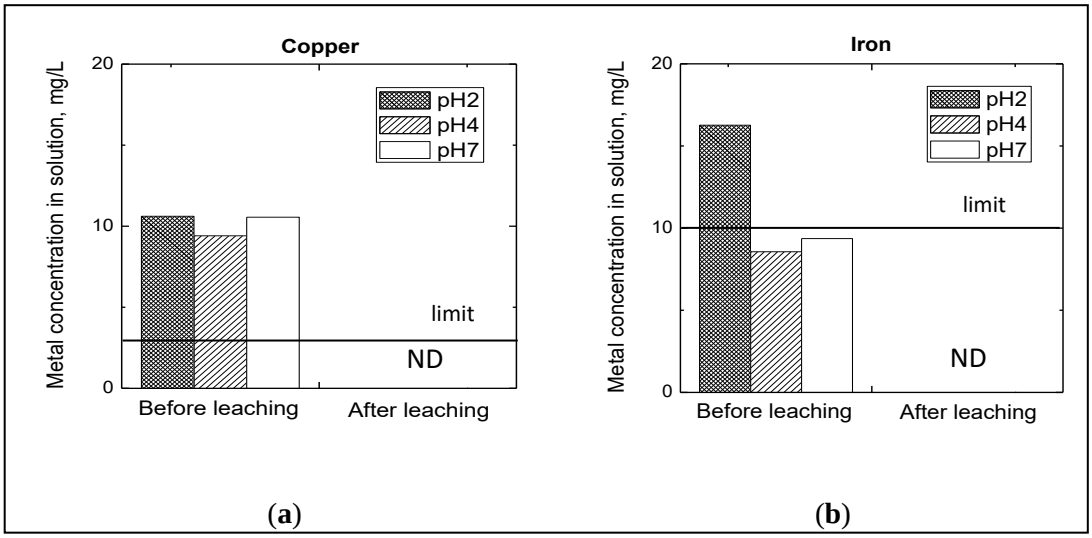

Figure 4.5: Metal concentration in the solution obtained from the elution test of mine tailings (before leaching) and solid residue (after leaching): (a) copper; (b) iron. ND= not detected.

4.1.3.3 Electrowinning of the simulated stripped solution

Current efficiency is an important parameter in electrowinning as it indicates the effectiveness of the electrowinning process. Ferric ion concentration is known to have negative interactions that significantly affect the current efficiency of copper electrodeposition during electrowinning. Therefore, to evaluate the efficiency of carrying out the electrowinning process on the obtained stripped copper solution obtained after solvent extraction of the leach solution from tailings' concentrate leaching, it is relevant to examine the current efficiency of the electrowinning process due to the inevitable Fe contamination during leaching. Figure 4.6 shows the influence of ferric ion concentration on the current efficiency of copper electrodeposition. As expected, a strong inverse relationship is observed, as the ferric ion concentration increases, the current efficiency of copper electrodeposition decreases. This is due to the presence of iron in the copper electrolyte which undergoes reduction from Fe^{3+} to Fe^{2+} at the cathode and re-oxidation to Fe^{3+} from Fe^{2+} at the anode. The cycle proceeds and consumes power that could be used for the deposition of copper. Considering the obtained Fe concentration of 1.4 g/L in the stripped solution, the expected current efficiency is approximately 95%, which is in the upper limit of the industrial range of 85 – 95% [3] (p. 358). Current efficiency loss was determined to be 2.8% per g/L of ferric ions, which agrees with Khouraibchia and Moats [27] 's empirical model of current efficiency (equation 4.7) and Schlesinger et al., [3] (p. 361)'s findings that current efficiency drops by approximately 2.5% for each addition of 1 g/L of ferric ions.

$$\text{Current efficiency (Khouraibchia and Moats [27] 's empirical model)} = 88.19 - 4.19 * [Fe^{3+}](g/L) + 0.52 * [Cu^{2+}](g/L) + 1.81 * 10^{-3} * j(A/m^2) - 6.83 * 10^{-3} * [Cu^{2+}]^2(g/L) + 0.028 * [Fe^{3+}](g/L) * [Cu^{2+}](g/L) + 4.015 * 10^{-3} * [Fe^{3+}](g/L) * j\,(A/m^2 \quad (4.7)$$

Where j is the current density.

Alongside targeting a low Fe concentration in the stripped solution, enriching copper concentration was also an important factor during the extraction process. To demonstrate the

importance of obtaining a high Cu^{2+} concentration in the stripped solution, the effect of three copper concentrations (25, 35, and 45 g/L) on current efficiency during electrowinning was investigated. The Fe^{3+} concentration in the electrolyte was varied from 0 to 1.5 g/L for each copper concentration investigated. Figure 4.7 displays the results obtained, showing that current efficiency losses are higher on dilute copper solutions than on concentrated copper solutions. From the gradients of the three plots, current efficiency loss per g/L of Fe^{3+} was determined and shown in table 4.2. A solution of 45 g/L copper concentration had the lowest current efficiency loss. This could be explained by that a high Cu^{2+} concentration in the electrolyte constantly provides sufficient copper ions to the cathode surface, thus improving deposition rate as well as the copper current efficiency [21]. Das and Krishna [22] also wrote that increasing the bath Cu^{2+} concentration increases the electrolyte viscosity, which impedes the distribution of Fe^{3+} over the cathode surface. Therefore, in this investigation, obtaining a high copper concentration of 44.8 g/L significantly contributed to achieving a good current efficiency of about 95%.

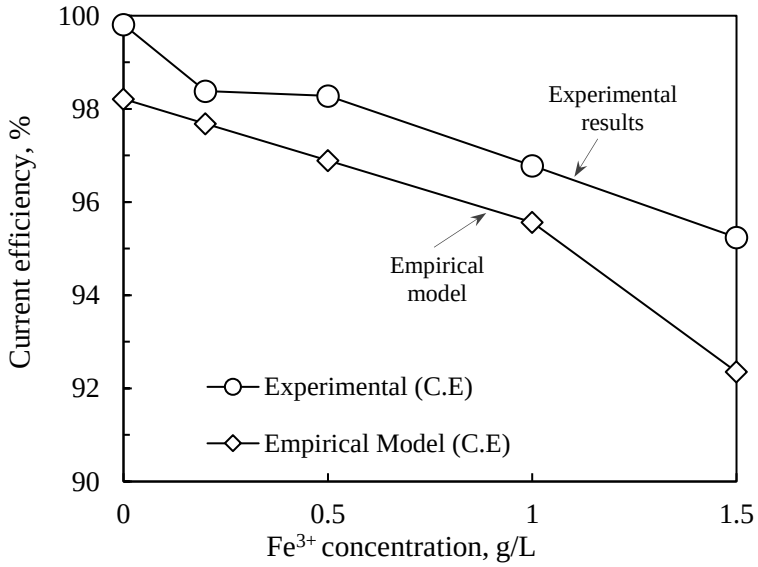

Figure 4.6: Effect of Fe^{3+} on current efficiency (C.E) of copper deposition. (Conditions: current density; 250 A/m^2, 40 ^oC, electrolysis time; 4 hrs., Cu^{2+} concentration; 45 g/L.

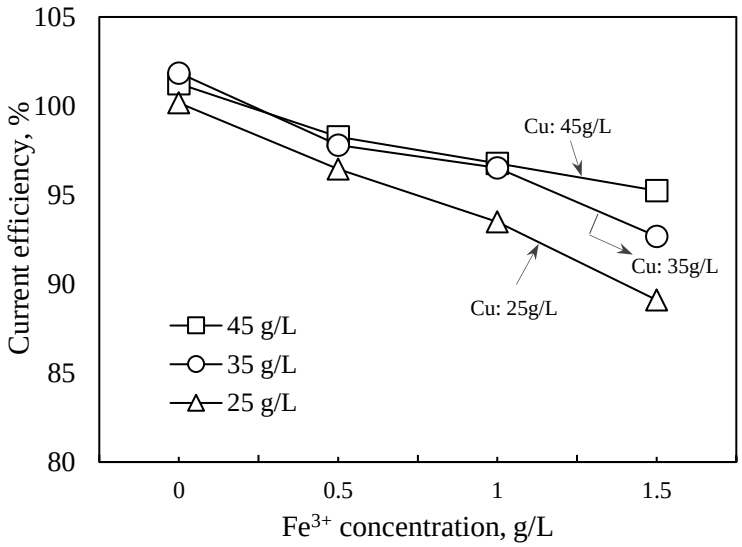

Figure 4.7: Effect of Fe^{3+} and Cu^{2+} concentration on Cu current efficiency. (Conditions: current density; 250 A/m^2, temperature; 40 °C, electrolysis time; 4 h).

Table 4.2: Effect of copper concentration on current efficiency loss per g/L of Fe.

Cu^{2+} concentration (g/L)	**Current efficiency losses (loss per g/L Fe (%))**
25	3.62
35	2.88
45	1.95

In hydrometallurgical processes like these, where pyrite is vital to the leaching stage, the Fe contamination to the stripped solution is inevitable. Therefore, obtaining a high copper concentration in the stripped solution is important as it is less susceptible to current efficiency losses during electrowinning. Since the electrowinning experiments were conducted using synthetic solutions, the expected current efficiency of the real solution obtained from solvent extraction may be slightly lower than that obtained when utilizing a synthetic solution. This is due to the complexity of the stripped solution composition because of several other impurities that may cause side reactions. However, current efficiency loss due to ferric ions reduction has

been found to have a significant effect on current efficiency compared to other impurities which showed no effect [23]. Therefore, the results obtained from electrowinning of a simulated solution can be highly comparable to those obtained from electrowinning the real stripped solution under optimized conditions.

4.1.4 Summary of processing mine tailings

This study demonstrated that leaching the mine tailings could alleviate the possible environmental effects the mine tailings can pose if left untreated, while simultaneously valorizing the mine tailings. As an AMD preventative technique, the removal of pyrite from the mine tailings through oxidative high-pressure leaching was successively achieved, resulting in the formation of hematite in the solid residue. The obtained residue from leaching the mine tailings, and the original sample of the mine tailings, were subjected to standardized elution tests. The eluded metal concentrations for the solid residue could meet the Ministry of the Environment of Japan's set limits for copper and iron in the wastewater discharge, while the original mine tailings exceeded the set limits, thus confirming the reduced environmental loading of the proposed copper recovery process.

A viable copper recovery process for re-treatment of the mine tailings was developed by employing hydrometallurgical methods of high-pressure leaching, solvent extraction, and electrowinning. During high-pressure leaching, the generation of sulfuric acid due to pyrite oxidation promoted copper leaching kinetics when water was used as a leaching medium, thus yielding a high copper leaching rate of 94.4%. Under the optimized solvent extraction conditions, over 93.7% of copper was extracted from the PLS while most of the iron was left in the organic phase. A high copper stripping efficiency of 97.4% was obtained resulting in an enriched solution containing 44.8 g/L Cu and 1.4 g/L Fe. Due to a minimized iron carryover from the stripped solution, electrowinning power consumption by iron was greatly reduced and the current efficiency for copper electrodeposition was over 95%.

4.2 Processing of complex carbonaceous sulfide ore

4.2.1 Introduction

Carbonaceous sulfide ores host polymetallic minerals characterized by carbonates (dolomite, calcite, magnesite, etc.) and carbonaceous materials (inorganic/elemental carbon and organic carbon) [1]. These deposits often contain substantial mineral grades of economic importance. However, the beneficiation of these deposits is extremely difficult due to their mineralogical complexity and lack of advanced processing technologies [2,10,11]. In recent years, the depletion and decline of copper ore grades have encouraged the research and development of beneficiation technologies that can concentrate and recover copper more efficiently from complex ores that contain harmful and high amounts of impurities. Efficient processing of these complex ores is beneficial in sustaining the world's growing demand for copper. The treatment of copper ores by the pyrometallurgical process is responsible for about 80 % of the world's copper production [12]. However, this process has several restrictions to treat other copper sulfide ores with organic and inorganic materials, silica, arsenic, and polymetallic (zinc, lead, cobalt, and PGE) [13]. Flotation of carbonaceous sulfide ore is a challenge due to the fine-grained intergrowth of valuable minerals with impurities of organic carbon and carbonates [13,14]. High reagent consumption has also been associated with gangue minerals present in these complex ores [15,16]. This study focuses on the application of a direct high-pressure leaching system for efficient dissolution of copper from complex carbonaceous sulfide ore which contains chalcopyrite, carbonates, and organic carbon. Sulfuric acid which is readily available from existing pyrometallurgical plants is used as a leaching medium. The effect of other key parameters such as temperature, total pressure, and pulp density on copper leaching efficiency was evaluated. The separation efficiency of copper and iron is highly considered in this process, because of the known codissolution of copper and iron in acidic media and the subsequent challenges caused by iron contamination in the downstream processes. To selectively precipitate copper over iron and other dissolved impurities from the leachate, the sodium hydrosulfide (NaSH) sulfidization method was used.

4.2.2 Methodology

4.2.2.1 Material

A copper ore sample from Southeast Asia was used in the leaching experiments. The chemical composition of the ore is indicated in table 4.3. The sample was dissolved in aqua regia, and chemical analysis was performed using inductively coupled plasma optical emission spectroscopy (ICP-OES) to determine the metal content. The sulfur content was determined by the ion chromatography method. Organic carbon was determined by the deduction method after the measurement of total carbon and inorganic carbon. Total carbon was determined by oxidatively decomposing the ore sample in a pyrolysis reactor of an electric furnace at 1000°C with pure oxygen injection of 300ml/min. The amount of carbon dioxide generated and absorbed was used to calculate the total amount of carbon in the sample. Inorganic carbon was measured by acidification of the ore sample with hydrochloric acid in the presence of nitrogen gas flow in a rubber stoppered flask fitted with an absorption apparatus. The amount of carbon dioxide absorbed was used to calculate the total inorganic carbon. Other elemental components were determined using X-ray fluorescence spectrometry (XRF) (Cu Kα, Ni filters). Mineralogical analysis of the ore was performed using an X-ray diffractometer (XRD, Rigaku RINT 2200V) and the results are shown in figure 4.8. The main gangue minerals observed were quartz (SiO_2), dolomite ($CaMg(CO_3)_2$), and calcite ($CaCO_3$).

Table 4.3: Chemical composition of the complex carbonaceous sulfide ore.

Element	Al	Ca	Cu	Fe	Mg	SiO_2	S	As	Org. C	Inorg. C
Grade (wt.%)	4.55	12.16	2.08	5.37	3.91	24.60	1.92	41 ppm	0.98	4.55

4.2.2.2 Experimental procedure

4.2.2.2.1 High-Pressure leaching

Leaching experiments were carried out in a stainless-steel autoclave (Nitto Koastu, Japan) equipped with a Teflon vessel (200 mL), heating mantle, temperature controller, and a variable speed stirrer (figure 2.15). The slurry samples were prepared by mixing 5 – 20 g of the ore sample with 50 mL of sulfuric acid solution (0.2 – 1 mol/L) to achieve different pulp densities. The optimum particle size of -106 µm was used throughout the experiments. The autoclave system, enclosing the slurry sample was heated to the desired set temperature (100 – 180 °C). Once the intended temperature was reached, oxygen (O_2) gas was injected into the slurry vessel at a controlled total pressure ($P_{total} = P_{vapor} + P_{oxygen}$) of 0.5 – 2.0 MPa. The stirring speed was kept constant at 750 rpm. The solution pH and Eh were measured before and after experiments using TPS WP-80 pH/ORP meter with a double junction Ag/AgCl/ saturated KCl probe. After the set reaction time, the autoclave system was cooled, and the obtained slurry solution was filtered. The copper and iron concentrations in the PLS were determined using ICP-OES. Solid residues were dried overnight in an oven (60 °C) and analyzed by XRD. Additionally, the mineralogical transformation of the solid residues was studied by an electron probe micro-analyzer (EPMA) using JEOL-JXA-8230.

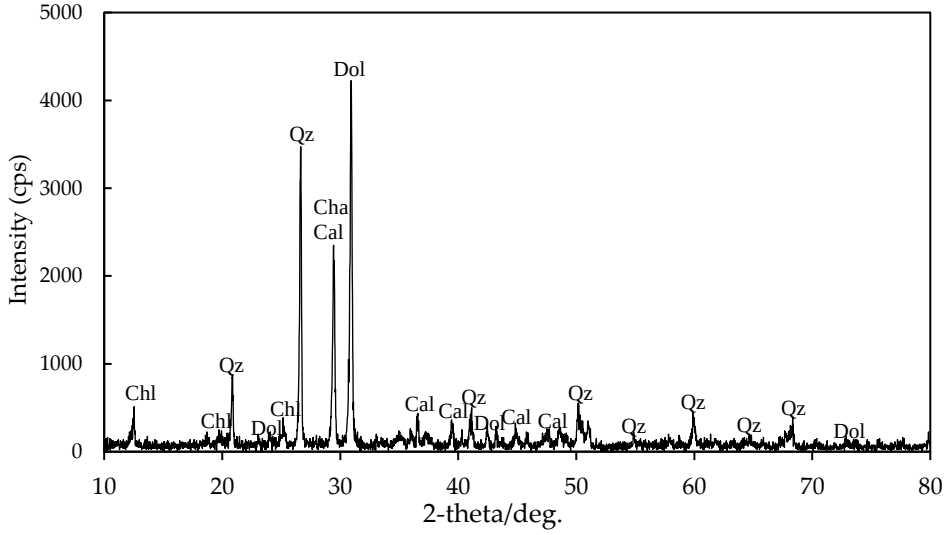

Figure 4.8: The results of XRD analysis of complex carbonaceous sulfide ore. **Dol**: Dolomite ($CaMg(CO_3)_2$), **Cal**: Calcite ($CaCO_3$), **Chl**: Chlorite ($(MgFeAlSi)O_{10}(OH)_8$), **Qz**: Quartz (SiO_2), **Cha**: Chalcopyrite($CuFeS_2$).

4.2.2.2.2 Determination of free acidity

The free acidity of the PLS solution was determined by direct titration to a pre-determined pH point, in the absence of a complexing agent. The analyte solution was prepared using distilled water and 0.1 mol/L sulfuric acid solution to attain a pH of 3.0. The analyte solution was set over a magnetic stirring unit with a pH meter mounted into the solution. Exactly 1.0 ml of the PLS was added to the analyte. The starting point of the burette containing 0.05 mol/L sodium carbonate (Na_2CO_3) was noted. Titration was then carried out by adding the Na_2CO_3 solution into the analyte up to the pre-determined endpoint of the initial pH (3.0). The final burette reading was recorded to determine the total volume of Na_2CO_3 solution added. The titration tests were run three times and the average values were used to calculate free acidity. Free acidity was determined by utilizing the reaction of 1 mol of Na_2CO_3 with 1 mol of H_2SO_4 (equation 4.8) and free acidity in 1.0 ml of PLS was calculated by equation 4.9.

$$H_2SO_4 + Na_2CO_3 = Na_2SO_4 + H_2O + CO_2 \quad 4.8$$

$$\text{Free acidity [FA] (g/L)} = Na_2CO_3\ (L) \times 98.08\ H_2SO_4\ (g/mol) \times 0.05\ (mol/L)\ Na_2CO_3 \quad 4.9$$

4.2.2.2.3 Precipitation of copper by NaSH sulfidization

Precipitation tests by NaSH sulfidization were conducted in 5 ml centrifugal tubes using a high-speed mixer (Eyela, CM-1000). A NaSH solution of 0.1 mol/L was prepared and dosed in relation to the total moles of copper in the pregnant leach solution. The precipitation tests were conducted at room temperature with a fixed shaking speed of 800 rpm. The effects of Cu:NaSH molar ratio (1:1, 1:1.2, 1:1.4, 1:1.6, 1:1.8 and 1:2) and shaking time (1, 5 and 10 minutes) were investigated. The concentrations of Cu and Fe in the residual solution were determined using ICP-OES. The precipitates were filtered and dried before XRD analysis was performed to characterize the sulfide precipitate generated. The pH and oxidation-reduction potential (ORP) were measured before and after precipitation tests.

4.2.3 Results & Discussions

4.2.3.1 High-Pressure leaching

4.2.3.1.1 Effect of sulfuric acid (H_2SO_4) concentration

The effect of H_2SO_4 concentration on the leaching behavior of copper and iron is shown in figure 4.9, which shows that the extraction of metals generally increases as the H_2SO_4 concentration is increased. Thus, showing that sulfuric acid concentration has a significant role in the extraction of copper from the complex carbonaceous sulfide ore. Other studies of similar mineralogical components also showed that an increase in acid concentration yielded a positive effect on the leaching of chalcopyrite [17 – 20]. Figure 4.9 shows that Cu was selectively leached over Fe at a sulfuric acid concentration of 0.6 mol/L, but as the sulfuric acid concentration further increased, the extraction of Fe increased sharply, minimizing the copper/iron selectivity. The key observation at this condition was hydrolysis of ferric iron into jarosite which was separated with the solid residue (figure 4.10). The highest copper and iron extraction percentages achieved were 97.55% and 95.37% respectively at a sulfuric acid concentration of 1.0 mol/L. The mean standard error for Cu and Fe extractions was estimated to be 2.7% and 3.5%, respectively. The Cu and Fe concentration in the pregnant leach solution was 2.43 g/L and 5.35 g/L respectively. Despite the appreciable amount of iron dissolved at 1.0 mol/L H_2SO_4, the direct leaching of copper in complex carbonaceous sulfide ore is still a viable option because of the high copper dissolution of 97.55%. Therefore, 1.0 mol/L H_2SO_4 was used for the subsequent leaching experiments.

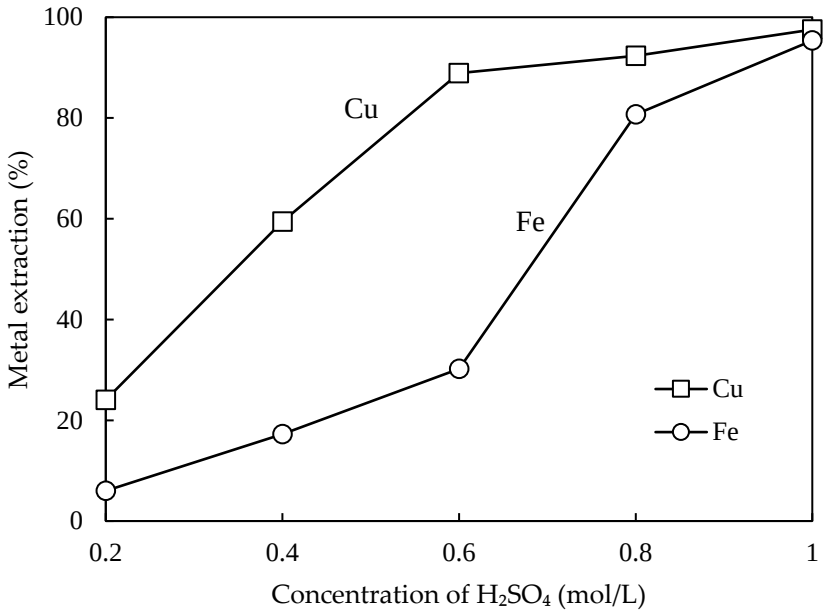

Figure 4.9: Effect of sulfuric acid concentration on the copper and iron extraction behaviors. (Conditions: 100 g/L pulp density, 60 min, 750 rpm, 160 °C, 1.0 MPa total pressure).

Table 4.4: Change in slurry pH before and after leaching

H_2SO_4 concentration mol/L	Slurry pH	
	before leaching	after leaching
0.2	0.81	5.79
0.4	0.63	1.68
0.6	0.44	0.85
0.8	0.27	1
1	0.13	0.42

Table 4.4 shows the change in slurry pH before and after leaching with respect to the different sulfuric acid concentrations. For all the investigated sulfuric acid concentrations, the slurry pH increased after the leaching tests. This indicates that the consumption of sulfuric acid is necessary for the reactions of chalcopyrite and carbonate minerals (calcite, dolomite) as in equations 4.10 – 4.12.

$$4CuFeS_2 + 17O_2 + 2H_2SO_4 \rightarrow 4CuSO_4 + 2Fe_2(SO_4)_3 + 2H_2O \quad 4.10$$

$$CaCO_3 + H_2SO_4 \rightarrow CaSO_4 + CO_2 + H_2O \quad 4.11$$

$$CaMg(CO_3)_2 + 2H_2SO_4 \rightarrow CaSO_4 + MgSO_4 + 2CO_2 + 2H_2O \quad 4.12$$

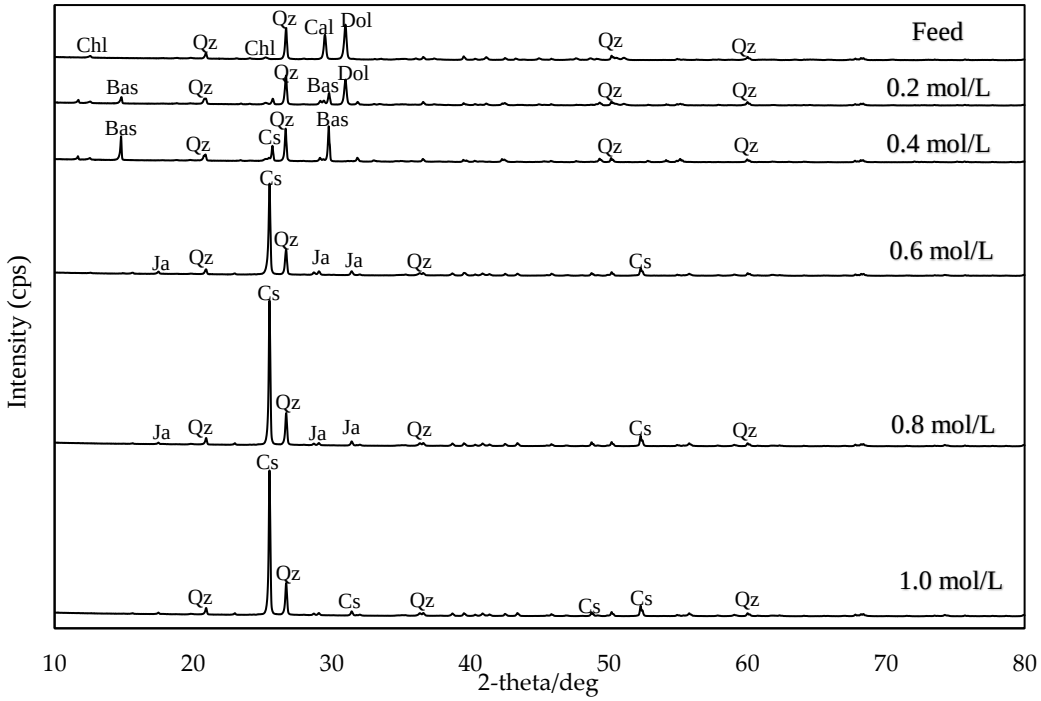

Figure 4.10: The XRD patterns of solid residues at different H_2SO_4 concentrations (Conditions: 100 g/L pulp density, 60 min, 750 rpm, 160 °C, 1.0 MPa total pressure). **Qz**: Quartz, **Cal**: Calcite, **Dol**: Dolomite, **Chl**: Chlorite, **Bas**: Bassanite, ($CaSO_4.1/2H_2O$), **Cs**: Anhydrite/ Calcium Sulfate, ($CaSO_4$), **Ja:** Jarosite, ($H_3O(Fe_3(SO_4)_2(OH)_6)$).

The XRD analysis was done on the leach residues obtained after leaching tests of different H_2SO_4 concentrations (figure 4.10). The intensity of quartz peaks remained unaltered in all the leach residues. The diffraction peaks of bassanite ($CaSO_4.1/2H_2O$) were observed in leach residues of 0.2 – 0.4 mol/L H_2SO_4 tests. Bassanite is usually formed when gypsum ($CaSO_4.2H_2O$) is transformed through energy-intensive dehydration (equation 4.13). At higher H_2SO_4 concentrations (0.6 – 1.0 mol/L), the main component in the leach residues was calcium sulfate ($CaSO_4$) generated by equations 4.11 and 4.12. Hydronium jarosite ($H_3O(Fe_3(SO_4)_2(OH)_6)$) peaks were only noted in residue samples of 0.6 and 0.8 mol/L H_2SO_4 concentrations. Equation 4.14 shows the formation of hydronium jarosite through hydrolysis of the ferric sulfate.

$$CaSO_4.2H_2O \rightarrow CaSO_4.1/2H_2O + 3/2H_2O \qquad 4.13$$

$$3Fe_2(SO_4)_3 + 14H_2O \rightarrow 2H_3O(Fe_3(SO_4)_2\,(OH)_6) + 5H_2SO_4 \qquad 4.14$$

4.2.3.1.2 Effect of pulp density

A high pulp density is important as it allows a high metal concentration in the PLS that is efficient for further upgrade processes such as solvent extraction. Figure 4.11 shows the change in metal extractions as the H_2SO_4 concentration was increased from 1.0 mol/L to 3.0 mol/L utilizing a slurry sample of 300 g/L pulp density. The highest percentage of copper leached was 70.2% at an H_2SO_4 concentration of 1.5 mol/L. A further increase in sulfuric acid concentration did not improve the dissolution of copper but maintained an extraction percentage of around 60%. Iron dissolution increased with increasing sulfuric acid concentration, achieving a high of 86% at an acid concentration of 3.0 mol/L. Figure 4.11 also shows that as the sulfuric acid concentration was increased, the residual acidity in the PLS also increased, but the extraction of copper did not improve. Therefore, the decrease in copper extraction as the pulp density is increased is not attributed to the insufficient amount of sulfuric acid required for leaching.

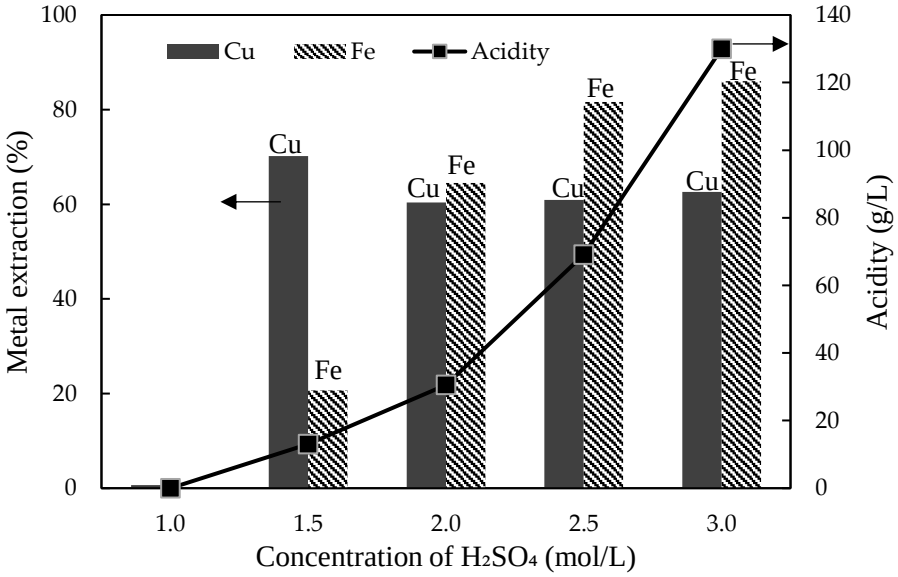

Figure 4.11: Effect of H_2SO_4 concentration on copper and iron extraction behaviors. (Conditions: 300 g/L pulp density, 60 min, 750 rpm, 160 °C, 1.0 MPa total pressure).

Table 4.5: Change in slurry pH before and after leaching of 300 g/L pulp density slurry sample at different sulfuric acid concentrations and the metal concentration in the PLS.

H_2SO_4 concentration, mol/L	Slurry pH before leaching	Slurry pH after leaching	Cu in PLS, g/L	Fe in PLS, g/L
1.0	-0.05	6.40	0	0
1.5	-0.18	1.51	5.19	2.97
2.0	-0.30	1.09	4.55	9.04
2.5	-0.39	0.70	4.44	11
3.0	-0.46	0.42	4.59	13.5

Change in slurry pH before and after leaching of the slurry sample of 300 g/L pulp density as well as the metal concentration in the pregnant leach solution is displayed in table 4.5. When the H_2SO_4 concentration was 1.0 mol/L, the slurry pH changed from an acidic pH of -0.05 to a neutral pH of 6.40, while the copper and iron dissolution was nil. This is due to the rapid acid consumption and depletion by the carbonates and clay minerals present in the system. An increase in acid concentration to 1.5 mol/L supported copper dissolution yielding the highest copper concentration in solution of 5.19 g/L and the lowest iron concentration of 2.97 g/L. Thereby, a good selectivity of copper over iron during leaching can be achieved using a high pulp density of 300 g/L.

The leach residue from 300 g/L pulp density and 2 mol/L H_2SO_4 leaching experiment were analyzed using EPMA (figure 4.12) to examine the hindering factor that results in the inefficient dissolution of copper. When using mapping analysis, Si and Ca were observed around the undissolved chalcopyrite in the leach residue. In various analyzed areas of the residue, the majority of the observed chalcopyrite was not corroded and was found embedded in quartz, which is one of the main gangue minerals in the ore. This confirms that a high pulp density significantly increased the viscosity of the slurry and resulted in poor mixing of the reactants. As a result of the decreased acid to solid contact, the chalcopyrite locked in quartz remained un-leached resulting in low copper extraction.

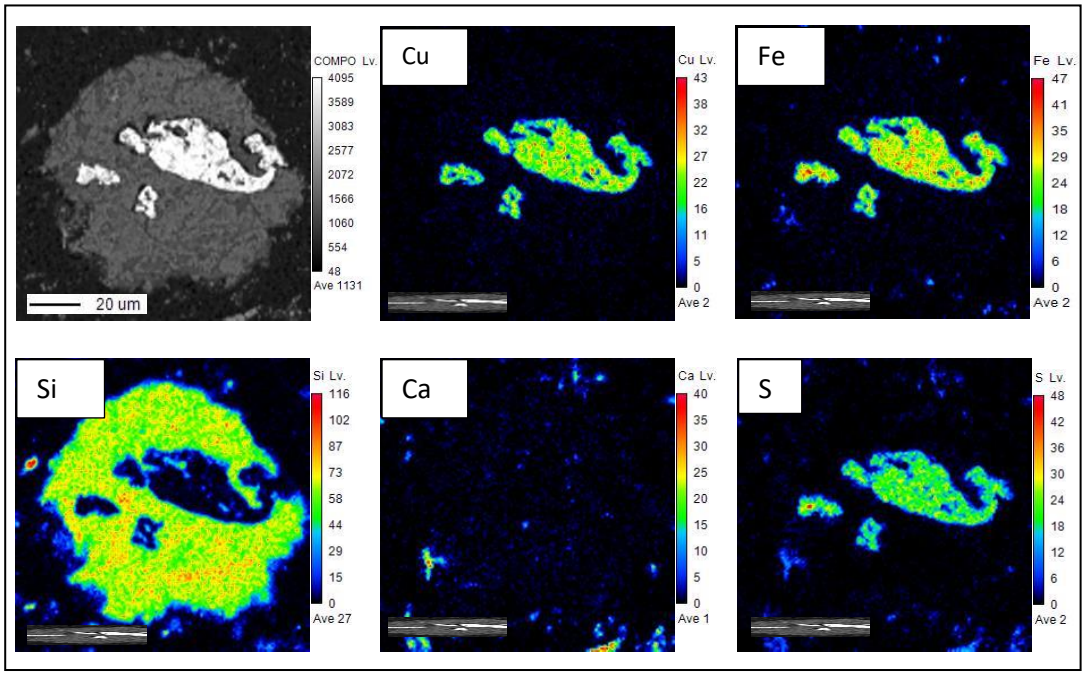

Figure 4.12: EPMA results showing the elemental mapping of the leach residue (Conditions: 300 g/L pulp density, 2.0 mol/L H_2SO_4, 60 min, 750 rpm, 160 °C, 1.0 MPa total pressure).

4.2.3.1.3 Effect of free acidity

The effect of free acidity was examined with respect to the dissolution behavior of copper and iron, and the results are displayed in figure 4.13. A relationship between free acidity and the leaching efficiency of copper and iron was established in all the investigated pulp densities. The copper extraction reached its maximum when free acidity was about 10 g/L, then slightly decreased, and remained constant with further increase of free acidity. Contrary to copper, the iron leaching efficiency increased with increasing free acidity and attained its maximum level when the free acidity was approximately 40 g/L. The error estimates of free acidity on metal extractions at 100, 200, and 300 g/L pulp densities are 5.6%, 7.7%, and 5.1%, respectively. The free acidity trends with respect to the metals leaching efficiencies, strongly suggest that the selective leaching of copper and iron from the carbonaceous ore is possible and can be controlled by adjusting the free acidity of the leachate. When free acidity is adjusted to 10 g/L, copper can be dissolved in solution while iron remains in the solid residue. It can thus be

concluded that free acidity is an important parameter in the leaching process of copper from the complex carbonaceous sulfide ore.

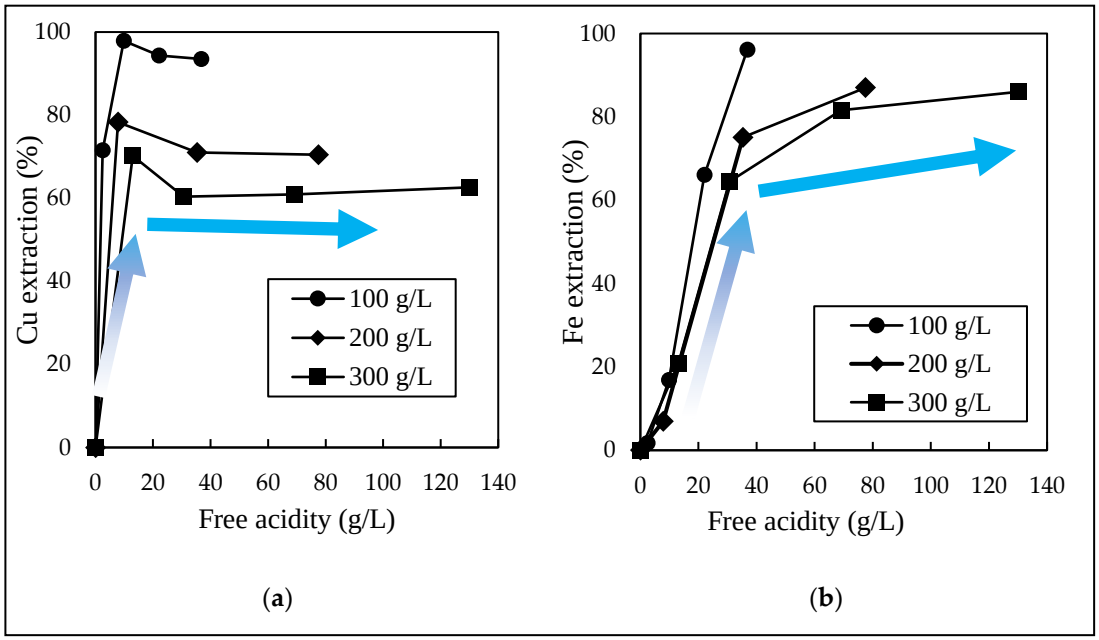

Figure 4.13: The effect of free acidity on dissolution behavior of (a) copper and (b) iron. (0.2 – 3.0 mol/L H_2SO_4 concentration, 1.0 MPa total pressure, 160 °C, 100 – 300 g/L pulp density, 60 min).

Figure 4.14 (a) shows a linear correlation between log[Fe] concentration and log[free acidity] in the pregnant leach solution, with a good correlation coefficient of 0.929. The relationship between Fe concentration in the PLS and free acidity can thus be presented as in equation 4.15. This implies that the extraction of Fe from the complex carbonaceous sulfide ore is dependent on the free acidity of the slurry. On the contrary, there was no correlation found between Cu concentration in the PLS and free acidity. A relationship was also established between free acidity and H_2SO_4 acid concentration used for leaching at different pulp densities (figure 4.14(b)). Such a relationship is important as it allows for the determination of H_2SO_4 consumption, especially when dealing with carbonate minerals. When utilizing a slurry sample of 100 g/L pulp density, free acidity can be expressed as in equation 4.16. Since a relationship exists between Fe concentration in the PLS and free acidity (equation 4.15), a direct relationship between Fe concentration in the PLS and sulfuric acid concentration used for

leaching can be deduced by a combination of equations 4.15 and 4.16. This indicates that Fe tenors in the PLS can be controlled directly through adjustment of the sulfuric acid concentration used for leaching. Therefore, a means for iron precipitation and removal with the solid residue during leaching may be possible. The Fe concentrations obtained from experimental results were found to agree with those calculated from equations 4.15 and the derived equations from figure 4.14(b) with an error margin of less than 2 g/L Fe.

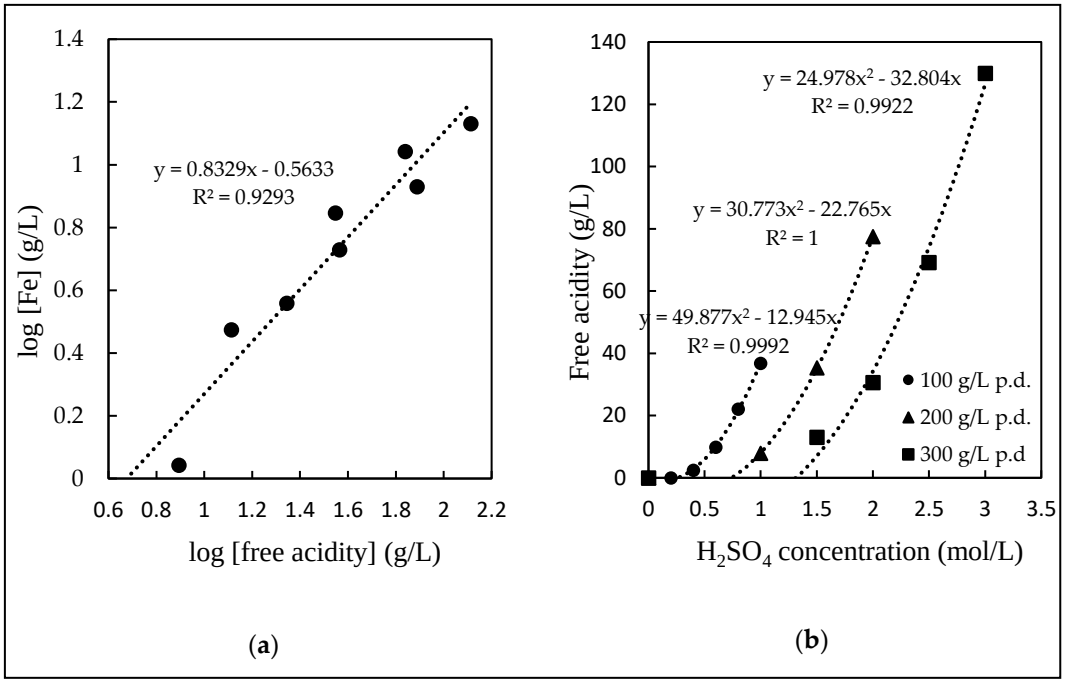

Figure 4.14: (a) The correlation of log [Fe] (g/L) as a function of log [free acidity] (g/L) in the pregnant leach solution (0.2 – 3.0 mol/L H_2SO_4 concentration, 1.0 MPa total pressure, 160 °C, 100 – 300 g/L pulp density, 60 min); (b) The correlations of free acidity and H_2SO_4 concentration (mol/L) (1.0 MPa total pressure, 100 – 300 g/L pulp density, 160 °C, 60 min).

During the leaching of carbonaceous sulfide minerals, iron is released from chalcopyrite ($CuFeS_2$) and chlorite $(MgFeAlSi)O_{10}(OH)_8$), and the initial consumption of sulfuric acid injected into the system is mainly by the reactions of the dissolution of chalcopyrite and carbonate minerals (calcite, dolomite) as illustrated in equations 4.10 – 4.12. During HPL, the Fe^{2+} is further oxidized by oxygen to Fe^{3+}, followed by the hydrolysis of Fe^{3+} to form jarosite.

This mechanism results in acidification of the leaching system through the generation of sulfuric acid via equation 4.14.

$$\log [Fe] = 0.833 \log[\text{Free acidity}] - 0.563 \quad (4.15)$$

$$\text{Free acidity (g/L)} = 49.877[H_2SO_4]^2 - 12.945[H_2SO_4] \quad (4.16)$$

4.2.3.1.4 Precipitation of copper by NaSH sulfidization

To recover the dissolved copper from the leachate, the sodium hydrosulfide (NaSH) sulfidization method was used to selectively precipitate copper over iron and other impurities. Using NaSH, copper is mostly precipitated as copper sulfide (synthetic covellite) via equation 4.17, while iron remains in the residual solution. Leachate (Cu: 3.08 g/L and Fe: 5.28 g/L) obtained from a direct high-pressure leaching experiment of 100 g/L pulp density, 1.0 mol/L H_2SO_4, 160 °C, and 60 minutes was used for these precipitation tests.

$$2CuSO_4 + 2NaSH \rightarrow 2CuS + Na_2SO_4 + H_2SO_4 \quad (4.17)$$

Figure 4.15 (a) shows the results of copper precipitation rate from the leachate at different NaSH molar ratios and a constant shaking time of 10 minutes. The precipitation rate of copper gradually increased with increasing NaSH addition. A low copper precipitation rate of about 45% was observed at the Cu: NaSH molar ratio of 1:1. Copper was not detected in the residual solution at Cu: NaSH molar ratios of 1:1.8 and 1:2, which indicates that more than 99.9% of copper was precipitated. Figure 4.15 (b) shows a consistent copper precipitation rate of more than 99.9% under all the investigated shaking times (1, 5, and 10 minutes). Therefore, the shortest residence time can be recommended to achieve a good separation of copper from iron during copper precipitation. At Cu: NaSH=1:1.8, shaking time: 10 minutes, the pH slightly declined from 1.129 to 1.080 due to the acidic conditions enhanced by equation 4.17. The oxidation-reduction potential (ORP) was measured before and after precipitation of copper to be 527 and -94 mV respectively, indicating a greatly reducing ORP for precipitation of copper.

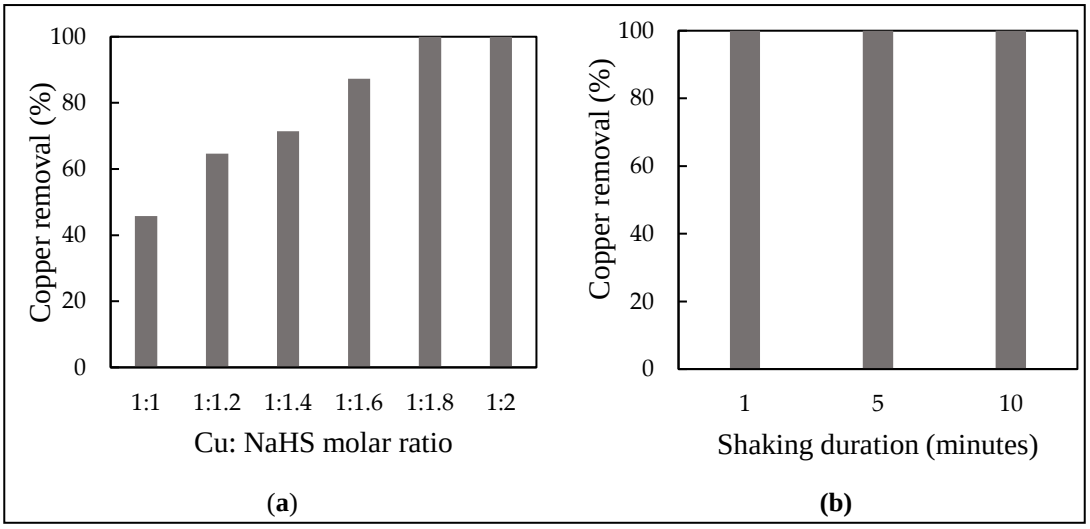

Figure 4.15: Copper removal after precipitation as a function of (a) Cu: NaSH ratio at room temperature, shaking speed, 800 rpm, and shaking duration, 10 minutes. (b) Shaking duration at room temperature, Cu: NaSH molar ratio, 1:1.8 and shaking speed, 800 rpm.

The obtained copper precipitate (Cu: NaSH=1:1.8, shaking time: 10 minutes) was analyzed to determine its chemical composition. The copper and iron content were determined to be 61.2% and 1.21% respectively, indicating a very low iron co-precipitation of about 1.05%. XRD pattern (figure 4.16) confirmed that the generated precipitate is copper sulfide.

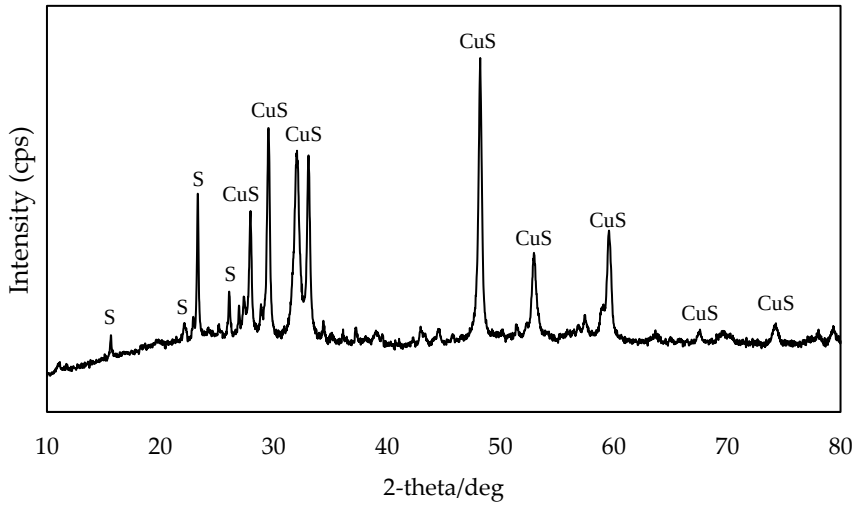

Figure 4.16: The XRD pattern of the precipitate generated by NaSH sulfidization (Cu: NaSH=1:1.8, shaking time: 10 minutes). CuS: copper sulfide, S: sulfur.

4.2.4 Summary of processing carbonaceous sulfide ore

A metallurgical process for selective extraction of copper and iron from complex carbonaceous sulfide ore using high-pressure leaching and sulfide precipitation methods was studied. The high-pressure leaching of complex carbonaceous sulfide ore in oxygenated sulfuric acid solution was performed and the extraction of copper increased with increasing sulfuric acid concentration, and conversely declined when pulp density was increased due to an increased slurry viscosity and resistance in the diffusive mass transfer of reactants. Selective dissolution of copper from an iron can be achieved by controlling free acidity in the pregnant leach solution (PLS). Free acidity analysis showed that the maximum copper and iron extractions were achieved when free acidity was approximately 10 g/L and 40 g/L, respectively, confirming that selective dissolution/separation of copper and iron can be achieved through efficient control of free acidity in the pregnant leach solution. The concentration of iron (g/L) in the pregnant leach solution was found to be dependent on free acidity. A linear relation between log[Fe] concentration and log[free acidity] was established as follows: log [Fe] = 0.833 log[Free acidity] - 0.563. Relationships were also established between free acidity and H_2SO_4 acid concentration used for leaching at different pulp densities. Under these leaching conditions: 100g/L, 1 M H_2SO_4, 160 °C, and 1.0 MPa total pressure, the highest copper extraction achieved was 97.55% with a copper concentration of 2.43 g/L in the PLS. Precipitation of copper from the PLS by NaSH sulfidization was investigated and more than 99.9% of copper was recovered at a Cu: NaSH molar ratio of 1:1.8.

4.3 Conclusion

The objective of this chapter was to explore the possibility of applying the developed hydrometallurgical processes to different kinds of materials for the efficient recovery of valuable metals. The two types of materials used are the flotation tailings from Bor Mine in Serbia and carbonaceous sulfide ore from Southeast Asia. The following findings were made:

Flotation tailings: When a combination of hydrometallurgical processes of high-pressure oxidative leaching (HPOL), solvent extraction (SX), and electrowinning (EW) was utilized to recover copper from the mine tailings, a total copper recovery of 86% was obtained, moreover, pyrite which was primarily in the mine tailings was converted into hematite after HPOL. Stability evaluation of the solid residue confirmed almost no elution of metal ions, confirming the reduced environmental loading of mine tailings through re-processing.

Carbonaceous sulfide ore: Using high-pressure leaching and sulfide precipitation methods, a high copper extraction of 97.55% could be achieved with a copper concentration of 2.43 g/L in the PLS. More than 99.9% of copper was recovered with no co-precipitation of iron when precipitation of copper from the PLS by NaSH sulfidization was used.

Therefore, based on the obtained results, it is possible to apply the developed hydrometallurgical processing technologies to different types of materials, that is; low grade, high-impurity content, and/or complex materials, for efficient metal recovery. The results show the importance of developing advanced hydrometallurgical processes as they are adaptable to processing various types of materials.

References

1. Chimonyo, W., Fletcher, B. and Peng, Y. (2020). 'Starch chemical modification for selective flotation of copper sulfide minerals from carbonaceous material: A critical review'. Minerals Engineering, 156, 106522.
2. Krausmann, F., Gingrich, S., Eisenmenger, N., Erb, K. H., Haberl, H. and Fischer-Kowalski, M. (2009). 'Growth in global materials use GDP and population during the 20th century'. Ecological Economics, 68(10), 2696–2705, doi: 10.1016/j.ecolecon.2009.05.007.

3. Schlesinger, M. E.; King, M. J.; Sole, K. C.; Davenport, W. G. Extractive Metallurgy of Copper, 5th ed.; Elsevier: UK, 2011; pp. 68, 356, 358, and 361.
4. Muravyov, M. I.; Bulaev, A. G.; Kondrat'eva, T. F. Complex treatment of mining and metallurgical wastes for recovery of base metals. Minerals Engineering, 2014; 64, 63–66. doi: 10.1016/j.mineng.2014.04.007
5. Park, I.; Tabelin, C. B.; Jeon, S.; Li, X.; Seno, K.; Ito, M.; Hiroyoshi, N. A review of recent strategies for acid mine drainage prevention and mine tailings recycling. Chemosphere, 2019; 219, 588–606. doi: 10.1016/j.chemosphere.2018.11.053
6. Chen, T.; Lei, C.; Yana, B.; Xiao, X. Metal recovery from the copper sulfide tailing with leaching and fractional precipitation technology. Hydrometallurgy, 2014; 147–148, 178–182. doi: 10.1016/j.hydromet.2014.05.018
7. Antonijevi´c, M. M.; Dimitrijevi´c, M. D.; Stevanovi´c, Z. O.; Serbula, S. M.; Bogdanovic, G. D. Investigation of the possibility of copper recovery from the flotation tailings by acid leaching. Journal of Hazardous Materials, 2008; 158, 23–34. doi: 10.1016/j.jhazmat.2008.01.063
8. Huang, Z.; Jiang L.; Wu, P.; Dang Z.; Zhu N.; Liu, Z.; Luo, H. Leaching characteristics of heavy metals in tailings and their simultaneous immobilization with triethylenetetramine functioned montmorillonite (TETA-Mt) against simulated acid rain. Environmental Pollution, 2020; 266, 115236. doi: 10.1016/j.envpol.2020.115236
9. Li, X., Gao, M., Hiroyoshi, N., Tabelin, C. B., Taketsugu, T., and Ito, M. Suppression of pyrite oxidation by ferric-catecholate complexes: An electrochemical study. Minerals Engineering, 2019; 138, 226–237. doi: 10.1016/j.mineng.2019.05.005
10. Mudd, G. M. (2012). 'Key trends in the resource sustainability of platinum group elements'. Ore Geology Reviews, 46, 106–117, doi: 10.1016/j.oregeorev.2012.02.005.
11. Calvo, G., Mudd, G., Valero, A. [Alicia] and Valero, A. [Antonio]. (2016). 'Decreasing Ore Grades in Global Metallic Mining: A Theoretical Issue or a Global Reality?'. Resources, 5(4), 36, doi: 10.3390/resources5040036.

12. Schlesinger, M.E., King, M.J., Sole, K.C., and Davenport, W.G. (2011). 'Extractive metallurgy of copper, 5th Edition'. Oxford, UK: Elsevier pp. 252 – 256.
13. Liao, Y., Zhou, J., Huang, F. and Wang, Y. (2015). 'Leaching kinetics of calcification roasting calcinate from multimetallic sulfide copper concentrate containing high content of lead and iron'. Separation and Purification Technology, 149, 190–196, doi: 10.1016/j.seppur.2015.05.042.
14. Matuska, S., Ochromowicz, K. and Chmielewski, T. (2018). 'Pressure leaching of sulfide concentrate produced by Lubin Concentrator (KGHM "Polska Miedz" SA, Poland)'. Physicochemical Problems of Mineral Processing, 54(3), 781-792.
15. Liu, Z., Xiang, Y., Yin Z., Wu, X., Jiang, J., Chen, Y., and Xiong, L. (2016). 'Oxidative leaching behavior of metalliferous black shale in acidic solution using persulfate as oxidant'. Transactions of Nonferrous Metals Society of China (English Edition), 26(2), 565–574, doi: 10.1016/S1003 6326(16)64145-6.
16. Gredelj, S., Zanin, M. and Grano, S. R. (2009). 'Selective flotation of carbon in the Pb-Zn carbonaceous sulfide ores of Century Mine, Zinifex'. Minerals Engineering, 22(3), 279–288, doi: 10.1016/j.mineng.2008.08.005.
17. Ntengwe, F. W. (2010). 'The Leaching of Dolomitic-Copper Ore Using Sulfuric Acid Under Controlled Conditions. The Open Mineral Processing Journal, 3, 60–67. doi: 10.2174/1874841401003010060.
18. Dávila-Pulido, G. I. and Uribe-Salas, A. (2014). 'Effect of calcium, sulfate, and gypsum on copper-activated and non-activated sphalerite surface properties'. Minerals Engineering, 55, 147–153, doi: 10.1016/j.mineng.2013.10.006.
19. Cerda, C. P., Taboada, M. E., Jamett, N. E., Ghorbani, Y. and Hernández, P. C. (2017). 'Effect of Pretreatment on Leaching Primary Copper Sulfide in Acid-Chloride Media'. Minerals, 8(1), 1, doi: 10.3390/min8010001.
20. Chetty, D. (2018). 'Acid-Gangue Interactions in Heap Leach Operations: A Review of the Role of Mineralogy for Predicting Ore Behaviour'. Minerals, 8(2), 47, doi: 10.3390/min8020047.

21. Owais, A. Effect of electrolyte characteristics on electrowinning of copper powder. Journal of Applied Electrochemistry, 2009; 39, 1587–1595. doi:10.1007/s10800-009-9845-y

22. Das, S. C.; Gopala Krishna, P. Effect of Fe (III) during copper electrowinning at higher current density. International Journal of Mineral Processing, 1996; 46, 91–105. doi:10.1016/0301-7516(95)00056-9

23. Moats, M. How to evaluate current efficiency in copper electrowinning. In Separation Technologies for Minerals, Coal, and Earth Resources; Young C. A.; Luttrell G. H.; Society for Mining, Metallurgy, and Exploration, Inc., (SME)), Colorado, USA, 2012; pp. 333-339.

24. Han, B.; Altansukh B.; Haga K.; Stevanović Z.; Jonović R.; Avramović L., Urosević, D; Takasaki, Y; Masuda, N; Ishiyama, D; Shibayama, A. Development of copper recovery process from flotation tailings by a combined method of high-pressure leaching–solvent extraction. Journal of Hazardous Materials, 2018; 352, 192–203. doi: 10.1016/j.jhazmat.2018.03.014.

25. McDonald, R. G.; Muir, D. M. Pressure oxidation leaching of chalcopyrite. Part I. Comparison of high and low temperature reaction kinetics and products, Hydrometallurgy, 2007; 86(3–4), 191–205. doi: 10.1016/j.hydromet.2006.11.015

26. Ministry of the Environment, Government of Japan. Uniform National Effluent Standards (Last update: October 21, 2015). Available online: https://www.env.go.jp/en/water/wq/nes.html (accessed on Mar 30 2021)

27. Khouraibchia, Y.; Moats, M. Evaluation of copper electrowinning parameters on current efficiency and energy consumption using surface response methodology. Proceedings of the 217th ECS Meeting, Vancouver, Canada, 2010; Abstract #1378.

Chapter 5. Conclusion

Metallurgical waste is globally being explored as a potential secondary resource of valuable metals due to the depletion of primary ore resources. Hydrometallurgical processing is lately being preferred as an alternative route from conventional pyrometallurgical processing for metal extraction because of its great potential to process complex and low-grade ores with reduced environmental implications. This research aims to develop an efficient hydrometallurgical process to recover Ni, Cu, and Co from discarded copper/nickel granulated smelter slag. The high-pressure oxidative acid leaching (HPOAL) method was used due to its advantages of increased reaction kinetics, enhanced metal selectivity, and the generation of stable residues. This technology was further applied to low-grade secondary material (flotation tailings) and a difficult-to-treat complex ore of high impurity content (carbonaceous sulfide ore), for the extraction of copper. This Ph.D. thesis consists of five (5) chapters, chapter 2 and 3 fully address the hydrometallurgical technologies used for the process development of treating the smelter slag for the recovery of Ni, Cu, and Co. Chapter 4 presents the application of the developed hydrometallurgical processes to different materials for metal recovery.

5.1 Summary of this thesis

Chapter 1: This chapter introduces the pyrometallurgical production of nickel, and copper from sulfide nickel ore, including the description of the smelting process that results in the generation of slag as a waste product. A worldwide current situation regarding the production statistics and predicted data is outlined. Slag is explained and how metal losses are incurred in slag. Environmental consequences due to discarded slag are demonstrated. The importance of re-processing slag is outlined, as well as the objective of this research. The technologies and analytical methods used in this research are introduced. Previous research studies related to the re-processing of slag are cited.

Chapter 2: In this chapter, the results of various leaching parameters' influence on atmospheric leaching and high-pressure leaching of slag are discussed. The characterization of the electric furnace slag sample is firstly illustrated, which showed that the slag sample has an amorphous structure and the dominant mineral composition is fayalite with the matte phase locked in the fayalite phase. The valuable metals content of Ni, Cu, and Co were 0.36%, 0.36%, and 0.17%. Various leaching parameters such as sulfuric acid concentration, temperature, oxidant concentration/total pressure, and leaching time were investigated during the leaching of slag. The atmospheric leaching results showed poor extractions of Ni below 40%, with high Fe dissolution of about 80% when utilizing 1.0 M sulfuric acid and 0.6 M hydrogen peroxide reagent suite. The formation of a passive layer of amorphous silica was suspected to hinder oxidant access for sulfides dissolution and/or Fe precipitation.

On the other hand, under optimized leaching conditions, high-pressure oxidative acid leaching yielded excellent extractions of Ni, Cu, and Co from slag with the highest metal recoveries of Ni, Cu, and Co of 99%, 84%, and 99%, respectively with low Fe extraction of less than 2%. Acidity and temperature are important parameters for optimum dissolution of valuable metals from slag and control the stability of silicic acid to prevent polymerization to silica gel which clogs dissolution pores and hinders slag leaching. Leach residue elution tests were performed for evaluation of their environmental stability.

Chapter 3: The objective of this chapter is to selectively separate metal ions from the pregnant leach solution (PLS) using various separation and enrichment techniques. The solvent extraction technique was used to effectively extract and enrich copper from a simulated leach solution obtained from the high-pressure leaching of the smelter slag. The multicomponent leach solution contained 0.3 g/L Cu, 0.34 g/L Ni, 0.13 g/L Co, and 2.96 g/L Fe. Batch solvent extraction tests were carried out using a countercurrent two-stage mixer settler extraction column. Copper was selectively extracted using LIX 984N (10%v/v) with

Isoper M as a diluent and stripped with sulfuric acid (H_2SO_4) solution. Fundamental parameters influencing the extraction process such as pH, mixing speed, H_2SO_4 concentration, and organic/aqueous (O/A) phase ratio were investigated. For copper enrichment in solution, a combination of two extraction stages and two stripping stages were employed. About 97% of copper was extracted from the simulated solution with coextraction of Fe, Ni, and Co of about 5.90%, 1.47%, and 2.53%, respectively. A final Cu-rich solution of about 23 g/L Cu was obtained with a very low Fe concentration of 0.05 g/L and no Ni and Co coextraction in the second stage. Additionally, for iron removal from the Ni/Co raffinate solution, more than 99% of iron was precipitated at pH 4 by the addition of a calcium carbonate ($CaCO_3$) suspension, with low coprecipitation of nickel and cobalt of around 3.68% and 2.27%, respectively. Subsequently, 99.3 % nickel and 99.9% cobalt were co-precipitated from the solution by potassium amyl xanthate (PAX) solution (55 g/L) at pH 6 forming Ni and cobalt xanthates. Selective dissolution of nickel xanthate using ammonia solution was achieved while more than 99% Co remained as cobalt xanthate precipitate, which was roasted and recovered as CoO powder of about 25 wt.% Co.

Chapter 4: This chapter presents the application of high-pressure leaching technology to extract valuable metals from other metallurgical waste material (flotation tailings) and a complex ore of high impurity content (complex carbonaceous sulfide ore). High-pressure leaching was used to treat the flotation tailings to convert the AMD supporting minerals to more stable forms, for reduction of environmental loading while simultaneously valorizing the mine tailings. A combination of hydrometallurgical processes of high-pressure oxidative leaching (HPOL), solvent extraction (SX), and electrowinning (EW) were utilized to recover copper from mine tailings. An overall copper recovery of 86% was obtained, while pyrite, which is primarily in the mine tailings, was converted into hematite after HPOL. A stability evaluation of the solid residue confirmed almost no elution of metal ions. Complex carbonaceous sulfide ores are extremely difficult to treat due to their mineralogical complexity and impurities of organic carbon and carbonates. This study focuses on the development of a

hydrometallurgical process for efficient copper extraction from complex carbonaceous sulfide ore which contains chalcopyrite, carbonates (dolomite and calcite), and carbonaceous gangue minerals. High-pressure leaching of complex carbonaceous sulfide ore in oxygenated sulfuric acid solution was performed. Selective dissolution of copper from an iron can be achieved by controlling free acidity in the pregnant leach solution (PLS). The highest copper extractions achieved was 97.55% respectively. More than 99.9% of copper was precipitation of copper from the PLS by NaSH sulfidization.

Chapter 5: Conclusion

This chapter provides a summary of the data discussed in the previous chapters, highlighting the major findings and conclusions of each chapter. An overall process flow chart of the developed hydrometallurgical processes for valuable metal recovery slag is presented. Future work recommendations are also outlined.

5.2 Process flowsheet for the recovery of Cu, Ni, and Co from smelter slag

A summary of the developed hydrometallurgical processes for the recovery of copper, nickel, and cobalt from the smelter slag is shown in figure 5.1.

The process flow consists mainly of the following processes sequentially:

i. High-pressure oxidative acid leaching of slag
ii. Solvent extraction of copper
iii. Selective precipitation of iron
iv. Xanthate complexation of nickel and cobalt
v. Ammoniacal dissolution of nickel xanthate
vi. Calcination of cobalt xanthate

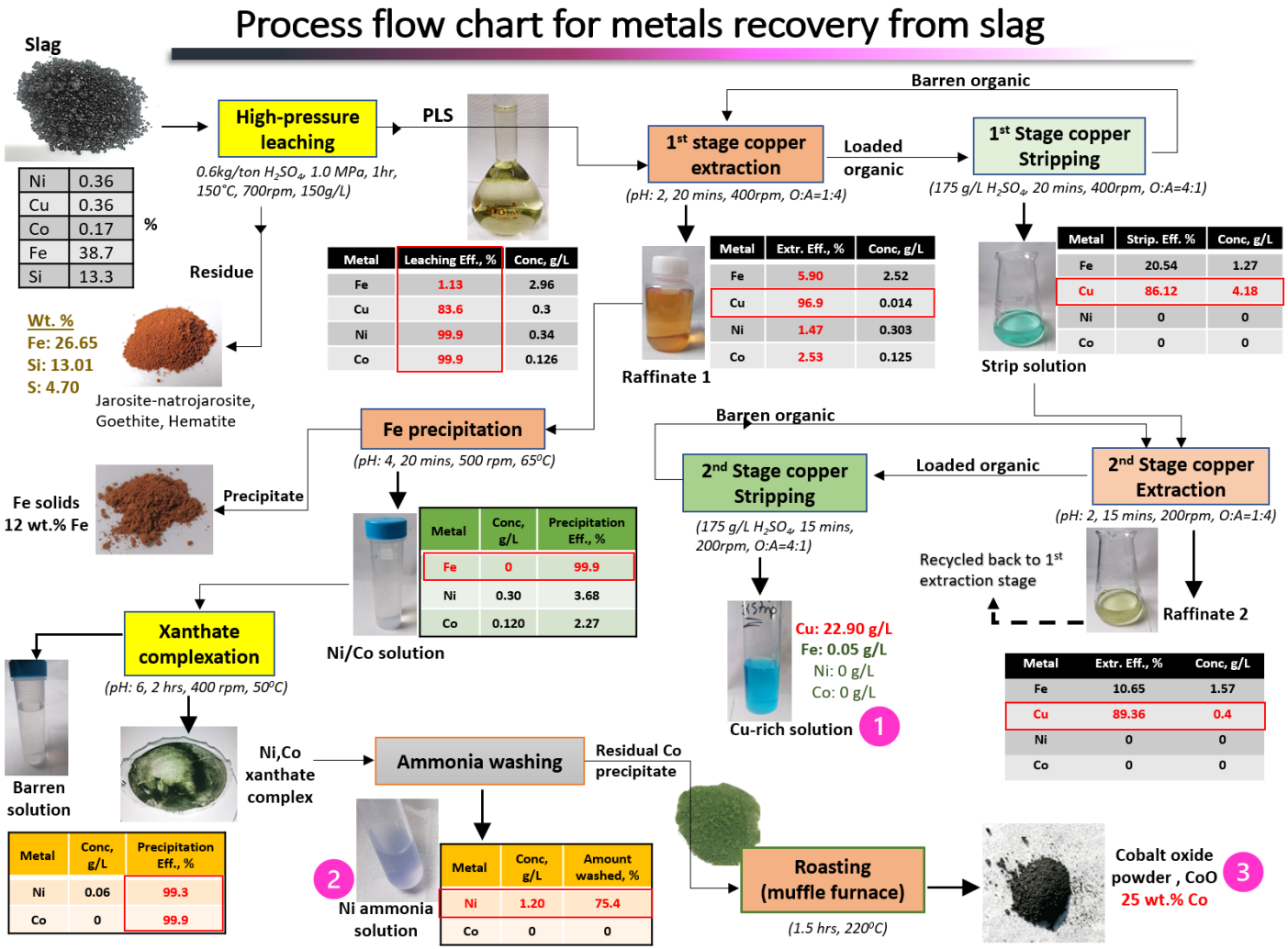

Figure 5.1: The process flowchart of the developed hydrometallurgical processes for recovery of Ni, Cu and Co from smelter slag

5.3 An economic evaluation of the proposed process

An approximated economic evaluation for processing the slag using the proposed technologies was evaluated as shown in Tables 5.1 and 5.2. Table 5.1 shows the financial benefit from the metal values utilizing the current prices from the London Metal Exchange (LME), and the estimated tonnage of metal content in slag that could be recovered. The total amount of metals was valued at around 10.2 billion USD. The value of Fe has been included due to the possibility of further utilizing the waste material as feed in the steel industry after additional processing.

Table 5.1: The economical benefit of metal values from slag

	Price (USD/ton)	**Total recovery**	**Wt.% in slag**	**Amount, tons**	**Value, $**	**Metal production ton/yr.**	**Value, $/yr.**
slag	free		100	32,000,000		800,000	
Cu	9,127	81	0.36	115,200	1,051,430,400	2,332.80	21,291,466
Ni	27,172	94.1	0.36	115,200	3,130,214,400	2,710.08	73,638,294
Co	82,000	99.9	0.17	54,400	4,460,800,000	1,358.64	111,408,480
Fe	125	99.9	38.7	12,384,000	1,541,808,000	309,197.52	38,495,091
				Total:	**10,184,252,800**		**244,833,331**

The cost of processing the slag was estimated based on the yearly production of Cu, Ni, and Co when the throughput of slag is around 800, 000 tons, which is equivalent to the yearly generation of slag by the smelter in Botswana. Table 5.2 displays the cost of processing slag according to the technology employed. Other factors, such as depreciation values, labor costs, transportation, and other miscellaneous administrative expenses were not taken into account during the economic evaluation estimation. High-pressure leaching capital costs were estimated to be 50,000 USD/annual tons of nickel produced from slag[*], while the high-pressure operational cost was estimated to be 8,000 USD/ton of nickel produced[*]. The sulfuric acid is considered to be readily supplied by the sulfuric acid plant from an operating smelter. The solvent extraction capital costs were estimated to be 500 USD/annual tons of Cu produced, while the operational costs and reagents costs were each estimated to be 0.05 USD/ kg Cu

[*] Australian Journal of Mining, Dec, 2010, Commodities, pg. 12.

produced†. The complexation process had the highest costs of 318 million USD per year, due to the high cost of the ammonia solution (60 USD/L). Therefore, an alternative reagent should be considered in the future to render the slag processing economical. Another option to have a positive economical benefit from processing slag is to recover both Ni and Co simultaneously in the solid form via the calcination method without the expensive ammonia washing step. On the other hand, environmental benefits that cannot be quantified are also realized.

Table 5.2: The estimated processing cost of slag per year

1. HPOAL	**Cost (USD)**	
Sulfuric acid (50 USD/ton)	free	
HPAL capital, (50,000 USD/annual ton Ni)*	135,504,000	
HPAL operation (4 USD/ton Ni)*	21,680,640	
	Total:	157,184,640
2. Solvent extraction (SX)		
SX capital (500 USD/annual ton Cu)†	1,166,400	
SX operation (0.05 USD/kg Cu) †	116,640	
Reagents (0.05 USD/kg Cu)	116,640	
	Total:	1,399,680
3. Fe removal		
$CaCO_3$ (50 USD/ton)	2,968,296	
Operation cost	116,640	
	Total:	3,084,936
4. Complexation		
NaOH (300 USD/ton)	178,098	
PAX (1300 USD/ton)	35,204,285	
NH_3 (60 USD/L)	283,048,696	
Operation cost	116,640	
	Total:	318,547,719
5. Calcination		
Operation cost (0.177 USD/KWh)	21,000	
	Total:	21,000
TOTAL	1st year (Capital and operation)	**480,237,975**
	2nd year (operation only)	**343,567,575**

† Schlesinger et al. Extractive metallurgy of copper, 5th Edition, pg. 437.
*Australian Journal of Mining, Dec, 2010, Commodities, pg. 12.

5.4 General conclusions

The growing global industrialization has resulted in an increased demand for metals, however, the mining industry is currently faced with challenges of depletion of primary ore sources which is threatening future supply and developments. The increasing complexity and impurity level of ores have also rendered the conventional processing methods inefficient. This Ph.D. research, mainly addresses these two main challenges, by utilizing metallurgical waste as a secondary source of metals and employing advanced hydrometallurgical techniques to efficiently extract valuable metals (nickel, copper, and cobalt) from smelter slag. By employing these advanced hydrometallurgical processes on other materials; metallurgical waste material (flotation tailings) and a complex ore of high impurity content (complex carbonaceous sulfide ore), high metal recoveries were still obtained. Therefore, developing advanced hydrometallurgical processes that are adaptable to various types of materials is of uttermost importance as it can ensure future metal sustainability.

5.5 Recommendations

Based on this Ph.D. outcome, the importance of developing advanced hydrometallurgical processes that are adaptable to processing various types of materials for future metal sustainability is demonstrated. Development of these advanced processing technologies to efficiently recover value metals from resources that are complex or challenging to process, is a great step towards the development of greener technologies that have a reduced environmental loading. The application of these advanced processing technologies may be the key to realizing a low carbon future, as well as ensuring the future availability of resources.

The following recommendations can thus be made:

- Metallurgical waste, such as the copper/nickel smelter slag presents a potential source of secondary raw material for metals such as copper, nickel, and cobalt production.

- Advanced hydrometallurgical techniques exhibit robust processing in handling different types of materials and achieving very high metal extractions along with the production of benign residue. Therefore, investments in development of these technologies are highly necessary to avoid future disruptment of metal supply.

- These advanced technologies can be incorporated into operational or future metallurgical operations worldwide to process the on-going generated waste material or reprocess the old discarded metallurgical waste for efficient metal recovery while achieving a sustainable metallurgical process.

ACKNOWLEDGEMENTS

I would like to extend my most sincere gratitude to my supervisor Professor Atsushi Shibayama for his guidance, valuable advice, and support throughout the course of my studies and research. His consistent encouragement and great focus motivated me to work hard with dedication and perseverance. I am deeply indebted for his unwavering patience and belief in me which empowered me to realize my potential and have a positive outlook for my future goals and professional development. I would like to also thank Professor Tsuyoshi Adachi, Professor Yasushi Watanabe, Professor Youhei Kawamura, and Professor Gjergi Dodbiba for their valuable comments and feedback which significantly contributed to the improvement of my research work and thesis.

I am also grateful to Associate Professor Kazutoshi Haga for his support in my studies and for being available and approachable to offer help, advice, and assistance at any time to ensure my studies and well-being are a success. Without his help, it truly would have been difficult. I feel immense gratitude to Associate Professor Yasushi Takasaki, who guided and mentored me in the early stages of my research and patiently led me through the use of technical types of equipment. I also would like to thank Dr. Altansukh Batnasan for his valuable suggestions and advice that significantly enhanced the technical writing of my manuscripts. The members of Shibayama laboratory, I humbly appreciate their acceptance and assistance in numerous ways.

I am deeply grateful to Dr. Gwiranai Danha, the Botswana International University of Science and Technology (BIUST), and BCL Mine in Botswana for their constant support and commitment to fostering the collaboration of this research. Their kind cooperation and provision of the smelter slag sample are truly appreciated.

I would like to acknowledge the financial support of the Program for Leading Graduate Schools, (New Frontier Leader Program for Rare metals and Resources), the Japanese Government (MEXT) Scholarship, and other organizations that financially supported my studies and made it possible to conduct this research.

Most importantly, I want to thank my husband for his unconditional love, patience, and being supportive for my studies. And my family for always encouraging me to keep shining!

Labone Lorraine Godirilwe

2022

DEDICATIONS

This Ph.D. thesis is dedicated to my spiritual father and life mentor Senior Prophet T.B. Joshua (12.06.1963 – 05.06.2021) and moreover, to my loving mother and life inspiration Keresepe Angelinah Kereilemang (08.02.1970 – 10.09.2021).

Publications in This Ph.D. Thesis

1. Peer-Reviewed Journal Papers

(1). **Godirilwe L.L.,** Takasaki Y., Haga K., Shibayama A., Sato R., Takai Y. (2021). The Role of Lead in Suppressing Passivation of High Silver-containing Copper Anodes During Electrorefining. *International Journal of the Society of Materials Engineering for Resources*, Vol.25, No.1/2.

○ (2). **Godirilwe, L.L.**, Haga, K., Altansukh, B., Takasaki, Y., Ishiyama, D., Trifunovic, V., Avramovic, L., Jonovic, R., Stevanovic, Z., Shibayama, A. (2021). Copper Recovery and Reduction of Environmental Loading from Mine Tailings by High-Pressure Leaching and SX-EW Process. *Metals*, 11, 1335. https://doi.org/10.3390/met11091335

○ (3). **Godirilwe L.L.**, Magwaneng R.S., Sagami R., Haga K, Batnasan A., Aoki S., Kawasaki T., Matsuoka H., Mitsuhashi K., Kawata M., Shibayama A. (2021). Extraction of copper from complex carbonaceous sulfide ore by direct high-pressure leaching. *Minerals Engineering*, 173, 107181. https://doi.org/10.1016/j.mineng.2021.107181

○ (4). **Godirilwe L.L.**, Haga K., Batnasan A., Danha G., Shibayama A. (2022). Recovery of copper, nickel, and cobalt from smelter slag using high-pressure oxidative acid leaching, solvent extraction, and xanthate complexation. *Hydrometallurgy*, Manuscript number: HYDROM-D-22-00239 (***under review***).

○ (5). **Godirilwe L.L**., Haga K., Batnasan A., Shibayama A. (2022). Selective leaching of copper and removal of arsenic from enargite by high-pressure oxidative leaching. *The Resources Processing Society of Japan*, Manuscript number: 2021-16 (***under review***).

2. International Conferences Proceedings

○ (1). **Godirilwe L.L.,** Haga K., Danha G., Takasaki Y., Shibayama A. Selective extraction of nickel, copper, and cobalt from a smelter slag in Botswana. *Proceedings of the XXX International Mineral Processing Congress (IMPC2020)*, pp 2451 – 2461. The Southern Africa Institute of Mining and Metallurgy (SAIMM). Cape Town, South Africa, (2020). (Reviewed).

(2). Godirilwe L.L., Takasaki Y., Kawamura S., Haga K., Shibayama A., Sato R., Takai Y. Effect of lead addition on passivation behavior of high silver−containing copper anode during electrorefining. *Proceedings of The 15th International Symposium on East Asian Resources on Recycling Technology (EARTH2019).* S5-R5-3. The Korean Institute of Resources of Resources Recycling (KIRR). Pyeongchang, Korea, (2019), (Reviewed).

○ (3). **Godirilwe L.L.,** Haga K., Danha G., Shibayama A. Selective leaching of valuable metals from a smelter slag by high-pressure oxidative acid leaching (HPOAL). *The Ninth International Conference on Materials Engineering for Resources (ICMR2021)*. The Society of Materials Engineering for Resources of Japan. [Online], (2021) (Reviewed).

3. Domestic conference proceedings

(1). **Godirilwe L.L.,** Takasaki Y., Kawamura S., Haga K., Shibayama A., Sato R., Takai Y. The Influence of Pb Addition on Passivation Behavior of High Silver-containing Copper Anode During Electrorefining, *The 29th Japan Society for Materials Physics and Materials Conference*, Akita, Japan, (2019).

Other symposiums, seminars, and meetings

(2). **Godirilwe L.L.,** Takasaki Y., Haga K., Shibayama A. The effect of lead addition on passivation behavior of high silver−containing copper anode during electrorefining. *16th International Symposium JSPS Core-to-Core Program International Symposium; "Challenges facing the Sustainable Development of Mineral and Energy Resources"*. [Online], (2020).

○ (3). **Godirilwe L.L.,** Haga K., Danha G., Shibayama A. Leaching of cobalt, nickel, and copper from granulated electric furnace slag of BCL copper-nickel smelter. *International Symposium on "Establishment of Research and Education Hub on Smart Mining for Sustainable Resource Development in Southern African Countries"*. International Center for Research and Education on Mineral and Energy Resources (ICREMER). Osaka, Japan, (2019).

○ (4). **Godirilwe L.L.,** Han B., Takasaki Y., Haga K., Shibayama A. Copper recovery from tailings by high-pressure leaching-solvent extraction-electrowinning (HPL-SX-EW) process, [Poster]. *ICREMER and Leading Program Symposium; Joint collaboration of the Southern African Universities and Japan*. Tokyo, Japan, (2018).